The Institute of Paper Chemistry

Appleton, Wisconsin

Doctor's Dissertation

Gas Chromatographic Characterization of Absorbent Cellulose Surfaces

Peter A. Mazurak

January, 1979

GAS CHROMATOGRAPHIC CHARACTERIZATION OF ADSORBENT CELLULOSE SURFACES

A thesis submitted by

Peter A. Mazurak

B.S. 1964, University of Nebraska, Lincoln

M.S. 1966, University of Wisconsin, Madison

M.S. 1975, Lawrence University, Appleton

in partial fulfillment of the requirements
of The Institute of Paper Chemistry
for the degree of Doctor of Philosophy
from Lawrence University,
Appleton, Wisconsin

January, 1979

TABLE OF CONTENTS

SUMMARY

Gas adsorption has long offered promise of becoming a useful tool for characterizing papermaking properties of cellulose fiber surfaces. The same fundamental surface force fields which govern aqueous interactions also cause physical adsorption of gases by fiber surfaces. Work in this field has long been restricted by the demanding, tedious, and time consuming experimental techniques involved with measurement of adsorption isotherms by vacuum techniques. Difficulties involved with the analysis of adsorption isotherms have also limited application of the resulting characterizations of fiber surfaces.

In recent years a gas chromatographic approach for adsorption studies has come into wider use. This technique allows calculation of adsorption isotherms from chromatograms of adsorbate injections on adsorbent packed columns. Although this technique is much faster and more convenient than vacuum measurements, adsorption isotherms still have to be analyzed to produce a surface characterization. This thesis develops a new approach for characterizing adsorbent surfaces based on direct use of gas chromatographic retention data.

A surface adsorption index (SAI) has been defined as the difference in retention volumes between large and very small injections of adsorbate on an adsorbent packed column. Consideration of mechanisms of adsorbate transport along the column indicated that the proposed SAI values should be predominantly influenced by sorbate-surface interactions. An experimental program was designed to investigate the general behavior of surface adsorption indices and to compare SAI characterization of a surface with results of thermodynamic analyses of adsorption isotherms.

Experimental results have shown SAI values to be strongly dependent on adsorbate-adsorbent interactions. SAI values were found to be directly proportional to adsorbent mass and specific surface area. These indices were independent of carrier gas flow rate, density of column packing, or column length as long as the column diameter remained constant. Temperature dependence was neither linear nor logarithmic since various thermal factors influenced transport of different concentrations of adsorbate along the column.

A series of cotton fiber surfaces modified with physically adsorbed stearic acid was characterized by both the SAI approach and traditional isotherm analyses. Hexanol and decane were used as adsorbates. Decane SAI values were directly proportional to coverage of fiber surfaces with stearic acid. Changes in the slope of hexanol SAI values plotted as functions of stearic acid surface coverage indicated a variation in the mechanism of hexanol adsorption occurred when fiber surfaces became more than half covered with stearic acid. Isotherm analysis yielded no parameters directly proportional to stearic acid surface coverage, but was able to elucidate changes in the mechanism of hexanol adsorption as stearic acid surface coverage increased.

Changes in the behavior of isosteric heats and entropies of adsorption for hexanol on fiber surfaces modified with physisorbed stearic acid indicated that below 40% stearic acid surface coverage, initially adsorbed hexanol molecules apparently cluster together forming more favorable hexanol adsorption sites. At and above 50% stearic acid coverage this clustering mechanism was eliminated.

SAI values must be measured at constant temperature and equal adsorbate vapor pressure for meaningful comparisons to be made between adsorbent surfaces. Adsorbates must be compounds with low saturation vapor pressure and incapable of penetrating or swelling the adsorbent surface. Well defined standard sur-

faces must be available for relative comparisons of SAI values. The SAI approach characterizes a surface as to the relative degree of interaction with a particular adsorbate compared to a standard surface of known properties. The usefulness of an SAI characterization depends on choice of adsorbate, specific nature of adsorbate-adsorbent interactions and availability of standard surfaces.

Surface adsorption indices were shown to be quite useful for relative evaluation of selected surface properties. Although detailed information concerning the nature of adsorption mechanisms requires analysis of adsorption isotherms, surface adsorption indices should allow wider application of gas adsorption to routine characterization of the surface composition of cellulose fibers with respect to their papermaking properties.

INTRODUCTION

In a very general way papermaking may be viewed as a collection of interactions occurring on cellulose fiber surfaces. Among the many interactions are chemical reactions with dyes and sizing agents, hydrogen bonding of fines and other fibers, and physical adsorption of retention aids, fillers, and pigments. By characterizing cellulosic surfaces, information allowing enhancement of desirable surface interactions or inhibition of unwanted interactions should be obtainable.

Traditional chemical analyses of cellulose for lignin content, carbonyl groups, etc., determine bulk properties but give little information about fiber surfaces. Ultramodern surface analysis techniques such as Secondary Ion Mass Spectrometry (SIMS) or Electron Spectroscopy for Chemical Analysis (ESCA), give detailed surface information where applicable. However, equipment for these techniques is quite costly. Experimental techniques are difficult to master, and the approaches are not always well suited to cellulosic materials.

Gas adsorption has long offered promise of becoming a useful tool for characterization of cellulosic surfaces. Gases physically adsorb through interactions with surface force fields. An adsorbate gas capable of hydrogen bonding could give information about the ability of cellulosic surfaces to hydrogen bond during paper formation. An adsorbate preferentially adsorbing on lignin might be useful for evaluating lignin distribution on cellulosic surfaces. These are but two examples of the potential usefulness of gas adsorption experiments for cellulose fiber characterization. Ideally, gas adsorption offers possibilities for measurement of many cellulose surface characteristics, a few of which are listed in Table I.

TABLE I

SURFACE CHARACTERISTICS MEASURABLE BY GAS ADSORPTION

Fraction of surface favorable for hydrogen bonding

Amount of surface lignin

Amount of surface hemicelluloses

Amount of surface benzene extractables

Concentration of surface hydrophobic groups

Concentration of surface polar groups

Use of gas adsorption for cellulose surface evaluation has been complicated by two basic factors. First are limitations imposed by the tedious, time consuming vacuum techniques usually used to measure adsorption isotherms. These constraints have been almost eliminated by application of inverse gas adsorption chromatography. Adsorption isotherms are calculated from gas chromatograms of pure adsorbates injected onto columns packed with adsorbent. Time required to determine a single isotherm is reduced from days to a few hours.

The second serious limitation to practical use of gas adsorption has been difficulties with the required analysis of adsorption isotherms necessary to produce a surface characterization. Analyses are based on mathematical models of adsorption processes. These models are highly complex, containing several adjustable parameters. The model is fitted to experimental data by graphical or computer techniques. Parameter values resulting from this fit characterize the surface. Sometimes these parameters can be related to adsorbent characteristics such as surface area. Often, however, parameters provide no useful adsorbent characterization. The technique developed by Brunauer, et al. in the 1930's remains the most widely known of these approaches (1).

In a recent thesis, Steven Papanu (2) sums up the field of gas adsorption quite nicely:

> "The study of physically adsorbed gas on solids has traditionally divided itself into two subdisciplines that can be labelled simply as theoretical and practical. The theoretical subdiscipline has, historically, studied the adsorption process on simple or well-defined substrates and has sought to develop detailed models of that process in terms of molecular energetics. Simultaneously, practically oriented investigators have accepted various theories, more or less without questioning their validity, to study complex adsorbents of particular interest to them. Succinctly put, one subdiscipline has concentrated on the adsorbate behavior while the other has studied adsorbents."

Gas adsorption on cellulose has been concerned with both aspects presented by Papanu. However, the basic impetus for studying gas adsorption on cellulose has always been a practical interest in characterizing cellulose fiber surfaces. The present work develops a practical, rapid approach for direct utilization of inverse chromatographic retention volumes for characterization of cellulose fiber surfaces. This approach is not dependent on any particular theoretical model of the adsorption process.

BACKGROUND OF THESIS PROBLEM

ADSORPTION OF GASES BY A SURFACE

FORCES INVOLVED IN GAS ADSORPTION

Forces responsible for gas adsorption are identical to those holding a solid together. At the surface these forces do not abruptly end, but reach out into space. This is a result of surface atoms not being surrounded on all sides by other adsorbent atoms. These "unfulfilled" surface atoms generate the force fields which cause adsorption.

Adsorbate gas molecules interact with adsorbent surfaces through forces which are common to both species. Physical adsorption results from the interaction of Van der Waals forces, which consist of London dispersion forces and electrostatic forces. No transfer or sharing of electrons between adsorbate molecules and the surface occurs in physisorption. Chemisorption involves a chemical reaction between adsorbate molecules and the adsorbent surface. Chemisorption produces heats of adsorption comparable to heats of chemical reactions. Physisorption results in much lower heats of adsorption.

Attractive forces responsible for physical adsorption of gases may be categorized as either polar or nonpolar. Nonpolar forces are functional for all gas-solid systems. Polar forces arise from surface polar groups which produce an electrostatic field reaching out from the adsorbent surface. A polar gas molecule can interact directly with this field by classical electrostatic interactions. Also, the electron distribution of a nonpolar adsorbate molecule may be polarized by this field. The resulting induced dipole then interacts with the surface field.

Cellulose molecules are held together by chemical bonds between adjacent glucose units forming the polymer chain. These molecular chains are in turn held together by a combination of Van der Waals forces and hydrogen bonds. In this manner the unit cells, micelles, microfibrils, and finally cellulose fibers are formed. This arrangement varies, forming both amorphous and highly ordered, crystalline regions. Cellulose surfaces would be expected to interact with gases through general, nonpolar-type and polar-type forces. Also, adsorbates exhibiting hydrogen bonding capability would have an additional mechanism for interaction with the surface. Water vapor is an extreme example of this type of adsorbate. Polar-type and hydrogen bonding forces would result primarily from surface hydroxyl groups but surface carbonyl and carboxyl groups may also be formed during pulping or other treatments.

EARLY GAS ADSORPTION WORK ON CELLULOSIC SURFACES

Early workers (3,4) gathered adsorption data for carbon dioxide and nitrogen on cellulosic surfaces. Emmett and DeWitt (5) studied nitrogen adsorption on paper. Hunt, et al. (6) studied surface areas of water-dried and benzene-dried cotton linters using nitrogen adsorption and BET isotherm analysis. Haywood (7) determined surface areas for a number of water-dried and acetone-dried hardwood ray-cell samples. Haselton (8) undertook a systematic study of gas adsorption on cellulosic surfaces. He studied adsorption of N_2, CO_2, and n-butane on a variety of cellulosic substrates. Experimental isotherms were analyzed by application of the BET model (p. 19). By measuring BET surface areas of unbonded, water-dried fibers and handsheets made from these fibers, Haselton was able to calibrate the optical scattering technique for determining relative bonded areas of paper.

Merchant (9) and Sommers (10) extended the work of Haselton. BET analysis was used to follow changes in surface area as water swollen cellulose fibers were dried from a variety of solvents. Upon initial drying, a never-dried cellulose fiber was found to suffer an irreversible loss of some of its internal surface area. Subsequent cycles of swelling with water followed by drying caused more and more loss of this internal surface area. These findings have important implications to the recycling of fibers. The techniques of solvent replacement drying were developed during this work. The WAN (water, alcohol, nonpolar solvent) drying technique of Merchant preserves the water swollen structure of cellulose through replacement of water with methyl alcohol, followed by exchange to a nonpolar solvent such as n-pentane. Sommers explored critical point drying of cellulose using liquid carbon dioxide as the final solvent.

These early workers all used some type of vacuum adsorption apparatus. In this technique adsorbent is packed into a Pyrex tube and sealed onto a vacuum line capable of achieving at least 10^{-6} torr. Next, the adsorbent is thoroughly out-gassed to remove all adsorbed contaminants. After out-gassing, the adsorbent tube is thermostated at the desired temperature. Adsorbate gas is admitted and allowed to come to equilibrium with the adsorbent.

At equilibrium, adsorbate vapor pressure is measured. To determine the amount of gas adsorbed, two methods are commonly used. In gravimetric adsorption experiments the adsorbent is weighed directly in vacuo with a McBain quartz spiral balance or some other type of vacuum microbalance. Less convenient are volumetric determinations, where the volume of adsorbate admitted to the tube is carefully premeasured. From the pressure drop during achievement of equilibrium, the volume of gas adsorbed by the solid is calculated. For more complete descriptions of this type experiment see Brunauer (1).

These experimental techniques require much time to master. Vacuum systems are notorious for developing minute leaks which are difficult to track down. A stopcock opened at the wrong time or turned in the wrong direction can spell disaster. Equilibrium is sometimes reached quite slowly for certain systems. If significant sorbate-surface interactions occur, the adsorbent may undergo important changes during extended equilibration. One of the greatest limitations to the usefulness of gas adsorption has been these time consuming, exacting experimental measurements. Often, several months are required just to gather experimental data for one system.

INVERSE GAS ADSORPTION CHROMATOGRAPHY

Gas adsorption may be viewed as a time phenomenon. Consider a gas-solid system. Gas molecules are constantly colliding with the surface. If conditions are such that adsorption does not occur, these collisions are totally elastic. Nonadsorbed gas molecules simply bounce off the solid surface. If the gas adsorbs, however, collisions lead to increased residence times for gas molecules on the surface. This time is very short and desorption soon occurs. At equilibrium, the number of adsorbing molecules equals the number of desorbing molecules and the surface has a certain steady-state population of adsorbed molecules. No one particular molecule remains on the surface very long. DeBoer estimates residence time as about 10^{-3} sec for a physisorbed molecule (11).

A gravimetric vacuum experiment measures directly the increased surface population of adsorbate molecules. A volumetric experiment measures the decrease in gas phase molecules which have been adsorbed. Both these experiments are indirectly measuring the increased average residence time of an adsorbate molecule on the surface. Gas adsorption chromatography measures this residence time in a more direct manner.

Gas chromatography developed from a combination of gas adsorption and column chromatography (12). Initial experiments involved columns packed only with adsorbent materials. With the advent of gas-liquid chromatography (13) and its subsequent rapid development as an analytical tool, gas adsorption chromatography became of secondary importance. In addition to becoming valuable for analysis of mixtures, gas-liquid chromatography provided a convenient means for studying solution thermodynamics of volatile solutes in nonvolatile solvents (14). In a like manner, gas adsorption chromatography can be used to study the interactions between injected adsorbate molecules and an adsorbent column packing material. Braun and Guillet (15) have termed this application "inverse" gas chromatography.

Surface studies of adsorbents by inverse chromatography are experimentally relatively simple. The adsorbent material is packed into a gas chromatography column. The packed column is connected to a standard gas chromatograph. Inert (nonadsorbing) carrier gas flows through the column. Pure adsorbates ("probe" molecules) are injected. Based on behavior of retention volume with injection size and temperature, traditional adsorption data may be calculated. Inverse gas adsorption chromatography investigates column packing materials by injection of known pure substances, in contrast to analytical chromatographic separations of unknown injected mixtures.

Inverse chromatographic studies are much more rapid and convenient than vacuum adsorption experiments. Several excellent reviews of the subject have been published (15-18). This technique effectively eliminates one of the limitations to routine gas adsorption surface characterization, the exacting and time consuming experimental work. Gas chromatographic techniques allow routine use of organic adsorbates such as alcohols and ketones. These materials would be quite difficult to work with in a vacuum apparatus due to low saturation

vapor pressures. Gas chromatographic "out-gassing" of contaminants is also quite easy. Carrier gas is simply allowed to flow through the adsorbent column for several hours or days.

EXPERIMENTAL GAS ADSORPTION DATA

The Adsorption Isotherm

The adsorption isotherm plots amount of gas adsorbed by the solid as a function of adsorbate vapor pressure at constant temperature. The amount of gas adsorbed is usually expressed as volume or weight adsorbed per gram adsorbent. Units of millimoles or micromoles adsorbed per gram adsorbent are also common, especially when several different adsorbates are being compared. Amount adsorbed is also expressed as fractional surface coverage, θ. A surface coverage of $\theta = 1$ corresponds to monolayer coverage; $\theta = 2$, to surface coverage by two layers; and so forth, as many multilayers of adsorbate molecules cover the surface.

Brunauer, et al. (19) have classified experimental adsorption isotherms into five types. Figure 1 shows this classification. Type I corresponds to monolayer adsorption and is typical of chemisorption or micropore filling (20). Type II is the most common type of isotherm found for purely physical adsorption and corresponds to multilayer formation. Type III is less common, resulting from a heat of adsorption less than or equal to the heat of liquefaction of the adsorbate. Types IV and V correspond to Types II and III, respectively, with an upper limit to pore volume.

Glueckauf (21) first related the shape of an elution chromatogram to the corresponding isotherm for adsorbate on adsorbent. For ideal analytical gas chromatography, a linear isotherm obeying Henry's Law is desired. In this case the resulting chromatogram is Gaussian. Injections of different sizes

have equal retention times. Very few linear isotherms are found for gas-solid systems.

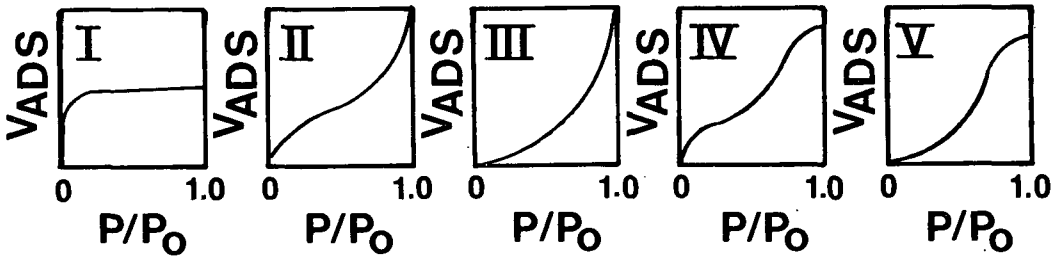

Figure 1. Five Classes of Isotherms According to Brunauer, et al. (19)

Gas adsorption for most real systems produces nonsymmetrical peak shapes, with diffuse leading or trailing edges. Retention time depends on amount injected and the resulting chromatographic peaks usually exhibit overlapping leading or trailing edges when superimposed. Kiselev and Yashin (22) show many examples of the chromatograms resulting from various isotherms. Adsorbate-surface interaction characterized by a BET Type III isotherm results in chromatograms with diffuse leading edges. Increasing the amount injected produces chromatograms with common leading edges. BET Type I interactions produce chromatograms with diffuse trailing edges. Larger injections result in chromatograms with common trailing edges. The BET Type II sigmoidal isotherm has two distinctly different types of behavior depending on amount injected. Small injections result in chromatograms with overlapping trailing edges. Large injections result in common leading edges. This behavior is shown in Fig. 2. In summary, isotherms concave to the pressure axis cause diffuse trailing edges of chromatograms while isotherms convex to the pressure axis produce diffuse leading edges. A BET Type II isotherm is partially concave and partially convex to the pressure axis.

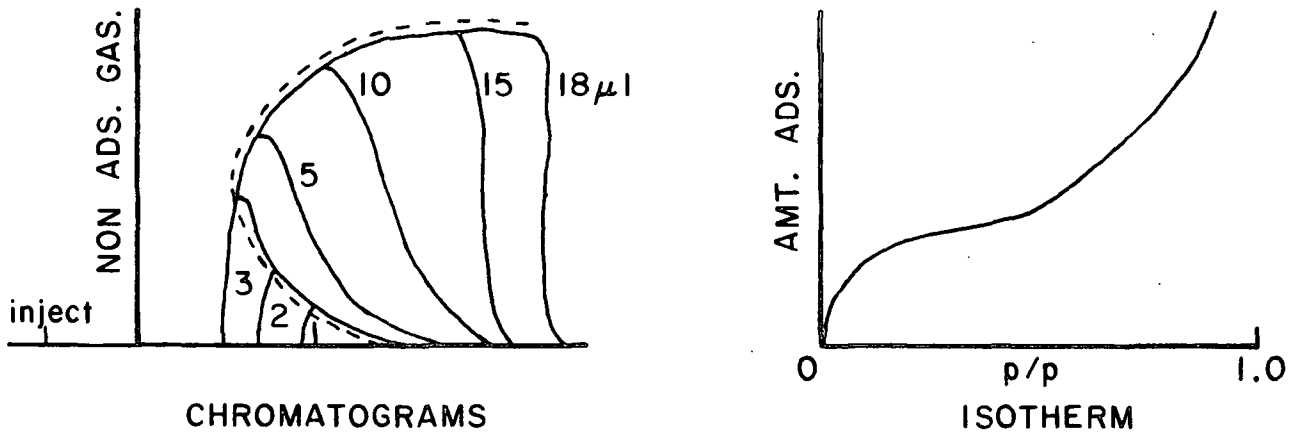

Figure 2. Behavior of BET Type II Isotherms on the Chromatograph

The dashed line in Fig. 2 indicates the diffuse common boundary for a BET Type II isotherm. This diffuse boundary is directly related to the adsorption isotherm. Glueckauf (21), Gregg (23), Huber and Gerritse (24), and Kiselev and Yashin (22) all developed the mathematical relationship between these quantities. Appendix I presents a complete derivation of this relationship. Briefly stated, chromatograph detector response is directly related to adsorbate vapor pressure. The amount of gas adsorbed is directly proportional to chart area between elution of an injection of nonadsorbed gas and the diffuse common boundary of the superimposed chromatograms. Adsorbate vapor pressure may be calculated at any detector response from the equation:

$$p(\text{mm Hg}) = ghRT/wD, \qquad (1)$$

where D = detector sensitivity (chart area/μmole injected)

w = carrier gas flow rate (mL/min)

g = chart speed (linear chart measurement/min)

h = detector response (linear chart measurement)

R = ideal gas constant = 0.0624 (mL) (mm Hg)/(K°) (μmole)

T = temperature (°K)

The corresponding amount adsorbed at a given vapor pressure is calculated from the equation:

$$\frac{\mu\text{moles adsorbed}}{\text{gram adsorbent}} = \frac{S_a}{mD}, \qquad (2)$$

where m = mass adsorbent in column (g)

S_a = adsorbed area at peak height corresponding to adsorbate vapor pressure (chart area)

The adsorbed area, S_a, may be better visualized by reference to Fig. 3. Adsorbed gas has a longer retention time than nonadsorbed gas. This gas hold-up is due to adsorption. An injection of a nonadsorbed gas, such as methane, is made to determine column dead space and serve as a reference point for evaluation of the adsorption isotherm. The chromatogram in Fig. 3 is "backwards" from the chromatogram of Fig. 2 and represents use of a zero left recorder instead of the more common zero right recorder.

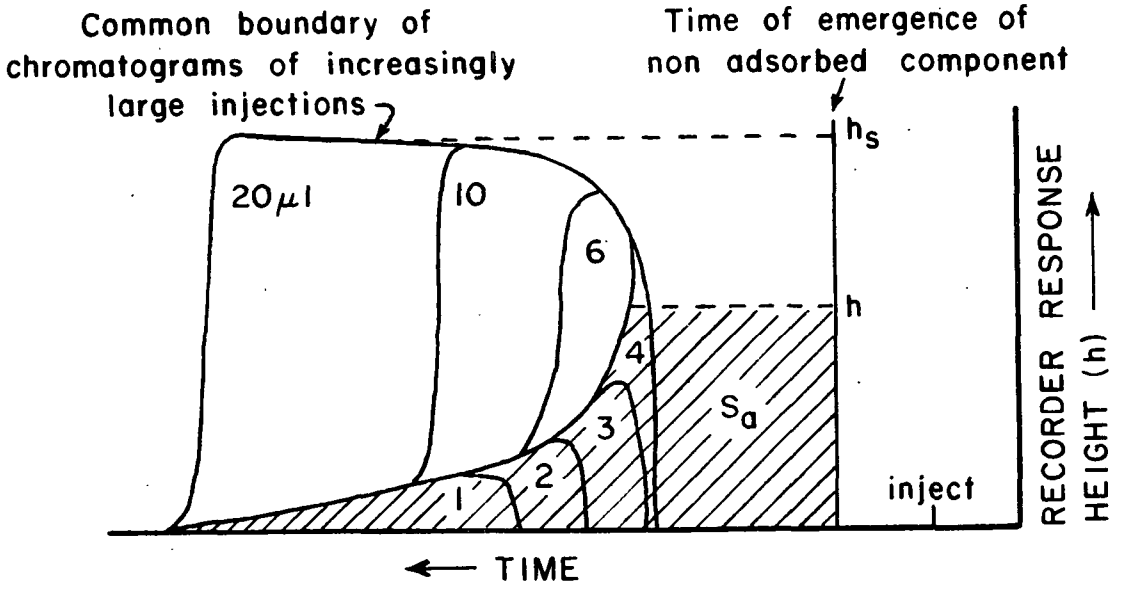

Figure 3. Adsorbed Area (Crosshatched) for Response Height h

This elution chromatographic technique is a nonequilibrium approach. Many complications which arise cannot be treated exactly. Among these are: non-

equilibrium in peak formation, noninstantaneous input peak profiles, and considerations of volume changes within the peak during adsorption. Although attempts have been made (25-27) to treat these factors exactly, such efforts may not be necessary. Huber and Gerritse (24) made an extensive comparison between elution chromatography experiments and equilibrium determinations. Isotherms were measured as described above and compared with isotherms determined from equilibrium chromatographic frontal analysis experiments and classical vacuum work. It was concluded that pressure drop across the column is the single most important factor influencing elution results. If pressure drop can be minimized, results of elution experiments are in very good agreement with equilibrium work.

The Adsorption Isobar

The adsorption isobar plots amount of gas adsorbed as a function of temperature at constant pressure. Adsorption isobars can be quite useful for detecting changes in the nature of adsorption. An adsorption isobar usually shows an exponential-like decrease in adsorption with increasing temperature. At some temperature a discontinuous, sharp increase in adsorption may occur, demonstrating onset of chemisorption. This discontinuity is again followed by exponential decay with respect to temperature. At a still higher temperature a second discontinuity may exist, corresponding to a second type of chemisorption, or penetration of adsorbate into the solid surface.

Adsorption isobars are not easy to measure directly in classical vacuum adsorption experiments. However, adsorption isobars are easily measured directly in chromatographic experiments. Since chromatogram peak height is directly proportional to vapor pressure, the adsorption isobar is equivalent to a plot of retention volume *versus* temperature at constant peak height. For a system exhibiting a linear isotherm, retention volume is independent of peak

height and the isobar is easy to evaluate. For systems with nonlinear isotherms, difficulties arise. Guillet (15) handles these problems by extrapolating retention volumes back to infinite dilution at each temperature. Data are plotted as the logarithm of infinite dilution retention volume versus reciprocal absolute temperature and termed "retention diagrams." Guillet and others (15,28,29) have made extensive use of these retention diagrams to study polycrystalline polymer solid-state transitions. Retention diagrams are, in fact, adsorption isobars and show behavior typical of these quantities. Penetration of adsorbate into a solid polymer often occurs at a glass transition, for example.

The Adsorption Isostere

The adsorption isostere plots data as variation of equilibrium pressure with temperature, corresponding to a constant amount of gas adsorbed. Each point on an adsorption isostere represents a pressure and temperature at which a fixed adsorbate surface concentration is in equilibrium with gaseous adsorbate molecules. The Clausius-Clapeyron equation allows calculation of the heat change for such a system. Slopes of $\ln p$ plotted as a function of $1/T$ for adsorption isosteres give heats of adsorption. Usually, heats of adsorption are not constant for different amounts adsorbed, but vary due to surface characteristics. Thus, the adsorption isostere is a valuable means of characterizing a surface. As such, it is always evaluated from isotherms measured at different temperatures. As is usually the case for thermodynamic treatments, application of the Clausius-Clapeyron equation assumes no particular model for the adsorption system.

Theoretically, the adsorption isostere should be quite easy to measure chromatographically. Very small (<0.1 μL) equal amounts injected at different temperatures should interact with corresponding areas of the surface. Different effective vapor pressures will be produced. A plot of peak height versus

temperature should be the adsorption isostere. Unfortunately, injections of identical very small quantities are impossible to make with any great accuracy. For linear isotherm systems, such as exist in most gas-liquid systems, a plot of retention time versus temperature is equivalent to the isostere. For most gas solid systems, however, retention time depends on amount injected as well as temperature. Therefore, adsorption isosteres are calculated from isotherms in most chromatographic work.

Summary

Adsorption data are usually measured and plotted as the adsorption isotherm. If adsorption isobars or isosteres are desired, the corresponding data points are read off a plot of several isotherms. Figure 4 illustrates this approach.

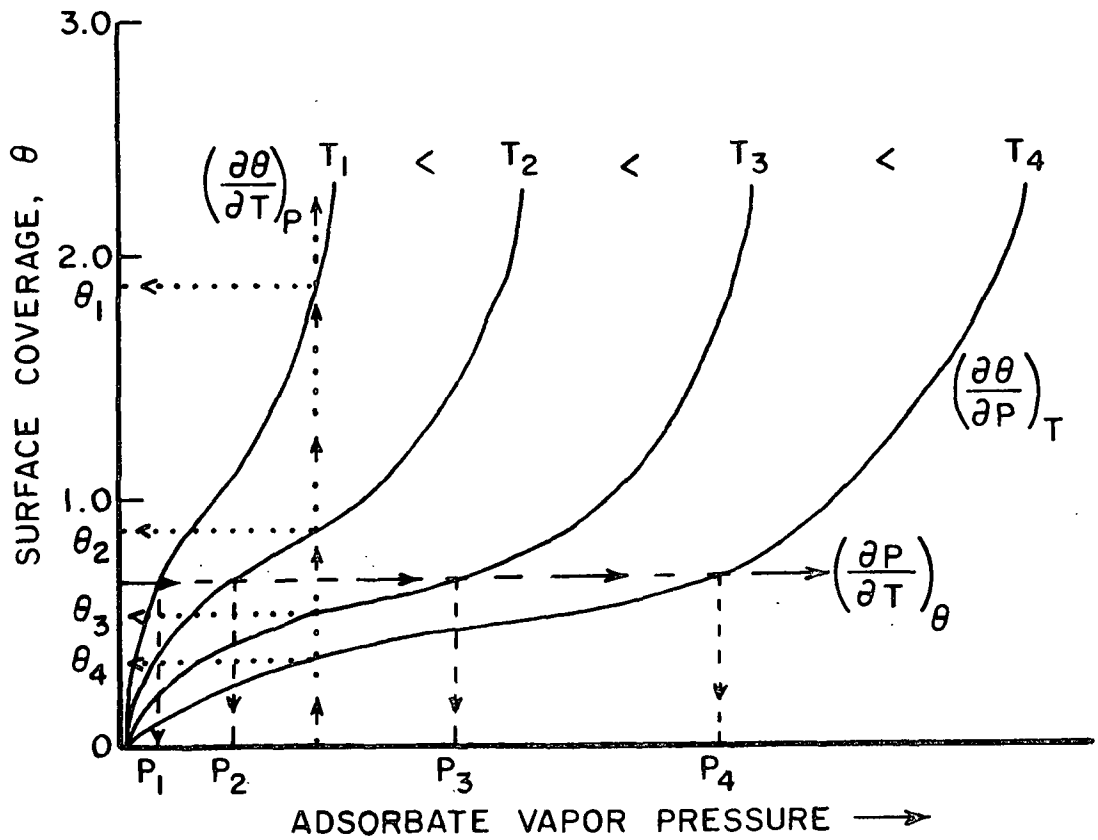

Figure 4. Adsorption Isotherms Used for Isobar and Isostere Calculations

Several adsorption isotherms, $(\partial\theta/\partial P)_T$, are determined experimentally and plotted on the same set of axes. The adsorption isobar, $(\partial\theta/\partial T)_P$, corresponds to a vertical (dotted) line drawn at some constant pressure. Values of θ corresponding to each temperature are read off the isotherms. In a similar manner the adsorption isostere, $(\partial P/\partial T)_\theta$, can be represented by a horizontal (dashed) line. Vapor pressure corresponding to each temperature are read off the isotherms. Adsorption isosteres will usually be determined for several values of θ, allowing investigation of the variation in heat of adsorption with surface coverage.

ANALYSIS OF ADSORPTION ISOTHERMS

The adsorption isotherm is nothing more than experimental data. Useful characterization of an adsorbent surface requires isotherm analysis. Figure 5 shows a typical BET Type II isotherm characteristic of multilayer physical adsorption. This type isotherm may be divided into three overlapping areas. At high adsorbate vapor pressures, adsorption is predominately due to capillary condensation of adsorbate. Analysis of this region by use of the Kelvin equation (30) can provide detailed information about the porous nature of the solid.

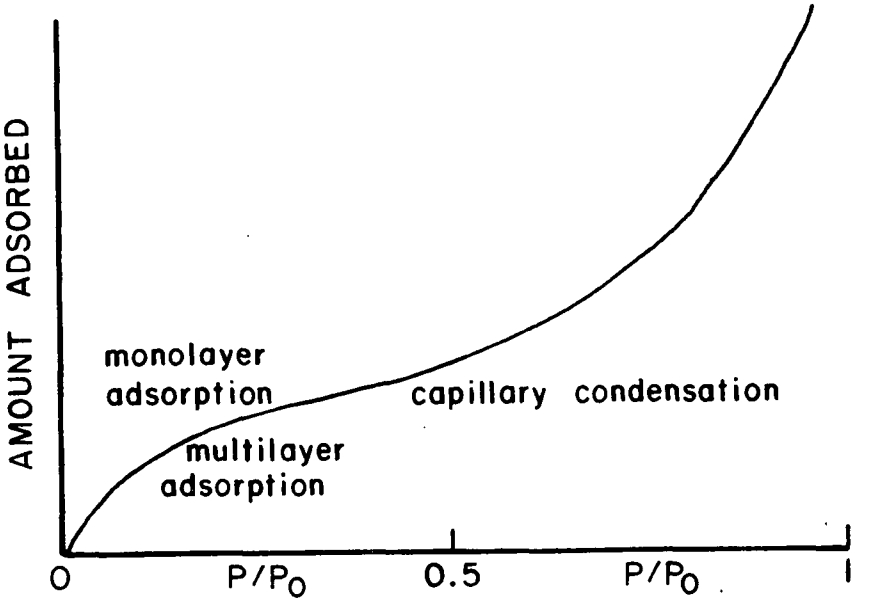

Figure 5. Typical BET Type II Adsorption Isotherm

For surface characterization other than porous structure, the monolayer region of the isotherm is of primary interest. After adsorption of several layers, the adsorbed phase becomes quite liquidlike and further multilayer adsorption will be governed mainly by adsorbate properties. Therefore, surface characteristics will influence adsorption primarily in the monolayer region. In this region the adsorption isotherm has a gently curving shape, concave or convex to the pressure axis.

Analysis of isotherms involves formulation of a mathematical model for the adsorption process. This model results in an equation for the adsorption isotherm. The equation contains several adjustable parameters. The analysis is valuable if these parameters can be related to physical characteristics of the surface. Experimental adsorption data are fitted to the isotherm equation. Early workers used graphical methods of fitting. Modern workers use computers for this task. Early models were relatively simple. Modern models can be as elaborate as computing facilities allow.

The smooth curve of the low pressure region of an adsorption isotherm can be easily fit to almost any equation having two or more adjustable parameters. Thus, a proposed model must do more than simply fit experimental data. A model to be used for isotherm analysis must be able to correctly predict temperature dependence of adsorption. In addition, correct behavior for heats of adsorption should be predicted. The parameters of the isotherm equation should have reasonable values and give good agreement with respective physical quantities that can be independently measured.

Analysis of adsorption isotherms has been the second basic limitation to the usefulness of gas adsorption. Most models fit experimental data but few fulfill all of the above criteria. Some model parameters are difficult to

relate to surface properties. Few model parameters have any relationship to papermaking properties.

MODELS OF HOMOGENEOUS ADSORBENT SURFACES

The Polanyi treatment (31) stands alone in that no isotherm equation is involved. The adsorbed phase is assumed to be similar to the atmosphere surrounding the earth. Treatment of experimental data results in a characteristic adsorption curve of a sorbate on a surface. This curve can be used to predict temperature dependence of adsorption. The Polanyi theory is generally applicable to mono- and multilayer adsorption on uniform or nonuniform surfaces. However, the extremely general nature of the theory which allows this general applicability also results in very little detailed information about the surface. Almost no detailed surface characterization is possible, although variations in heats of adsorption with surface coverage can be calculated.

Langmuir (32) modeled a uniform adsorbent surface with energetically equivalent adsorption sites. Lateral interactions between adsorbed molecules were ignored. Adsorption was restricted to a monolayer of localized, immobile film. Graphical treatment of adsorption data characterizes the surface with V_m, the amount of gas needed to produce monolayer coverage; and k, a general adsorbate-surface interaction constant. This model met with much initial success. However, it soon became apparent that temperature dependence was not well predicted for most systems, since Langmuir's model applies in general only to chemisorption.

Brunauer, et al. (33) extended Langmuir's model to multilayer adsorption. The same assumptions of surface uniformity and absence of lateral interactions of adsorbed molecules were made, but multilayer adsorption was allowed. Except

for the first adsorbed layer, heat of adsorption was assumed to be equal to heat of liquefaction for the adsorbate. Heat of adsorption for the first layer was assumed to be different from that of the other layers. Graphical treatment of experimental data yields V_m and c, a constant related to heat of adsorption of the first layer. This "BET" model is more generally applicable to gas adsorption than Langmuir's model. Temperature dependence is accurately predicted. However, consistent results are not produced when the theory is applied to low energy surfaces. In particular, V_m is dependent on the distribution of adsorptive site energies for a real, nonhomogeneous adsorbent.

MODELS OF HETEROGENEOUS ADSORBENT SURFACES

Real adsorbent surfaces are not uniform. Topographical variations such as edges, corners, ridges, fractures, cracks, and slip planes cover the surface. Each such area has a slightly different force field extending into space. Corners, for example, would be favorable places for gas adsorption, since two surfaces are available for interaction with a single adsorbate molecule. Unless the adsorbent is a highly purified element, such as a metal or carbon, chemical differences will exist at various locations on the surface. For cellulosic surfaces, carboxyl, carbonyl, and hydroxyl groups will provide high energy adsorption sites. Also for a natural product like cellulose, a very specific arrangement of surface molecules may be generated during biological production of the material. Subsequent processing may expose internal surfaces resulting in a mixture of surface types.

Thus, a realistic adsorption model should account for surface heterogeneity. DeBoer (11) demonstrates how monolayer adsorption on heterogeneous surfaces can produce experimental isotherms identical to the different types of multilayer isotherms discussed by Brunauer. In Brunauer's model the initial

knee of a Type II isotherm represents completion of monolayer coverage and onset of multilayer adsorption. DeBoer shows this knee can equally well be described by a series of adsorbate condensations occurring on areas of differing adsorption energy. Of course, in most real systems a combination of these two extremes must be functioning. For any real adsorbent, multilayer adsorption occurs at various sorbate vapor pressures on different adsorption sites.

Heterogeneous surfaces are treated as being composed of very small patches of different energies that adsorb independently of each other. Let $f(\varepsilon)$ be a function describing the distribution of adsorptive site energies on the surface. Let $\theta(\underline{P},\underline{T})$ be the experimentally observed isotherm, and $\theta(\varepsilon,\underline{p},\underline{T})$ be a function describing localized adsorption on a very small energetically homogeneous area of the overall heterogeneous adsorbent. The observed isotherm in the submonolayer region may be represented by:

$$\theta(P,T) = \int_0^\infty \theta(\varepsilon,p,T)\, f(\varepsilon)\, d\varepsilon \qquad (3)$$

This is a quite general equation and a great many solutions are possible. The applicability of a particular model will depend on the choice of $f(\varepsilon)$ and $\theta(\varepsilon,\underline{p},\underline{T})$.

Ross and Olivier (34) let $f(\varepsilon)$ be Gaussian and $\theta(\varepsilon,\underline{p},\underline{T})$ be the Hill-DeBoer equation, a two dimensional analog of the Van der Waals equation. This treats the adsorbed state as molecules with both size and lateral interactions which are mobile on the adsorbent surface. Model parameters are generated by graphical or computer fitting of experimental data to the adsorption model. The surface is characterized by $\underline{V}_\beta$, the monolayer coverage which is independent of site energy distribution; $\underline{U}'$, the mean adsorptive potential energy which is defined as the difference between the lowest energy states of vapor phase and adsorbed gas molecules; and γ, the heterogeneity parameter which determines the width of the adsorptive site energy distribution.

Barber (35) compared results of applying the Ross-Olivier (R.O.) and BET analysis techniques to adsorption isotherms of argon on cotton, oxidized cotton, rayon, and a variety of other substrates. Barber's work showed BET surface areas for cellulosic materials were in serious error, giving lower than geometric surface areas for rayon fibers. The R.O. analysis of the same data gave higher than geometric surface areas as was expected for a gas adsorption surface area determination. Barber found only slight differences in the R.O. parameters of $\underline{U}'$ and γ for different cellulosic surfaces. WAN dried cotton cellulose humidified to different levels gave identical results, showing the site energy distribution in this case was independent of available surface area. He concluded that the R.O. model was more applicable to low energy surfaces. The BET surface area apparently only represents that portion of the surface having an adsorption potential greater than the attraction of adsorbate molecules for each other.

Brown (36) extended the Ross-Olivier approach to multilayer adsorption. A more realistic log-normal distribution function was used. This eliminated the possibility of negative adsorption energy values and preserved the high energy tail found by Hoory (37) and others to be necessary if a distribution function is to accurately reflect adsorption on a highly heterogeneous surface. Up to five adsorbed layers were allowed on each small subpatch of the surface. Experimental data were fitted by a computer program. Argon, nitrogen, and $CFCl_3$ adsorption on alkali extracted, acid extracted, and untreated spruce holocellulose was studied utilizing a gravimetric adsorption apparatus. Argon and nitrogen isotherms fit the model quite well. The cellulosic surfaces were characterized by low, broad distributions of adsorptive site energies. Little difference was noted between various adsorbents. Trichlorofluoromethane isotherm analysis gave statistically meaningless parameters due to rapid multilayer buildup at very low surface coverages.

Modern models (38,39) for adsorption on heterogeneous surfaces do not assume any particular form for (ε). This is desirable if the true nature of the site energy distribution on the surface is to be investigated. Assumption of a particular form for (ε) usually assures generation of that form during analysis.

If gas adsorption is to become a useful technique for routine surface studies, a fast and straightforward analysis approach is necessary. This analysis must produce a useful surface characterization. In some cases, such as the work of Ross or Brown, a good deal of physical significance can be applied to model parameters resulting from analysis of adsorption on heterogeneous surfaces. However, in many cases, no attempt in this direction was made. The parameters are simply adjusted by computer until the best fit between model and experimental data is obtained. This "goodness of fit" is often cited as proof of applicability of the model. Adamson and Ling (40) sum up the situation quite nicely:

> "The results have excellent abilities for curve fitting as would any (multiparameter) equation since most isotherms are fairly regular in shape. There will in general exist other functions giving as good a fit and $\theta(P,T)$ has an indefinite number of solutions..... The usually smooth (energy) distribution function resulting should, therefore, be regarded merely as the physically most acceptable one of a large family of others."

INVERSE GAS ADSORPTION CHROMATOGRAPHY FOR SURFACE CHARACTERIZATION

Most investigations using inverse chromatography have applied classical approaches to isotherm analysis. Gray's group at the Pulp and Paper Research Institute of Canada has used inverse gas adsorption chromatography to study

cellulosic surfaces. Organic vapors of alcohols, ketones and alkanes were used as adsorbates. Adsorption isotherms were measured and analyzed by the BET technique (41). Several different sources of cellulose were utilized as adsorbents. Experimental data were also analyzed by the Polanyi treatment (42). Thermodynamic parameters were calculated by application of the Clausius-Clapeyron equation. Experimental data fit both the BET and Polanyi plots very well. The technique was also applied to humidified cellulose fibers (43,44). Humidified fibers would be impossible to study with vacuum techniques. Chromatographically this was quite easy to accomplish, requiring only humidification of the carrier gas.

Gray's application of inverse chromatography allows organic vapors to be conveniently used as adsorbates. In addition, experimental procedures are greatly simplified when compared to classical vacuum techniques. An isotherm can be determined in a few hours instead of several days or even weeks. However, Gray's work retains limitations imposed by isotherm analysis. Barber's work has clearly demonstrated the inapplicability of BET theory to cellulosic surfaces. The Polanyi treatment yields little detailed information.

A modern mathematical model might give a better surface characterization but would require detailed information about allowed energy and entropy levels of adsorbate molecules. All possible vibrational and rotational degrees of freedom must be considered. Changes in allowed molecular states during adsorption must be calculated. Organic adsorbates do not lend themselves to this type of analysis, since exact configurations of large adsorbed molecules are difficult if not impossible to determine.

A more convenient way to use inverse chromatography for surface characterization would be direct analysis of adsorbate retention behavior without calculation of adsorption isotherms. For a real, heterogeneous adsorbent,

surface distribution of adsorptive site energies governs interactions with adsorbates. This distribution may be calculated from a chromatographically measured isotherm by application of an adsorption model. However, this distribution also governs retention of adsorbate injections on adsorbent columns. Thus, in theory at least, calculation of the adsorptive site energy distribution should be possible directly from chromatographic retention data. The transport of an adsorbate injection along a column packed with adsorbent will be briefly considered before reviewing an approach involving a more direct use of gas chromatographic retention data for surface characterization.

An average adsorbate molecule experiences numerous adsorption-desorption cycles between injection and elution from an adsorbent column. The elution chromatogram represents the overall residence time distribution of injected adsorbate molecules. For a very small injection, effective adsorbate vapor pressure is so low that only the highest energy surface sites are favorable for adsorption. These sites allow adsorbate molecules to dissipate some of their kinetic energy. Molecules remain on the surface until this adsorption energy is regained by thermal agitation. The higher the site energy, the longer the surface residence time. Retention times of small injections are quite long.

A slightly larger injection causes higher effective adsorbate vapor pressure within the column. Adsorption on lower energy sites now occurs. Average surface residence time is decreased and initial retention time of the injection decreases. The chromatogram will be wider since a broader distribution of residence times results from adsorption on a greater range of site energies. Larger injections produce further decreases in retention time. Since higher energy sites are quickly covered, an average adsorbate molecule moves more rapidly along the column. The higher the vapor pressure, the more

adsorption sites are available. Initial retention time continues to decrease until a minimum value is reached. At this point adsorption of the first few layers is complete and the adsorbed state has become somewhat liquidlike in nature. Still larger injections cause bulk phenomena such as capillary condensation, but initial retention time remains at its minimum value. Adsorptive interactions always tend to maximize retention on an adsorbent column.

Rudzinski and coworkers (45-47) have developed a method for characterizing adsorbents directly from chromatographic data. The surface adsorptive site energy distribution is evaluated by graphical differentiation of initial retention volume plotted as a function of adsorbate vapor pressure. The adsorbate is assumed to be an ideal gas, both in the vapor and adsorbed phases. The condensation approximation of Hobson and Armstrong (48), Hobson (49,50), and Harris (51,52) is also applied. This approximation assumes condensation of adsorbate vapor on a very small homogeneous surface patch will occur at a specific adsorbate vapor pressure. The observed isotherm is a result of numerous very small, stepwise isotherms. Van Dongen (53) and Van Dongen and Broekhoff (54) point out that this approximation is correct only at 0°K. However, stepwise experimental isotherms reported by Dash (55) at 4°K, and by Davis and Pierce (56) at 200°K, and other workers (57) support application of the condensation approximation at higher temperatures. DeBoer (12) points out that this idea becomes more useful in describing adsorption as surface heterogeneity increases.

A plot of retention volume versus adsorbate vapor pressure is very closely related to the adsorption isotherm. Adamson has developed a method (40,58,59) for calculating adsorptive site energy distributions directly from experimental isotherms. The isotherm is used as the first approximation to the

integral site energy distribution. Repeated graphical integrations and recalculations of the isotherm are made until no change in the distribution occurs with further iteration. Both Van Dongen (53,54) and Morrison and Ross (60) point out that the condensation approximation is the unstated basis for Adamson's approach. Ross feels this approach is useful only for obtaining a rough, first-order approximation to the site energy distribution.

The Rudzinski approach is almost identical to Adamson's method, although derived entirely from considerations of chromatographic processes. The derivation presented by Rudzinski (Appendix II) is neither complete nor straightforward. Attempts to clarify and expand on this derivation have been made (61-63) but are only moderately successful. Rudzinski's site energy distributions are undoubtedly only rough, first-order approximations. They would be most applicable to very low coverages of mobile adsorbates on highly heterogeneous surfaces. Rudzinski makes no claims about the accuracy of his approach. Rather, he emphasizes the speed and simplicity of chromatographic measurements. He suggests this approach might be useful for quality control of adsorbent surfaces. Rudzinski used this approach to characterize silica gels (46,47) and diatomaceous earth (64).

APPROACH TO PROBLEM

Exacting, time consuming experimental techniques and uncertainties of isotherm analysis have combined to limit applications of gas adsorption for characterizing cellulose fiber surfaces. The work of Barber (35) and Brown (36) has shown that cellulosic surfaces are characterized by a low, broad distribution of adsorptive site energies with little difference between modified surfaces. Dietrich (65) found the cellulose surface electrostatic field to be quite low, indicating that surface hydroxyl groups are involved in a hydrogen bonded network with each other. Argon and nitrogen can interact with surfaces only through nonpolar and induced polar forces. Therefore, the hydrogen bonded surface network cannot be directly probed with these adsorbates. An adsorbate capable of interactions with the hydrogen bonded surface network would be expected to differentiate modified surfaces. Organic alcohols and ketones would be ideal for this purpose. To minimize penetration of organic adsorbates into dry cellulose surfaces, compounds consisting of more than four carbon atoms should be used (66). These slightly volatile compounds would be quite difficult to work with in a vacuum adsorption apparatus, but are easily used in gas chromatographic experiments.

Several workers have investigated interactions of organic liquids with cellulose. Thode and Guide (66) found a correlation between solubility parameters of organic liquids and their ability to swell cellulose. BET surface areas of water swollen, solvent-dried cellulose fibers were inversely proportional to cohesive energy density of the solvent. Cohesive energy density is defined as energy of vaporization divided by molar volume and provides a measure of attractive forces between solvent molecules. Robertson (67,68) investigated changes in tensile strengths and swelling of paper soaked in organic liquids.

Craver (69) used sonic velocity techniques to evaluate degree of interaction between organic liquids and cellulose. These studies all indicated that interactions between organic liquids and cellulose are governed by the cohesive energy density and hydrogen bonding ability of the liquid. This relation should also hold for adsorption of organic vapors, giving a tool for probing the hydrogen bonded cellulose surface by gas adsorption techniques.

However, for this tool to be of any value for routine characterization of cellulose fibers, a new approach for utilization of gas chromatographic adsorption data must be developed. Inverse gas chromatography provides a rapid, simple technique for gathering adsorption data. An equally rapid and simple analysis technique for using these data to evaluate surfaces is required. It may be inferred from Gray's work (42) that traditional analysis techniques applied to chromatographically measured isotherms do not give information particularly relevant to papermaking properties. Any new approach for utilization of chromatographic data should result in a surface characterization which can be directly related to properties important in papermaking.

Direct use of chromatographic data for surface characterization would be quite convenient. Analytical separation chromatography makes direct use of retention times and peak areas to characterize an injected mixture. Calibration curves for standard mixtures and/or internal standards are used to facilitate this operation. A similar approach should be possible for adsorbent surface characterization. Some instruments and procedures of this type have already been developed. The Rudzinski approach (47) calculates adsorbent site energy distributions directly from chromatographic data. Retention diagrams are quite useful for characterizing solid-state polymer glass transitions (28,29). The Institute Sorptometer (Appendix V) is one of a family of instruments allowing simple, rapid evaluations of adsorbent surface area (70,71).

All of these techniques make direct use of chromatographic data and characterize surfaces without calculation or analysis of adsorption isotherms. However, none of these characterizations is especially useful for describing the composition of fiber surfaces which may be related to papermaking properties.

Gas chromatographic retention data can be analyzed to give adsorption isotherms and adsorptive site energy distributions. Obviously, retention data are affected by the same factors influencing gas adsorption. These are: adsorbent surface area, adsorptive site energy distribution for the surface, nature of adsorbate-surface interactions, adsorbate vapor pressure and other adsorbate properties. Gas chromatographic retention times are also affected by the experimental operational variables of carrier gas flow rate, column length, and amount of adsorbent present. Specific retention volumes ($\underline{V_R}$), defined as product of retention time and carrier gas flow rate divided by adsorbent weight, would be expected to be fairly independent of operational variables. Retention volumes, therefore, should be quite valuable for characterizing surfaces.

The most common behavior exhibited by gas adsorption on a surface results in a BET Type II isotherm. For surface characterization, the low pressure region is of primary interest. In this region the surface influences adsorption to a maximum degree. This region corresponds to decreasing retention volume for a series of small injections of increasing size, as was shown in Fig. 2. A very small injection is strongly affected by adsorbate-surface interactions. However, adsorbate properties are also important. As injection size increases, retention volume decreases until a minimum, constant value is reached. This minimum retention volume should be affected primarily by adsorbate properties including saturation vapor pressure, adsorbate-adsorbate lateral interactions, and heat of vaporization. Therefore, the surface adsorption index (SAI), defined as maximum retention volume minus minimum retention

volume should be characteristic of adsorbate-surface interactions. Figure 6 demonstrates this approach. Distance III represents retention of a barely detectable injection. Distance I is the minimum retention of the adsorbate. Distance II is the SAI. SAI values should be independent of operational variables and quite dependent on surface characteristics.

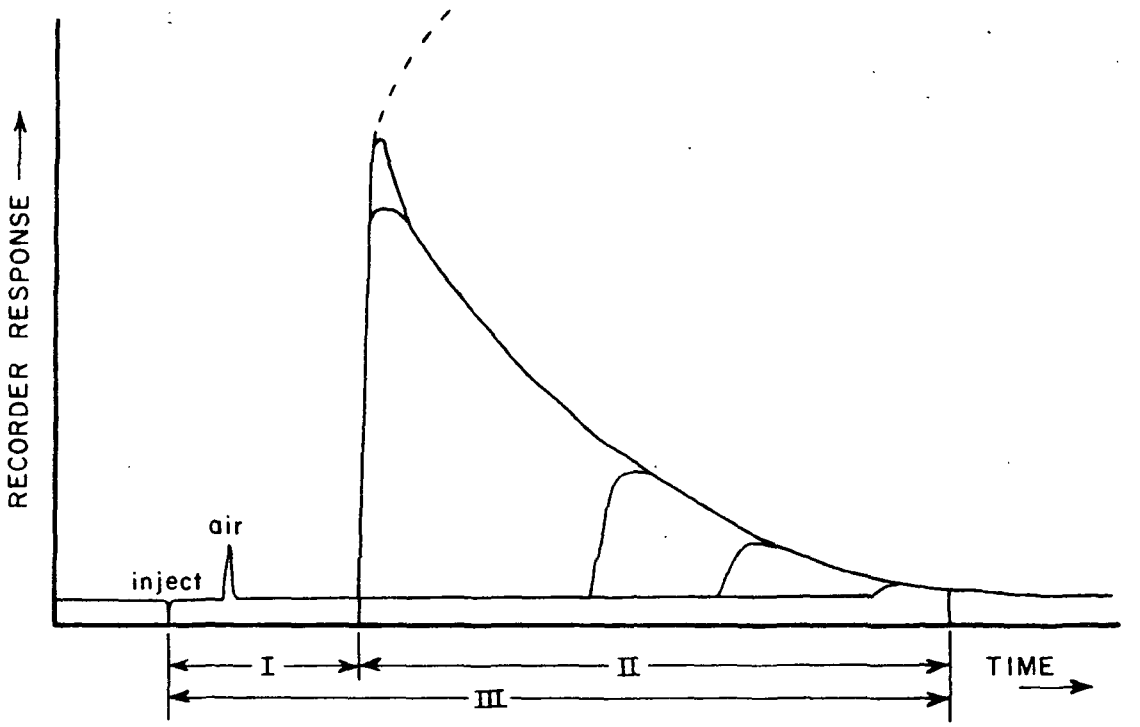

Figure 6. Superimposed Chromatograms for Low Pressure Region of BET Type II Adsorption Isotherm

The area between the composite chromatogram trailing edge and the air peak yields, upon analysis, the concave portion of a BET Type II isotherm, up to the "knee." The rectangular area between the minimum retention time and the air peak represents a linearly increasing amount of adsorption with adsorbate vapor pressure. Isotherm curvature is represented by the area between the minimum retention time and the composite trailing edge. The shape of this area (isotherm curvature) is affected by many factors including:

1. Monolayer completion
2. Onset, and perhaps completion, of multilayer adsorption
3. Surface heterogeneity, i.e., the adsorptive site energy distribution
4. Lateral interactions between adsorbed molecules
5. Equation of state for adsorbed molecules
6. Mobility of adsorbed molecules
7. Microporous nature of the adsorbent surface

Although some workers (72) identify minimum retention time as marking completion of the first adsorbed layer, the location of this point is controlled by all the above factors. SAI values are also influenced by these factors.

At any given adsorbate vapor pressure, a certain amount of adsorption will occur. If the adsorption isotherm were linear, this amount could be calculated from Henry's Law. However, for a gas-solid system exhibiting a BET Type II isotherm, Henry's Law behavior will not be followed. For gas-solid systems following BET Type II behavior, amount adsorbed in the low pressure region will be greater than the amount calculated by Henry's Law. This excess adsorption is due to the specific nature of the sorbate-surface interactions. Since retention volumes are directly proportional to amount adsorbed, the SAI value for an adsorbate is proportional to the amount adsorbed at a given vapor

pressure in excess of the amount which would have been adsorbed at that vapor pressure if the isotherm were linear.

Of course, SAI values will decrease with increasing adsorbate vapor pressure at constant temperature. Therefore, comparison of different surfaces should be done at equal adsorbate vapor pressures. Comparison between SAI values of different adsorbates on the same surface should also be done at equal adsorbate vapor pressures. SAI values would be quite easy to calculate from chromatographic data. Interpretation must be done relative to a standard surface. For instance, SAI values might be used to evaluate the amount of lignin on fiber surfaces. An adsorbate preferentially adsorbed by lignin would be used. SAI values greater than standard surface values would show more surface lignin than on standard fibers. Quantitative interpretations could result if a series of standard surfaces of known properties were available, allowing determination of a calibration curve.

The surface adsorption index approach appears to be a useful means of characterizing adsorbent surfaces by direct use of chromatographic retention volumes. This characterization should be as useful as more traditional methods of detailed adsorption isotherm analysis. The SAI approach matches the ease and simplicity of experimental techniques of inverse gas adsorption chromatography. The hypothesized usefulness of the SAI approach for surface characterization is the subject of this thesis.

The experimental program was designed to investigate the general behavior of surface adsorption indices and to compare SAI characterization with traditional isotherm analysis. First, the experimental conditions necessary to optimize SAI characterization of the surface were considered. SAI dependence

on chromatographic operational variables and adsorbent physical characteristics was investigated. Next, a series of cotton cellulose fibers was prepared which exhibited a well characterized variation in chemical composition of the fiber surfaces. This series of fibers was characterized by the SAI approach and also by several isotherm analysis techniques. The SAI approach proved to be quite useful for relative surface characterization. In many respects, the SAI characterization was more informative about the chemical composition of fiber surfaces than were the results of adsorption isotherm analysis.

GENERAL EXPERIMENTAL EQUIPMENT AND PROCEDURES

ADSORPTION CHROMATOGRAPH

An experimental chromatograph especially designed for adsorption studies on cellulose was constructed. Parts from several different analytical instruments not currently in use were combined during construction. Figure 7 is a schematic diagram of this instrument. A 30 x 18-inch cylindrical Pyrex jar served as the column oven (10). This large size facilitated construction of chromatography columns (9) from glass tubing. Temperature was regulated to ±0.1°C by a mercury thermal sensing element connected through a Precision Scientific electronic relay to three 500-watt heater knives (not shown). In operation only one heater was usually used to maintain temperature. A 10 ft by 1/4-inch copper cooling coil (not shown) was located at the bottom of the bath. A Little Giant Model SN-1A pump provided water circulation. Bath temperature was monitored with a 24-inch 2 to 55°C mercury in glass thermometer. It was possible to use any temperature between 10 and 75°C if desired.

Helium carrier gas was used. A capillary flow restrictor (1) allowed an easily set tank pressure of 25 psig to result in a flow rate of approximately 50 mL/min against atmospheric pressure. Nupro flow controllers (4) provided fine adjustment of carrier and reference gas flows. Approximate flow rates were monitored with spherical float rotameters (5). Exact flow rates were measured with a 25 mL soap bubble flowmeter attached to the proper vent port (18). A flow rate of 30 mL/min was used for most work. An injection port (6) from a Wilkens Aerograph 1520B chromatograph was used. This provided on column injection. The port was heated with a cartridge type heater. Temperature was monitored with a 6-inch 0 to 220°C mercury in glass thermometer. A temperature of 130°C provided instant vaporization of injected adsorbates. By proper

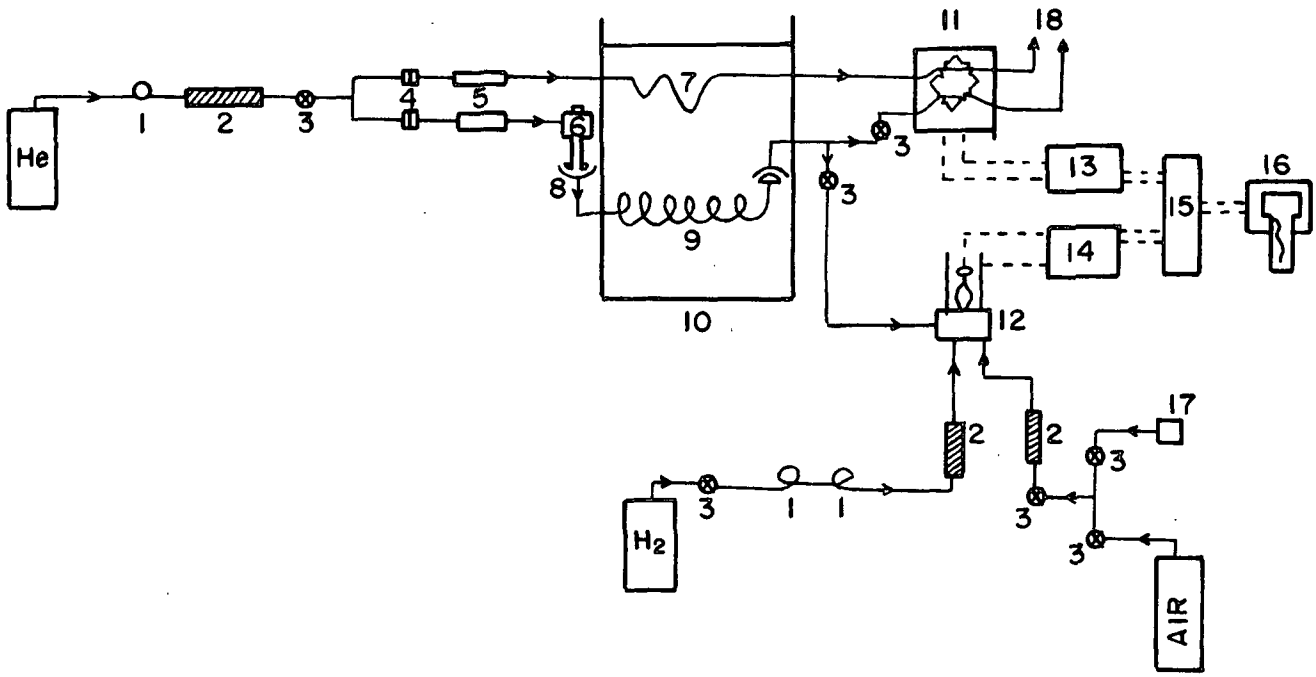

1. Capillary flow restrictors
2. Molecular sieve filters
3. On/off valves
4. Nupro flow controllers
5. Rotameter flowmeters
6. Injection port
7. Reference gas flow line
8. Ball and socket joints
9. Glass chromatographic column
10. Water bath
11. Thermal conductivity detector
12. Flame ionization detector
13. Thermal conductivity power supply/bridge
14. Dual differential electrometer
15. Power/output control panel
16. Strip chart recorder
17. Air pump
18. Vent ports

Figure 7. Schematic Diagram of Adsorption Chromatograph

positioning of shut off valves (3), adsorbate concentration could be monitored by either a thermal conductivity detector (11) or a flame ionization detector (12).

The thermal conductivity detector (11) and power supply/bridge circuit from a Wilkens Aerograph 1520B chromatograph were used to monitor large injections of highly volatile adsorbates. A detector oven was constructed from a large Glas Col heating mantle. Temperature was monitored with a 0 to 250°C Weston bimetallic thermometer imbedded in the detector block. A minimum of 24 hours after startup was required to stabilize detector temperature. A temperature of 160°C was normally used. The thermal conductivity detector responds to all adsorbate gases. Adsorbates which do not "burn," such as CO_2 or Cl_2, will not be detected by a flame ionization detector. However, thermal conductivity detectors are not as sensitive as flame ionization detectors. Also, the response of a thermal conductivity detector is quite nonlinear, while a flame ionization detector is linear in response over a wide range of adsorbate concentration.

The flame ionization detector block assembly from a Wilkens Aerograph Hy-Fy chromatograph was monitored with a Varian Aerograph Dual/Differential Electrometer of the most modern solid-state design. Hydrogen was provided from a cylinder. Air was supplied from an air pump (17) or a cylinder if extreme detector sensitivity was desired. All gases were filtered through 4 A molecular sieve filters (2) constructed from 1/2-inch stainless steel tubing. The flame ionization detector could not be used if adsorbate vapor pressure was above 20 mm Hg. Higher vapor pressures overloaded the electrometer. The detector block was housed in a transite oven and heated with a 100 watt cartridge heater. Temperature was monitored with a -10 to 200°C mercury in glass thermometer. A temperature of 130°C was normally used. All gas

flow lines from the water bath to detectors were wrapped in heating tape to prevent adsorbate condensation. Heating tape temperature was monitored by a 0 to 150°C Taylor bimetallic thermometer. Tapes were heated to 100°C. Temperatures of detectors, injection port, and heating tapes were controlled with separate variable voltage transformers.

The main power/output panel of a 1520B chromatograph provided power to the desired detector electronics. Output was recorded on an Esterline Angus Model E-1101-S, 10-inch strip chart recorder. This recorder allowed selection of 15 chart speeds from 8 inches/sec to 0.5 inch/hour. Chart spans of 1 mv to 100 v were provided. Normally, a 1 mv span was used with chart speeds of 1, 2, or 4 inches/minute.

ADSORBENTS

Stoneville 2B cotton fibers were selected as the adsorbent. Sommers (10) gives a complete description of this material. Cotton fibers contain no lignin or hemicellulose. Carboxyl and carbonyl content should be minimal. Therefore a very nearly pure cellulose surface was available for investigation.

PREPARATION OF ADSORBENTS

Raw cotton was sorted with tweezers to remove entangled debris. Approximately 10 g were sorted for each adsorbent batch. Average fiber length was shortened to about 5 mm by several passages through a paper cutter. This was necessary to facilitate packing of the fibers into chromatography columns. The sorted, chopped cotton was extracted for 24 hours with chloroform in a large Soxhlet extractor. This was followed by extraction for 24 hours with 95% ethanol. These two extractions removed any natural waxes from the fibers. Pectins were removed by boiling the extracted cotton 4 hours in 1% (w/w) caustic in a nitrogen atmosphere. After rinsing with distilled water the alkali treatment was repeated. Caustic treatment was done in a nitrogen atmosphere

to minimize alkali degradation of the cellulose. The treated cotton was rinsed in distilled water. Any residual caustic was neutralized by rinsing with 1% acetic acid. Rinsings with 500 mL quantities of distilled water were repeated until pH 7 was indicated with pH paper. The purified cotton was stored under distilled water until needed.

Initially it was thought desirable to have a slightly expanded surface to maximize adsorbate retention. Accordingly, after rinsing, the cotton fibers were solvent exchanged from water to methanol. A second solvent exchange to pentane was followed by drying at 80°C in a vacuum oven. Two cycles of humidification at 50% RH and drying at 105°C removed any entrapped pentane. WAN dried material was stored in an empty Drierite jar. No special precautions were taken during this "batch" WAN drying. Methanol and pentane were not dried. Solvent exchange was accomplished by rinsing, suspending and draining the fibers in open air. The resultant fibers were only slightly expanded. WAN drying was also carried out by passing water, methanol and pentane through a packed chromatography column which produced a more expanded surface unsuitable for inverse chromatography. In the region corresponding to capillary condensation, chromatograms would not give overlapping leading edges when superimposed. Apparently, complete equilibrium between the moving adsorbate injection and the expanded surface was not possible because of the highly porous nature of the fibers. Batch WAN dried and water-dried fibers did not give this problem.

Two 10 g amounts of batch WAN dried and two 10 g quantities of water-dried fibers were prepared. Water-dried fibers were prepared by removing bulk water on a 200 mm Buchner funnel, pressing between paper towels and drying 12 hours at 105°C. Water-dried fibers were also stored in empty Drierite jars.

Adsorbent surface areas were measured with the Institute Sorptometer by comparison with standard Whatman No. 1 filter paper assigned a surface area 1 m^2/g. Table II shows surface areas for raw cotton and purified cotton. Increase in surface area after extraction of waxes and pectins is probably due to increased surface roughness. Apparently waxes and pectins "fill in" about 0.2 m^2/g of surface area. Sorptometer precision was ±0.09 m^2/g regardless of adsorbent surface area.

TABLE II

ADSORBENT SURFACE AREAS

Material	Surface Area, m^2/g
Raw cotton	0.52
Extracted cotton	
Water dried	0.73
WAN dried	2.98

ADSORBENT GAS CHROMATOGRAPHY COLUMNS

Chromatographic columns were constructed from Pyrex glass tubing 6 mm, 7 mm, or 8 mm OD. Column lengths ranged from 4 ft to 16 ft. Most columns were constructed from a single length of 7 mm tubing bent into a "U" shape. Initially, columns were packed with gentle vacuum induced air flow of a few hundred milliliters per minute. About half a gram of adsorbent fibers were placed in a Waring Blendor. A quick pulse of 2-3 sec resulted in a heavy population of fibers stuck to the blendor walls and lid by static electricity. These were sucked off with a glass tube attached to one end of the column through a ball and socket joint. Fibers were held in the column by a length of glass rod which partially blocked the column exit. Fiber packing density was controlled by occasionally blocking and quickly releasing the air flow via

a finger placed over the end of the glass suction tube. The resulting "air hammer" effect can be easily controlled to pack fibers to any desired density. A 4 ft column could be packed with from 0.5 to 1.5 g of fibers by this technique.

Pyrex glass was chosen for column construction to allow monitoring of the column packing process. Void spaces within the column were easily eliminated. Columns longer than 10 ft could not be packed by vacuum flow from end to end. For longer columns a 2 inch Pyrex tee was constructed half-way along the column. The vacuum was drawn from this point and the column packed from both ends. After packing and weighing, the side arm was packed with Pyrex wool and sealed. Columns were weighed to the nearest 0.01 g before and after filling. After final weighing a small plug of Pyrex wool was placed in each end of the column. This protected the packing material from carrier gas heated by the injection port. Without this plug, the first inch of column packing rapidly discolored. Columns were attached to the chromatograph through 13 mm ball and socket joints secured with Manostat 12/30 ring couplings. Water bath level was maintained 1 cm below these joints. Heating tape began 1/2 cm above the joints. Aluminum foil was wrapped around the joints to eliminate any "cold spots." When not in use, ends of the columns were sealed with inverted serum bottle caps.

The Waring Blendor/suction packing technique resulted in the lighter, smaller fraction of the fibers being sucked into the column. Sorptometer measurements on residue fibers left in the blendor after packing gave a surface area of 1.33 m^2/g compared to 2.98 m^2/g for WAN dried fibers before packing began. Apparently this technique selectively packed columns with high surface area components. Indeed, BET analysis of adsorption isotherms for these WAN dried fibers gave a surface area of 3.78 m^2/g. Samples of adsorbent before packing, residue fibers after packing, and fibers removed from a column

were examined by scanning electron microscopy. Microphotographs at 100X and 300X showed no gross differences between the fibers. All fibers were somewhat twisted. Fibers removed from the packed column were more twisted than others. These microphotographs are on file at The Institute of Paper Chemistry, assigned Negative No. 2462-67.

All 4 ft columns were packed by a combination of vacuum packing and manual techniques. A 2 ft length of rod was inserted in one end of the column. Vacuum flow was used to pack the bend in the "U." Then the arms of the U-shaped column were packed by manipulating bunches of fibers with tweezers and a long glass rod. In this manner preferential fractionation of adsorbent fibers was minimized. A 4 ft column could be packed with slightly over 1.5 g of fibers in about an hour by this technique.

Packed columns should offer minimum resistance to carrier gas flow for elution chromatographic data to agree closely with equilibrium adsorption isotherms (23). Packed columns were checked for flow resistance as follows. An empty column of similar dimensions was attached to the chromatograph. Carrier gas flow was adjusted to 30 mL/min. The packed column was substituted for the empty column without changing carrier gas pressure or flow controller setting. Flow rate was checked again with a soap bubble flow meter. A typical 4 ft column of 7 mm OD tubing packed with 1.2 g reduced the flow to 29 mL/min. A 16 ft column of 6 mm OD tubing packed with 1.7 g reduced the flow to 26 mL/min. Four foot by 7 mm columns were used for most work. This assured both minimal resistance to flow and an entirely representative adsorbent sample.

ADSORBATES

PREPARATION OF ADSORBATES

Various reagent grade or better organic compounds were used as adsorbates. Each liquid was further purified by passage through a 4 ft x 1/2 inch column

of charcoal granules freshly activated by heating overnight at 450°C. Purified adsorbates were stored in 4 mL screw top glass vials sealed with Teflon-lined septums and Reacti-Vial lids. Half of each vial was filled with a mixture of charcoal granules and 4 A molecular sieve material. This served to absorb any water or oxidation products which might contaminate the adsorbate. The Reacti-Vial lid and septum allowed adsorbate sampling by syringe without exposure to atmospheric moisture.

SELECTION OF ADSORBATES

Adsorbate properties, especially vapor pressure, will have a strong influence on gas chromatographic retention behavior. Therefore, adsorbates should be selected to maximize surface effects on retention. Let:

$\underline{N}$ = amount adsorbate injected

$\underline{N}_{ads}$ = amount adsorbate in adsorbed phase

$\underline{N}_{gas}$ = amount adsorbate in gas phase

At any given time after injection, before elution begins,

$$\underline{N} = \underline{N}_{ads} + \underline{N}_{gas} \text{ must hold.}$$

The adsorbent packed into the column has a certain fixed surface area. For this surface to have a maximum effect on retention, $\underline{N}_{ads} > \underline{N}_{gas}$ is required. Cellulosic adsorbents used in this study do not have very large surface areas. If adsorbate saturation vapor pressure is high, $\underline{N}_{gas}$ will be high. This means $\underline{N}_{gas} > \underline{N}_{ads}$ and the surface would have little effect on retention volumes. If $\underline{N}_{gas} > \underline{N}_{ads}$ for two or more adsorbates, the surface will be ineffectual in differentiating between retention volumes. For instance, n-heptane, 2-butanone, and ethyl acetate would be expected to interact differently with cellulose. However, at 40°C, these compounds all have vapor pressures in excess of 100 mm Hg.

Retention volumes on a column packed with cotton cellulose were nearly identical and quite close to the retention volume of nonadsorbed air.

Retention volumes for 1 μL injections of several organic compounds with a wide range of saturation vapor pressures were measured on a column packed with WAN dried fibers at 50°C. Compounds with saturation vapor pressures above 100 mm Hg at 50°C had very small retention volumes. Between 10 and 100 mm saturation vapor pressure, retention volumes were inversely proportional to vapor pressure. Several compounds with saturation vapor pressures close to 10 mm Hg showed wide differences in retention volumes. These differences were closely related to the nature of the adsorbate. Alcohols had large retention volumes, alkanes small, ketones intermediate. This relationship was true only for compounds with low saturation adsorbate vapor pressures, showing the importance of the $\underline{N}_{ads}/\underline{N}_{gas}$ ratio.

Obviously, experimental conditions should be chosen to insure $\underline{N}_{ads}/\underline{N}_{gas}$ is maximized. This could be accomplished by adjusting temperature. An easier approach is to choose adsorbates which have low and nearly equal saturation vapor pressures in the experimental temperature range. A low saturation vapor pressure also insures minimal effects of column pressure changes during adsorption. Table III shows temperatures at which several compounds have vapor pressures of 10 mm Hg according to the Handbook of Chemistry and Physics, 47th edition. Any of these compounds would have saturation vapor pressures below 10 mm in the 30-55°C temperature range. Adsorbates from this table will show maximum effects of interaction with cellulosic surfaces. Several of these compounds, marked by an asterisk in Table III, were used as adsorbates on a column packed with cotton cellulose. n-Decane and n-hexanol were chosen as adsorbates for further work since they exhibited the largest range of retention behavior while maintaining BET Type II behavior. This pair of

materials would be expected to interact quite differently with cellulose. Hexanol should be capable of interacting with the hydrogen bonded network of hydroxyl groups on the surface. Decane can interact only through generally nonpolar type forces.

TABLE III

TEMPERATURES AT WHICH SOME ORGANIC COMPOUNDS HAVE SATURATION VAPOR PRESSURES OF 10 mm Hg

Compound	10 Mm Vaporator Pressure Temperature, °C
n-Decane[a]	55.7
1-Hexanol[a]	58.2
Diacetone alcohol[a]	58.8
Butyric acid	61.5
Methacrylic acid	60.0
2-Octanone[a]	60.9
Benzaldehyde[a]	62.0
α-Chlorotoluene[a]	60.8
Ethanethlonitrile	61.6
sec-Butyl glycolate	66.0
Cyclohexanol[a]	56.0
Benzenthiol	56.0
2-Chlorophenol	51.2
1,2-Dibromopentane	58.0
1,2-Dichlorobenzene[a]	59.1
Indene	58.5
1,4-Diethylbenzene	60.3
Diisoamyl ether[a]	57.0

[a]Compounds investigated as possible adsorbates.

INJECTION OF ADSORBATES

Adsorbates were injected with Hamilton standard 10 µL and 1 µL gas chromatography syringes. Injection sizes below 0.1 µL were not very reproducible. Although many techniques of syringe handling were tried, hexanol injection sizes could not be reproduced within ±25%. Decane reproducibility was much better, about ±5% for a 0.01 µL injection. This is apparently due to wetting differences in the metal capillary tip of the 1 µL syringe. Mixtures of decane and hexanol in n-hexane were investigated. Hexane is quite volatile and elutes rapidly. However, use of these mixtures was discontinued in order to avoid complications arising from adsorption of mixtures.

Before work was begun with a new adsorbate, the syringe was cleaned by withdrawing and discarding 10 syringe-fulls of acetone from a vial. Acetone was removed from the syringe by use of a syringe cleaner constructed from an injection port of a Wilkens Aerograph Model 1520B chromatograph. The port was heated to 180°C by a self-contained cartridge heater. The carrier gas input line was sealed and a vacuum drawn on the column connection of the port. The syringe needle pierced the injection port septum. The combination of high temperature and low pressure insured complete vaporization and removal of acetone. The procedure was especially effective for the 1 µL syringe where the entire volume is contained in the needle.

For determination of surface adsorption indices, small (0.05 µL) and large (2 µL) injections were made. For measurement of an isotherm, a series of about 10 injections in the 0.1 to 5 µL size range was made. Each injection point was marked on the chart with a spike caused by a momentary short circuit of the electrometer. A nonadsorbed gas was injected to measure column dead space and calculate gas hold-up time. Air was used for this purpose with the thermal conductivity detector. Methane (natural gas) was used with the flame

ionization detector. Individual chromatograms were superimposed by tracing on a light box.

INVESTIGATION OF FUNDAMENTAL PROPERTIES OF SURFACE ADSORPTION INDICES

Table IV demonstrates the usefulness of gas chromatographic retention data for characterizing adsorbate-surface interactions. BET parameters were calculated from chromatographically measured isotherms. These three adsorbates would be expected to interact differently with a cellulosic surface. However, BET surface areas only show a differentiation for diacetone alcohol. This difference is probably due to dimerization of diacetone alcohol molecules on the surface, resulting in two molecules covering less than two molecular areas as calculated from the liquid density. BET "c" values indicate only that decane interacts to a lesser degree than the alcohols.

TABLE IV

BET MODEL PARAMETERS COMPARED WITH GAS CHROMATOGRAPHIC RETENTION TIME FOR THREE ADSORBATES ON WAN DRIED COTTON FIBERS AT 58°C

Adsorbate	BET Surface Area, m^2/g	BET "c" Value	Retention Time of 0.5 µL Injection, min
n-Decane	3.82	3.8	5.4
Diacetone alcohol	2.54	14.6	8.0
n-Hexanol	3.74	14.8	11.6

Gas chromatographic retention times do differentiate between the three adsorbates. In spite of having two possible points for interaction with the network of hydrogen bonds on a cellulosic surface, diacetone alcohol interacts to a lesser degree than hexanol. Intramolecular hydrogen bonding may lessen

the ability of vapor phase diacetone alcohol molecules to interact with cellulose, or vapor phase diacetone alcohol dimers may exist. Gas chromatographic retention times are in agreement with the work of Robertson (67) which also ranks diacetone alcohol intermediate between primary alcohols and alkanes in ability to interact with cellulose.

Unlike retention time, SAI's will be independent of chromatographic variables. SAI's should be directly dependent on amount of adsorbent material. Column length, packing density, and carrier gas flow rate should have no effect on SAI values. SAI values will depend on adsorbent specific surface areas. However, determination of adsorbent surface areas will not always be convenient. Furthermore, in order to be directly dependent on specific surface area, the adsorptive site energy distributions for organic adsorbates on the surface must be quite similar to the distribution of the adsorbate (usually nitrogen) used to measure surface area. Therefore, the most useful surface characterization would be SAI/g values. No simple temperature dependence for SAI values would be expected, since different combinations of thermal factors influence transport of large and small injections along a column in different ways.

EXPERIMENTAL PROCEDURES

ADSORBENTS

WAN dried and water-dried cotton fibers were studied. Chromatographic columns from 122 to 488 cm long were packed with fibers. Bulk density ranged from 1.8×10^{-2} g/cm^3 to 5.3×10^{-2} g/cm^3. Flow rates of 20 mL and 30 mL/min were used. Adsorbent surface areas were measured with the Institute Sorptometer using nitrogen at 76°K as adsorbate and Whatman No. 1 filter paper for a standard surface.

SURFACE ADSORPTION INDEX MEASUREMENT PROCEDURES

The surface adsorption index is defined as the difference between maximum retention volume and minimum retention volume for an adsorbate on a particular surface. Minimum retention volume, $\underline{V}_{R_{min}}$, was quite easy to measure since this is a constant value for large injections. A constant retention volume for injections in the 1 to 5 μL range indicated that $\underline{V}_{R_{min}}$ had been reached. The shape of a chromatogram of an injection larger than necessary to yield $\underline{V}_{R_{min}}$ displays a diffuse leading edge concave to the time axis. A constant plateau level ends in an abrupt vertical drop. Thus, a single large injection producing a chromatogram with this characteristic shape will yield $\underline{V}_{R_{min}}$.

Maximum retention volume, $\underline{V}_{R_{min}}$, will depend upon adsorbate vapor pressure. To assure maximum adsorbent surface effects on $\underline{V}_{R_{min}}$, a very low adsorbate vapor pressure was selected. At $\underline{P}/\underline{P}_o \sim 0.001$, adsorption will be in the 0.01 monolayer region. Selecting adsorbates with low saturation vapor pressure values ($\underline{P}_o$) such as decane and hexanol also helps to insure maximum surface effect on SAI as was discussed earlier. Equation (1), p. 14, can be used to calculate detector response height ($\underline{h}$) corresponding to the desired adsorbate vapor pressure. However this requires determination of detector sensitivity, and a series of exactly sized, very small injections is difficult to make.

Based on an estimated surface area of 39 A^2 covered by one n-hexanol molecule, a 0.05 μL injection would cover 1 g of WAN dried cotton ($\sim$3 m^2) with 0.02 of a monolayer. An injection of this size at 45°C on a 488 x 0.4 cm column filled with 1.45 g of WAN dried cotton gave a peak about 1-inch high measured with the flame ionization detector at a range of 10^{-10}, sensitivity 16. Refer now to Fig. 8a and 8b. A hexanol peak height of 1/2 inch was picked as the $\underline{V}_{R_{min}}$ peak height for hexanol. To determine the corresponding peak height for

decane, 1 μL injections of decane and hexanol were made at decreased detector sensitivity. Peak areas, as measured with a Technicon integrator, resulted in a decane to hexanol sensitivity ratio of 1:1.7. Therefore, a decane peak height of 0.5 x 1.7 = 0.85 inch will correspond to the desired decane vapor pressure.

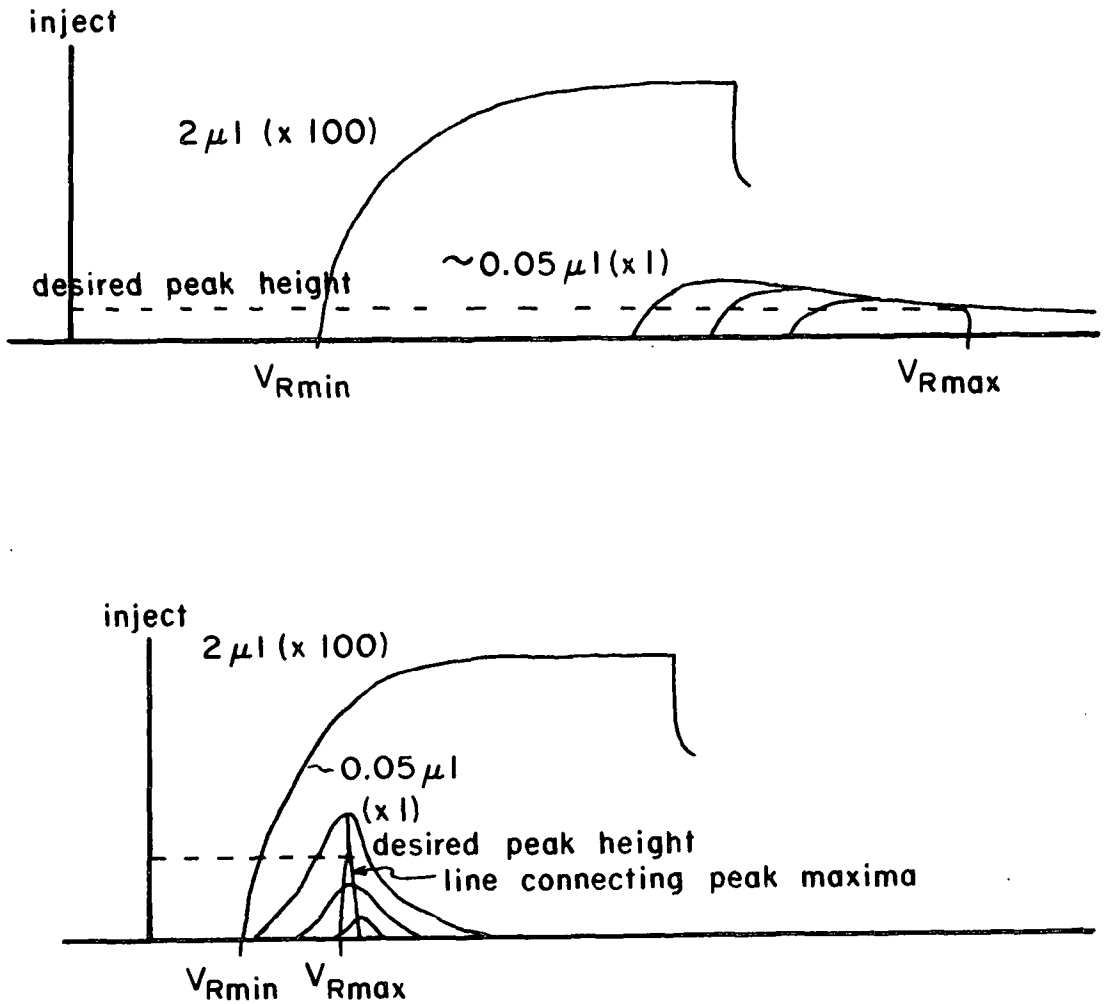

Figure 8. a) Retention Volume Measurements for Strongly Adsorbed Hexanol

b) Retention Volume Measurements for Weakly Adsorbed Decane

Small, slightly different sized injections of hexanol exhibit overlapping trailing edges. Thus, $\underline{V}_{R_{max}}$ can simply be measured at the desired peak height (1/2 inch) from the trailing edge of a suitably sized injection, as shown in Fig. 8a. Slightly different sized small injections of decane do not have overlapping trailing edges. To measure $\underline{V}_{R_{max}}$ for decane, peak maxima for two or more chromatograms very close to the desired peak height are connected by a straight line, as is shown in Fig. 8b. At the desired peak height (0.85 inch) along this line, a vertical line is dropped to the time axis. $\underline{V}_{R_{max}}$ is measured at this point on the time axis.

A single 0.05 μL injection of n-hexanol was sufficient to determine $\underline{V}_{R_{max}}$. However, at least three injections in the range of 0.03 to 0.08 μL were required to measure $\underline{V}_{R_{max}}$ for n-decane. $\underline{V}_{R_{min}}$ was determined from a single 2 μL injection of each adsorbate. Electrometer sensitivity was decreased to allow recording the entire peak of the larger injection.

Adsorbent material, column length, and temperature all affected the choice of chart speed. Hexanol retention data were measured at 0.5, 1 or 2 inches/min. Decane retention data were measured at 1, 2, or 4 inches/min. Chart speed was adjusted to produce a chromatogram 18 to 24 inches long. This length was convenient to handle, reproduce, and store. Retention distances were measured to the nearest millimeter, and converted to retention time using the appropriate chart speed. Retention volumes were calculated by multiplying retention time by carrier gas flow rate. Carrier gas flow rate was adjusted to 30 μL/min as measured at about 25°C and 740 mm Hg with a soap bubble flow meter.

EXPERIMENTAL RESULTS AND DISCUSSION

EFFECTS OF ADSORBENT MASS AND COLUMN DIMENSIONS ON SAI VALUES

Table V shows the effects of column dimensions and amount of adsorbent on SAI values. Results for Columns I and II show expected behavior. SAI values are independent of column length and packing density, and are directly proportional to amount of adsorbent. Both hexanol and decane exhibit the same behavior. Neither $V_{R_{max}}$ nor $V_{R_{min}}$ values alone will show these relationships.

TABLE V

EFFECTS OF COLUMN DIMENSION AND ADSORBENT MASS ON SAI VALUES FOR WAN DRIED COTTON FIBERS AT 45°C (Flow Rate 30 mL/min)

Column Description	Adsorbate	$V_{R_{min}}$, mL	$V_{R_{max}}$, mL	SAI, mL	SAI/g, mL
Col I	Hexanol	246	1500	1254	995
122 cm x 5 mm 1.26 g	Decane	150	309	159	126
Col II	Hexanol	263	1142	879	999
244 cm x 5 mm 0.88 g	Decane	171	282	111	126
Col IV	Hexanol	234	984	750	510(995)
488 cm x 4 mm 1.47 g	Decane	108	203	95	65(127)

Results for Column IV, however, indicate that column radius has an influence on SAI value. Calculations showed that in this case SAI values were directly proportional to the cube of column radius. Cube dependence may only be fortuitous, but a wall effect on retention is definitely indicated. Values in parentheses result from multiplication by $(2.5/2)^3$ which corrects for the smaller radius of Column IV. This correction gives SAI/g values

identical to those for Columns I and II. More experimental work should be done to further investigate effects of column radius on retention.

Fortunately, column diameter is relatively easy to control. Except for Column IV, all columns were constructed of 7 mm OD Pyrex tubing with an inside diameter of 5 mm.

EFFECT OF CARRIER GAS FLOW RATES ON SAI VALUES

If instantaneous equilibrium is reached between adsorbate molecules and adsorbent surfaces in the chromatography column, changing carrier gas flow rates should have no effect on retention volumes. Therefore, SAI values should be independent of carrier gas flow rate. Table VI shows the effect of carrier gas flow rate on hexanol and decane retention. These data indicate that carrier gas flow rates do not affect SAI values. Lack of agreement in Table VI is probably due to errors in measurement of flow rates and retention times since retention volumes of air at 30 and 20 mL/min agreed only to within ±6%.

TABLE VI

EFFECT OF CARRIER GAS FLOW RATE ON SAI VALUE FOR COLUMN IV

Adsorbate	Temp., °C	Flow Rate, mL/min	$\overline{V_R}_{min}$, mL	$\overline{V_R}_{max}$, mL	SAI, mL	SAI/g, mL/g
n-Hexanol	40	30	351	1350	999	680
		20	354	1350	996	678
n-Hexanol	50	30	228	717	489	333
		20	232	744	512	348
n-Decane	50	30	147	218	71	49
		20	147	229	82	55

Also, at slower flow rates an injection has more time to spread out due to diffusion. Since smaller injections would be affected more by diffusion because of their increased retention volumes, some increase in SAI values at slower flow rates is not too surprising.

EFFECT OF ADSORBENT SURFACE AREA ON SAI VALUES

SAI values should be directly proportional to adsorbent surface areas, assuming that a good method for estimating adsorbent surface areas is available. Three different reference adsorbents were compared: WAN dried fibers, water-dried fibers, and water-dried fibers which were then extracted with benzene, dried, rewetted with water and dried at 80°C in a vacuum oven. The last adsorbent served as a standard surface for stearic acid treated, water repellent fibers. Preparation of this reference adsorbent reproduces treatment made on water-repellent fibers. This procedure will be discussed at length later. Sorptometer surface areas were measured with nitrogen at 76°K. Table VII shows the results of surface adsorption index measurements on these three surfaces.

These results indicate that nitrogen, decane, and hexanol adsorption sites are distributed evenly over the cellulose fiber surfaces. Furthermore, on drying, these sites must all be reduced in number by equal relative amounts. If, on drying, hydrogen bonding sites were preferentially lost, SAI/m^2 values for hexanol would be different for WAN and water-dried fibers. The results for Column 5 reflect difficulties involved in measuring surface areas. Since sorptometer precision is ± 0.09 m^2/g, a good deal of uncertainty is present in the surface areas for Columns 4 and 5. SAI/m^2 values are probably not too valuable for characterizing adsorbents with specific surface areas less than 1 m^2/g. Some strongly held water molecules may also have been on the fiber surfaces of Column 5 since a lower temperature was used to dry these fibers.

TABLE VII

EFFECT OF ADSORBENT SURFACE AREA ON SAI VALUES AT 45°C

Column Number and Description	Adsorbate	SAI	SAI/g Adsorbent	SAI/m^2 Adsorbent Surface Area
Col. 1 — 1.26 g Ads. II — 298 m^2/g WAN dried, rehumidified, dried at 105°C	Hexanol	1254	995	334
	Decane	89	71	24
Col. 4 — 1.23 g Ads. III — 0.73 m^2/g water dried at 105°C	Hexanol	314	255	349
	Decane	23	19	26
Col. 5 — 1.23 g Ads. III — 0.83 m^2/g benzene extracted water dried at 80°C and 24 in. Hg vac.	Hexanol	387	315	380
	Decane	34	28	33

EFFECT OF TEMPERATURE ON SAI VALUES

The two retention volumes which are used to calculate SAI values actually represent two different types of temperature dependence. $\underline{V}_{R_{max}}$, measured at a constant peak height with changing temperature, is the adsorption isobar, $(\partial\theta/\partial\underline{T})_{\underline{P}}$. $\underline{V}_{R_{min}}$ temperature dependence can be related by the Clausius-Clapeyron equation to heat of adsorption in the vicinity of monolayer coverage. Thus, SAI values have no simple temperature dependence. Adsorption isobars usually exhibit an exponential decrease in amount adsorbed with increasing temperature. The Clausius-Clapeyron equation predicts exponential vapor pressure behavior as a function of reciprocal absolute temperature. Therefore, surface adsorption indices might be expected to display some type of exponential temperature dependence. However, no significance can be placed on SAI temperature dependence.

SAI values in the 40 to 50°C range were measured for hexanol and decane on Column IV. Hexanol values were more strongly temperature dependent than decane values, reflecting the stronger interactions of hexanol with cellulose. However, temperature dependence was not linear, nor was it logarithmic, and it did not fit the Clausius-Clapeyron equation. The SAI value is proportional to adsorption in excess of that for a linear isotherm (see discussion p. 30-32). Therefore SAI temperature dependence will be affected not only by heat of adsorption factors but also by increasing isotherm linearity with temperature. Heat of adsorption involves molecular level interactions while isotherm linearity is the macroscopic manifestation of a variety of effects.

COMPARISON OF SAI CHARACTERIZATION WITH ADSORPTION ISOTHERM ANALYSIS FOR A SERIES OF MODIFIED SURFACES

The previous section has shown that surface adsorption indices seem to be quite characteristic of adsorbent-surface interactions. Values are independent of gas chromatographic operational variables. To further test the usefulness of the SAI concept, a series of surfaces differing in a known manner was investigated. Ideally, these surfaces should be identical except for one well characterized difference. This difference should produce a dramatic change in adsorbate behavior.

Ferris (73) and Swanson (74) studied in detail interactions between stearic acid vapors and cellulosic surfaces. They identified three distinct states of adsorbed stearic acid on cellulose films: physically adsorbed on the surface; physically adsorbed in the porous surface structure; and chemically bonded by esterification with surface hydroxyl groups. They hypothesized that vapor phase stearic acid molecules dimerize upon adsorption. A very low monomer population is present due to dimer-monomer equilibrium. These monomers are capable of esterifying surface hydroxyl groups. The physisorbed dimers and chemisorbed monomers change the surface from a hydrophilic network of hydrogen bonded hydroxyl groups to a hydrophobic hydrocarbonlike surface.

Treatment of cotton fibers with stearic acid vapor was chosen as the method for preparation of a series of cellulose surfaces differing only by a single well characterized property, namely, coverage of fiber surfaces by stearic acid. No change in fiber morphology or bulk cellulose chemistry would be expected from this treatment. Modification of dry fibers is possible, eliminating the need for swelling and redrying of fibers. Cellulose degradation would not be a factor.

EXPERIMENTAL EQUIPMENT AND PROCEDURES

SURFACE MODIFICATION AND ANALYSIS

Treatment with Stearic Acid Vapors

An empty 1 lb Drierite jar served as the treatment chamber. One gram of stearic acid, tagged with 0.031 μCi/mg C-14, was coated onto the walls of the jar. See Appendix III for details of the preparation, dilution, and counting of the tagged stearic acid. Walls were coated by heating the horizontal jar until the acid melted (68°C). By rotating the jar while cooling, an even coating of solid stearic acid can be deposited on the walls. A sheet of 1 mm thick Teflon was perforated with 6 mm holes and rolled into a cylinder 5.5 cm x 15 cm. Fibers to be treated were placed inside the cylinder which was then centered in the acid coated jar. In this way fibers were prevented from coming into direct contact with the acid. A Teflon liner for the jar lid prevented reaction of stearic acid with the metal lid.

A Thelco drying oven allowed treatment at elevated temperatures. The jar was maintained in a horizontal position in the oven. A synchronous motor (Cramer Controls Corp. Type 117) located outside the oven was connected to the jar lid by a shaft through a hole in the side of the oven. This provided rotation at 2 rpm about an axis 2 cm off the jar's centerline. Rotation is necessary to prevent stagnation of heavy stearic acid vapors and insure uniform treatment of the fibers. A temperature of 90°C was used for treatment. At this temperature stearic acid melts and forms a pool which wets the jar wall during rotation.

To prevent condensation of vapors on cooler fiber surfaces, the entire oven/jar apparatus must be heated and cooled as a unit. Two gram batches of purified, water-dried cotton fibers were treated for various lengths of time.

After cooling, 0.1 g samples were removed for analysis. Treated fibers were stored in 4-oz screw capped jars until needed.

Surface Analysis

Water repellency of treated fibers was evaluated by placing a small (~0.01 g) bunch on water with a pair of tweezers. Water repellent fibers floated indefinitely, nonwater repellent fibers sank within one or two seconds. Surface areas of treated fibers were measured with the Institute Sorptometer.

Physically adsorbed stearic acid on the surface is extractable with boiling benzene. Stearic acid physically adsorbed in the porous surface structure is extractable only by a swelling solvent. Water at 25°C extracts this physically adsorbed acid but is incapable of breaking chemical bonds at such a low temperature. Chemically adsorbed acid can be extracted only by reaction with hydroxide ions.

Ferris and Swanson analyzed cellulose film surfaces by counting directly with a Geiger counter the adsorbed C-14 tagged material. Stearic acid was extracted by dipping small pieces of treated film into the proper solvent. After drying, the film was counted. Amount of each stearic acid species was calculated as the amount of activity removed by the corresponding solvent. Fiber surfaces cannot be counted directly with a Geiger counter. Therefore, after extraction, solvents were concentrated to 0.5 mL. Extracted stearic acid was counted directly with a liquid scintillation counter using a dioxane/napthalene counting cocktail. Samples of approximately 0.1 g were extracted in turn with 200 mL boiling benzene, 200 mL water at 25°C, and 30 mL boiling 0.01M KOH in methanol. Duplicate extractions with each solvent showed that one extraction removed all of each adsorbed acid species. See Appendix IV for complete details and data for this analysis.

This analytical technique is far from ideal. The main complication arises from an apparent reaction between stearic acid and the counting cocktail. This reaction caused the quenching constant and resultant count to change for the first 12 hours after mixing. The basic methanol extract was most troublesome in this respect. After 12 hours, a yellow color became apparent and quenching constants were quite low. All samples, therefore, were counted as soon as possible after concentration and immediately after cocktail was added. Triplicate samples of pure stearic acid agreed within ±6%. Duplicate samples of treated fibers agreed within ±5% for benzene and water extractions and ±8% for caustic extraction.

SELECTION AND PREPARATION OF SURFACES

Surfaces Modified by Chemisorption

Ferris and Swanson found water repellency was due entirely to chemisorption of stearic acid. Stearic acid adsorbs with the carboxyl group oriented toward the cellulose surface and the hydrocarbon tail extending into space. If these molecules are not chemically bonded to the surface, water is capable of "overturning" them by the mechanism first postulated by Yiannos (75). Chemically bonded stearic acid molecules would not desorb into the carrier gas. Therefore, it was initially planned to prepare a series of surfaces modified with chemically bonded stearic acid. All physically adsorbed acid can be removed after vapor phase treatment by extraction with boiling benzene and room temperature water.

Accordingly, untreated control fibers were extracted 4 hours with benzene in a small Soxhlet extractor, dried, soaked 1 hr at 25°C in 1 liter water, and dried at 80°C in a vacuum oven. Another sample of fibers was treated with stearic acid vapors for 130 hr at 90°C. These fibers were also extracted with benzene, room temperature water and dried at 80°C in a vacuum oven. Analysis showed these water repellent fibers had a stearic acid coverage of 0.28 POML.

A planar oriented monolayer (POML) refers to coverage based on orientation of stearic acid molecules. The surface area covered by one POML molecule is equivalent to the cross-sectional area of the extended stearic acid chain, 20 A^2. Ferris and Swanson showed that water repellency developed with as little as 0.10 POML of chemisorbed stearic acid. Apparently, the long hydrocarbon tails of firmly anchored chemisorbed stearic acid molecules vibrate and oscillate around, effectively shielding large areas of the surface from liquid water.

Surface adsorption indices for decane and hexanol on these two surfaces were measured. Hexanol values decreased from 298 mL/g for control fibers to 227 mL/g for water repellent fibers. For decane the values were 24 mL/g and 19 mL/g, respectively. Obviously, gaseous adsorbate molecules are not greatly affected by the cones of coverage swept out by stearic acid tails which can shield the surface from liquid water. A coverage of 0.28 POML chemisorbed acid is close to the maximum possible chemisorption reported. Therefore, a series of these surfaces would not produce the desired wide range of adsorbate behavior.

Surfaces Modified by Physisorption

Fibers modified only with physisorbed acid were easily prepared. Fibers treated for 24 hours at 90°C showed 0.75 POML stearic acid coverage. Only 0.03 POML chemisorption had occurred. Exposure times longer than 24 hours resulted in increased chemisorption. However, physically adsorbed acid on the surface and in the surface structure remained nearly constant at about 0.50 and 0.25 POML, respectively. Therefore, a formal coverage of 0.75 POML must indicate full coverage of the fibers with physisorbed stearic acid. Percent physisorbed stearic acid surface coverage was calculated using 0.75 POML = 100% coverage. Either the surface area of the fibers is lower than 0.70 m^2/g or one physisorbed acid molecule shields more than 20 A^2 of the surface.

Surface adsorption indices for hexanol and decane on 0.75 POML stearic acid covered fibers were nearly identical, 8 mL/g and 5 mL/g, respectively. This indicates that to gaseous adsorbate molecules fiber surfaces now appear hydrocarbonlike. The specific hydrogen bonding interactions between hexanol and the cellulose surface have been effectively eliminated. By exposing fibers for various times less than 24 hours, a series of surfaces differing only in stearic acid coverage was prepared. Modifying fibers by physisorption of stearic acid had the advantage of eliminating extraction and redrying of the treated fibers. At room temperature dissociation and chemisorption of physisorbed stearic acid dimers with surface hydroxyl groups is a very slow process, requiring many months. Surfaces were packed into columns and analyzed within two months of treatment.

Table VIII shows the series of surfaces prepared in this manner. For each surface, stearic acid adsorption is first listed as total acid adsorbed. This total adsorption is broken down into adsorption of each surface species. The uppermost number represents acid adsorbed on the surface which is extractable with boiling benzene. The middle number represents acid adsorbed in the porous structure of the fibers which is extractable by room temperature water. The lower number is the chemisorbed acid extractable only by saponification with boiling basic methanol. Surface analysis data for adsorbed stearic acid are presented in Appendix IV. Sorptometer data are contained in Appendix V.

Stearic acid is a liquid on the fiber surfaces at 90°C. Adsorption from the gaseous phase may occur preferentially in the porous surface or the molten acid may migrate across the surface, concentrating in the porous structure. Whatever the explanation, the porous structure is filled with stearic acid before adsorption on the surface is completed. Sorptometer surface areas show

TABLE VIII

COTTON FIBER SURFACES MODIFIED WITH STEARIC ACID VAPORS AT 90°C

Column Number	Hours Exposure	Total Acid Adsorbed, POML	Coverage, %	Stearic Acid Surface Species, POML	Sorptometer Surface Area, m^2/g
4	Untreated control		0	Water dried fibers	0.70
14	2.5	0.13	17	0.07 0.06	0.59
11	5	0.29	39	0.18 0.11 0.005	0.57
12	13	0.39	52	0.22 0.15 0.02	0.56
13	18	0.51	68	0.27 0.22 0.02	0.52
15	19	0.61	81	0.35 0.23 0.03	0.53
8	24	0.75	100	0.50 0.23 0.02	0.54
7	144	1.03	--	0.53 0.29 0.21	0.54
3	Unpurified raw cotton fibers				0.52
6	130	Water repellent fibers extracted with water and benzene		0.28	0.60

a decrease in surface area as stearic acid is adsorbed. This porous structure probably corresponds to surface roughness features for water-dried cotton fibers. After this surface is filled with 0.22 POML of stearic acid, surface area remains at a minimum of about 0.53 m^2/g. This value is for all practical purposes identical to the 0.52 m^2/g surface area of raw cotton fibers. Purification of raw cotton removes waxes and pectins, opening up the surface slightly. Adsorbed stearic acid fills in these surface features. The greatest decrease in surface area occurs first as the numerous very small porous features are filled. Larger pores fill later and require more stearic acid but contribute little to the total porous area. The water repellent fibers of Column 6 which were extracted with benzene and water to remove all physisorbed acid have a surface area of 0.60 m^2/g. This indicates that chemisorption occurs both on the surface and in surface features to the same degree.

Sorptometer surface area decreases by 0.16 m^2/g from 0.70 m^2/g for untreated fibers to 0.54 m^2/g for fibers completely covered with stearic acid. Table VIII shows that this decrease corresponds to adsorption of 0.23 POML/g of stearic acid filling the surface features. The area of 0.23 POML stearic acid is, interestingly enough, 0.16 m^2. This is probably only a coincidence, but may indicate that the average depth of these surface features is approximately the same as the length of a stearic acid chain, 25 A.

These modified fibers were packed into 122 x 0.5 cm Pyrex columns identified with an aluminum tag numbered as shown in Table VIII. This series of surfaces was analyzed both by the SAI approach and isotherm analysis procedures.

SURFACE ADSORPTION INDEX (SAI) CHARACTERIZATION

SAI values for n-hexanol and n-decane at 45°C were measured on Columns 11-15, 4 and 8. SAI's were determined by techniques already described. $V_{R_{max}}$ values

were measured at $P/P_o \sim 0.01$. Carrier gas flow rate was 30 mL/min. Retention volumes for Column 8 (0.75 POML) were also measured at flow rates of 20 mL/min. This work showed no serious problems due to absorption of n-hexanol or n-decane into the stearic acid surface phase. Slight absorption of n-decane was indicated by increased retention volumes at 20 mL/min, but this was not large enough to be troublesome.

ISOTHERM ANALYSIS TECHNIQUES

Chromatographic data suitable for calculation of adsorption isotherms were gathered for n-hexanol and n-decane at 5°C intervals from 35 to 55°C. Desorption of physisorbed stearic acid was not a problem even at 55°C. Detector base line increased slightly, but this was detectable only at detector sensitivities 100 times greater than those used for SAI measurements.

Hexanol behavior was studied on eight surfaces; the seven surfaces modified with physisorbed stearic acid and water repellent fibers modified with chemisorbed stearic acid. SAI values shown in Table IX, p. 75, indicated that decane behavior changed only slightly for the series of seven surfaces modified with physisorbed stearic acid. Therefore, decane isotherms were analyzed only on untreated control fibers (Column 4), 100% stearic acid covered fibers (Column 8), and 52% stearic acid covered fibers (Column 12). Thus, a total of 55 adsorption isotherms were experimentally measured. For each isotherm, carrier gas flow rate was checked and set to 30 mL/min before beginning to gather data.

From seven to ten chromatograms were determined for each isotherm. These chromatograms were superimposed by tracing on a light box. To calculate the adsorption isotherm from chromatograms, the common boundary for the superimposed chromatograms must be drawn, as shown in Fig. 9b. BET Type II isotherms are

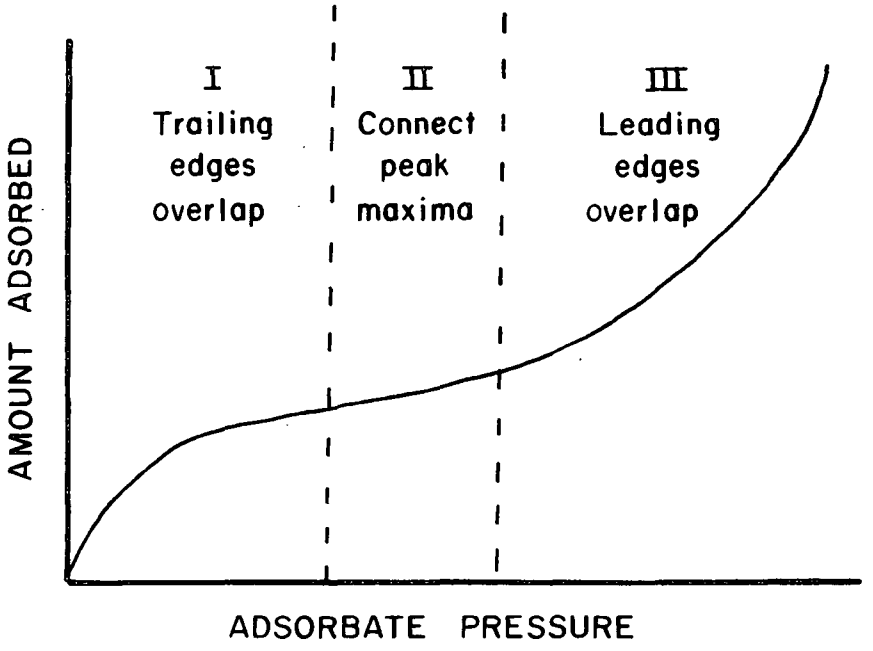

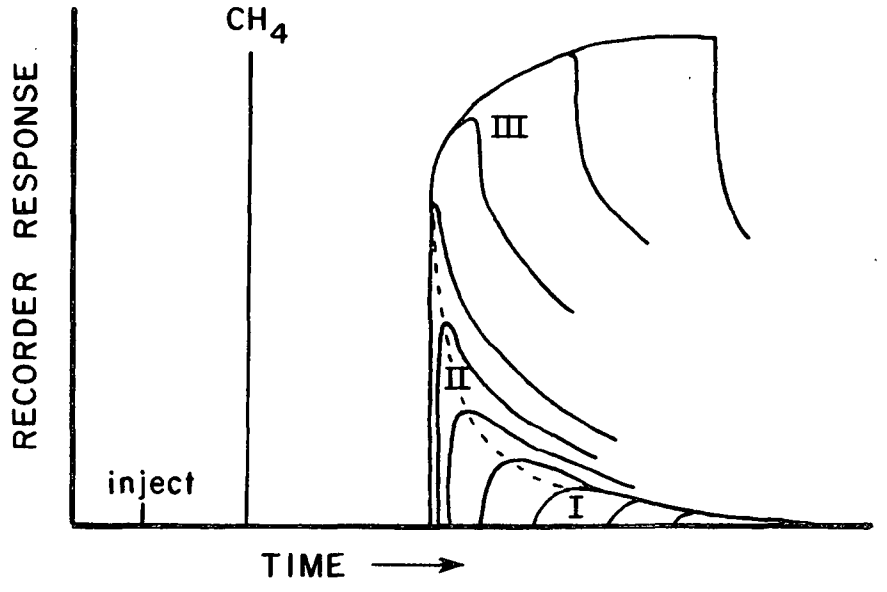

Figure 9a. Regions of a Sigmoidal, BET Type II Isotherm

Figure 9b. Chromatogram Common Boundary for BET Type II Isotherm

concave and convex to the pressure axis, as shown in Fig. 9a. Thus, chromatograms of small injections have overlapping trailing edges while large injections have overlapping leading edges. Between these two extremes is a transition region. This region corresponds to chromatograms with neither coinciding leading nor trailing edges. Here the chromatogram common boundary is determined by connecting peak maxima. Figure 9b shows chromatogram common boundary regions corresponding to BET Type II isotherms.

The chromatogram common boundaries were reduced photographically to a size suitable for digitization on the Institute's microcomparator. Each boundary was digitized at ∿150 points, punching four data points to a card. Programs were written for an IBM 360 computer to calculate and analyze adsorption isotherms by three different approaches. The Clausius-Clapeyron equation was applied to adsorption isosteres calculated from the five different temperature isotherms to determine thermodynamic adsorption parameters. Computer output was in the form of tables and graphs showing variations in heat, entropy, and Gibb's free energy of adsorption with surface coverage. Experimental data cover a range from $\theta = 0$ to $\theta = 2$. A rough estimate of the distribution of adsorptive site energies on the surface was calculated from the 45°C adsorption data by computer application of the Rudzinski approach [see p. 26 and References (45-47)]. Data at 35°C were also analyzed by calculating spreading pressure as a function of surface coverage. This gave an idea of the lateral mobility of adsorbed molecules on the surface. Derivation of spreading pressure from an adsorption isotherm is presented at a later point. Computer programs for adsorption data analysis are contained in Appendix VI, A-C.

Detector sensitivity was calculated for each isotherm by measuring chart areas of 0.1-0.4 μL injections. Measurements were made with a Technicon curve tracing integrator. Detector sensitivity was found to be constant (within

one standard deviation) 90% of the time. Detector air flow of at least 350 mL/min was necessary to accomplish this. Mean detector sensitivity was used to calculate isotherms unless the measured sensitivity varied more than one standard deviation from the mean value. In these cases the individual measured value for detector sensitivity was used. Detector sensitivity data and calculations are shown in Appendix VII.

EXPERIMENTAL RESULTS AND DISCUSSION

CHARACTERIZATION BY SURFACE ADSORPTION INDICES

Figure 10 shows retention volume data for decane and hexanol on physisorbed stearic acid modified surfaces. It might be supposed that surface adsorption indices are no more informative than retention volumes. Changes in adsorbate behavior are readily apparent in Fig. 10. However, column idiosyncrasies are evident. Note, for example, that all retention volumes for Column 15 (0.61 POML) are higher than expected. Column 11 (0.29 POML) also shows slightly higher than expected retention volumes for hexanol. $\underline{V}_{R_{min}}$ values for hexanol and decane are strongly influenced by the adsorbate heat of vaporization. Thus, hexanol ($\Delta\underline{h}_{vap}$ = 13.4 Kcal/mole) had a larger $\underline{V}_{R_{min}}$ than decane ($\Delta\underline{h}_{vap}$ = 11.4 Kcal/mole). Changes in fiber surface properties could not be very well illustrated if retention volumes instead of SAI values were compared.

Since SAI values are calculated as the difference of two retention volumes, column idiosyncrasies are eliminated. Figure 11 shows SAI values plotted as a function of POML stearic acid coverage for the series of physisorbed modified fibers. On untreated fibers there is a large difference between hexanol and decane SAI values. On 100% stearic acid covered fibers, hexanol and decane behaviors are nearly identical. Decane SAI values decrease linearly in proportion to stearic acid surface coverage. Hexanol SAI values also decrease with

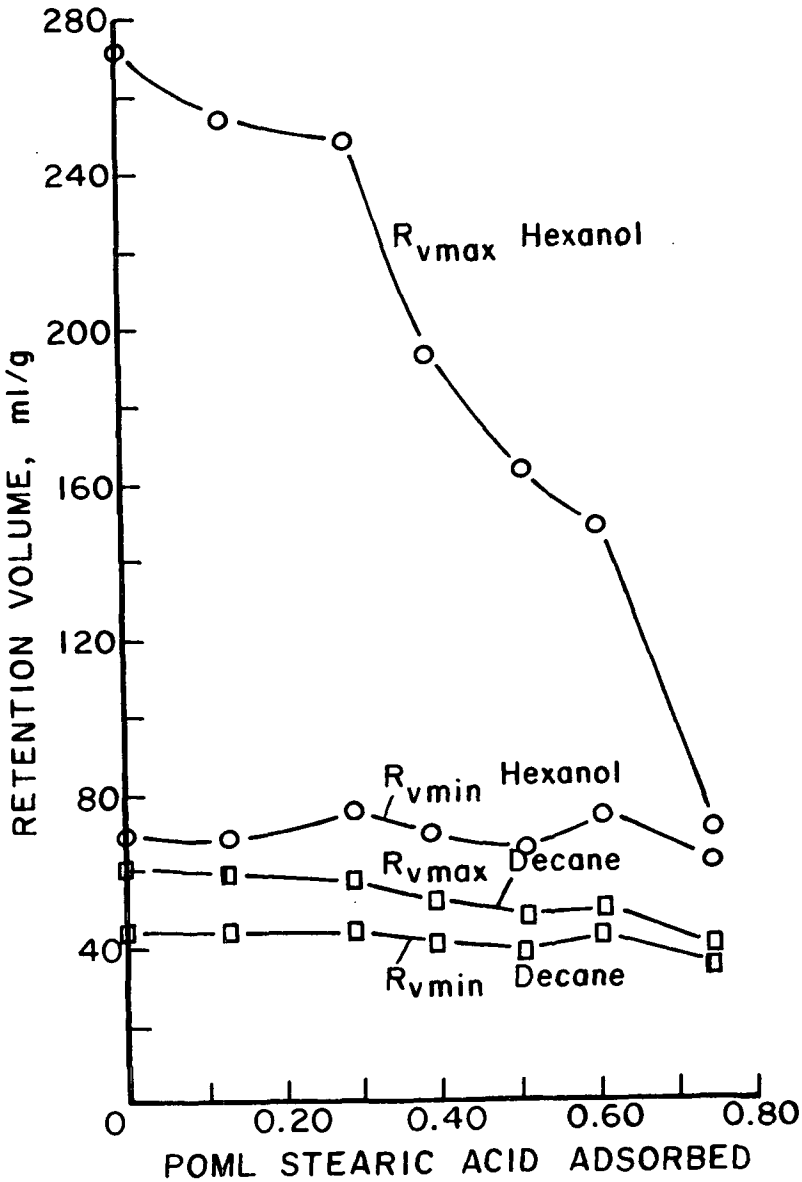

Figure 10. Retention Volumes for Decane and Hexanol on Stearic Acid Modified Fibers at 45°C

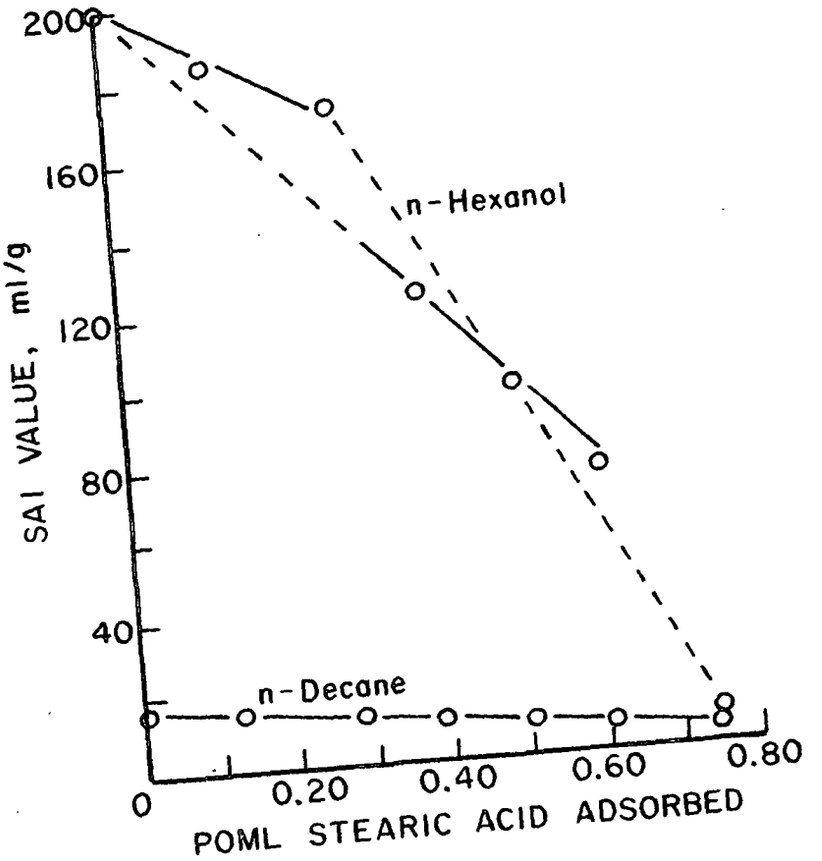

Figure 11. SAI Values for Hexanol and Decane on Stearic Acid Modified Surfaces at 45°C

increasing stearic acid coverage, but apparently in two different ways. At low stearic acid coverage, rate of decrease in SAI value is less than at higher coverages. Both decane and hexanol adsorb preferentially on uncovered cellulose. Decane adsorption seems to be directly proportional to the amount of uncovered cellulose. Hexanol adsorbs more strongly and specifically on cellulose. However, at low stearic acid surface coverages, hexanol adsorption is affected less by loss of unmodified cellulose surface than at higher stearic acid coverages of fiber surfaces.

This distinct change in hexanol behavior may not be readily apparent from the SAI values shown in Fig. 11. A smooth curve could be drawn through the hexanol SAI values, although two straight lines give a better fit to the data. Results of adsorption isotherm analysis presented in the next section confirm this hypothesized change in hexanol adsorption mechanism. The SAI analysis gives no detailed information about the nature of adsorption, only relative comparisons of adsorbate interaction with different surfaces.

Decane SAI values are small, but at a chart speed of 2 inches/min and carrier gas flow rate of 30 mL/min, 1 mL SAI corresponds to about 2 mm chart distance, which is easily measured. Therefore, a precision of ±1 mL for decane SAI values seems reasonable. Precision is not better due to difficulties in precisely marking the injection point on the chart. For hexanol, a chart speed of 0.5 inch/min was used resulting in an estimated precision of ±5 mL.

The SAI value for any surface in the series reflects adsorption on portions of the surface not covered by stearic acid. The minimum SAI value on 100% stearic acid covered fibers reflects adsorption on stearic acid. For decane, this value is significant in size compared to the SAI value on unmodified fibers. Therefore, for any surface in the series, $(SAI - SAI_{min})$ would reflect

unmodified cellulose influence on adsorption. If SAI* is the value for an adsorbate on untreated control fibers, the term $SAI - SAI_{min}/SAI^* - SAI_{min}$ represents the surface fraction of unmodified cellulose relative to control fibers. One minus this quantity represents stearic acid coverage.

Table IX shows results of SAI characterization of the series of physisorbed stearic acid modified fibers and chemisorbed stearic acid modified fibers. Because of changes in detector sensitivity due to inadequate air flow to the flame head, SAI values for Columns 5, 6 and 7 were measured at P/P_o of 0.005. SAI values for the series of physisorbed modified surfaces were measured at P/P_o of 0.01. This discrepancy results in higher SAI values for Columns 5 and 6. This demonstrates again that the SAI approach is a relative method. Standard surfaces must be used for characterization of a surface. Thus, the chemisorbed stearic acid modified, water repellent fibers in Column 6 must be compared with Columns 5 and 7. Columns 4 and 8 serve as standards for the series of surfaces modified by physisorbed stearic acid.

Figure 12 shows the quantity $1 - SAI - SAI_{min}/SAI^* - SAI_{min}$ for decane plotted as a function of stearic acid surface coverage. Decane SAI ratio is directly proportional to stearic acid coverage. The two asterisk points represent chemisorbed modified, water repellent fibers, with surface coverage calculated two different ways. The point falling on the line corresponds to 0.28% coverage, that is, POML coverage. The second point calculates percent coverage using 0.75 POML as 100% coverage. For chemisorbed stearic acid modified fibers, POML coverage seems to be correct. This implies that for physisorbed modified fibers, 100% coverage corresponds to 0.75 POML because the space occupied by each adsorbed dimer is larger than twice the POML chain cross-sectional area. Approximately 56 A^2 of surface seem to be covered by an average dimer instead of $2 \times 20\ A^2 = 40\ A^2$.

TABLE IX

SAI VALUES AT 45° FOR CELLULOSE SURFACES MODIFIED WITH STEARIC ACID

Column Number and Description	Hexanol SAI Values, mL/g	Decane SAI Values, mL/g	SAI Ratio = $1 - \left(\frac{SAI - SAI_{min}}{SAI^{a} - SAI_{min}}\right)$ Hexanol	SAI Ratio Decane
Col. 4 (0%) Control[a]	202[a]	17[a]	0.00	0.00
Col. 14 (17%) 0.13 POML	185	15	0.09	0.17
Col. 11 (39%) 0.29 POML	173	13	0.15	0.33
Col. 12 (52%) 0.39 POML	123	11	0.41	0.50
Col. 13 (68%) 0.51 POML	98	9	0.54	0.66
Col. 15 (81%) 0.61 POML	75	7	0.66	0.83
Col. 8 (100%) 0.75 POML	8	5	1.00	1.00
Col. 5 extracted[b] control	298[a]	24[b]	--	--
Col. 6 0.28 POML water repellent	227	19	0.26	0.28
Col. 7 1.03 POML water repellent	24	6	--	--

[a] Control fibers for physisorbed stearic acid modified fibers. To be used with Col. 8 as SAI_{min} to calculate SAI ratio.

[b] Control fibers for chemisorbed stearic acid modified fibers. To be used with Col. 7 as SAI_{min} to calculate SAI ratio.

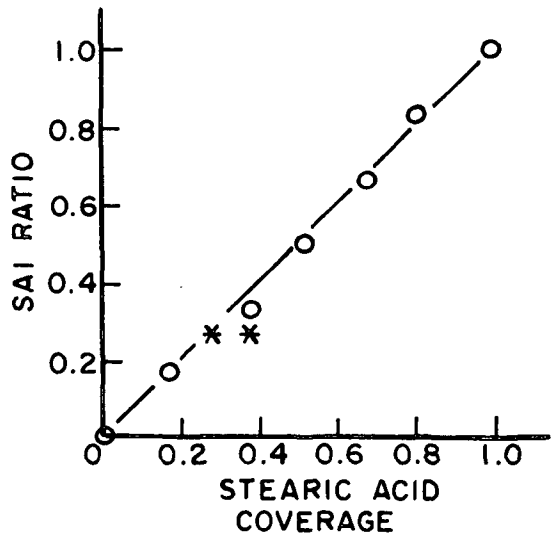

Figure 12. SAI Ratio for Decane on Stearic Acid Modified Fibers at 45°C

Preferential adsorption of decane by unmodified cellulose is sufficient enough to make decane a useful tool for characterizing stearic acid modified surfaces. Hexanol is very strongly adsorbed by cellulose. However, hexanol seems less suitable for direct characterization of stearic acid coverage. Figure 13 plots hexanol SAI ratio as a function of stearic acid fractional coverage. As in Fig. 11, hexanol behavior can be viewed as two distinct cases. Relative hexanol adsorption is affected to a lesser degree than decane adsorption. Presumably this is due to increased attraction of hexanol for unmodified cellulose. After about 40% of the surface is covered by stearic acid this preference is decreased somewhat. Note the good linearity between 0 and 40% coverage. Good linearity is also displayed between 50 and 80% coverage but with a different slope. The two asterisks correspond to chemisorbed stearic acid coverage calculated as explained previously for decane. The chemisorbed modified fibers fall closer to the second grouping, even though stearic acid coverage groups them with the low coverage surfaces. Apparently chemisorbed

stearic acid is more effective at shielding the surface from gaseous molecules than physisorbed acid species. The SAI ratio is nearly equal to POML coverage for chemisorbed modified fibers.

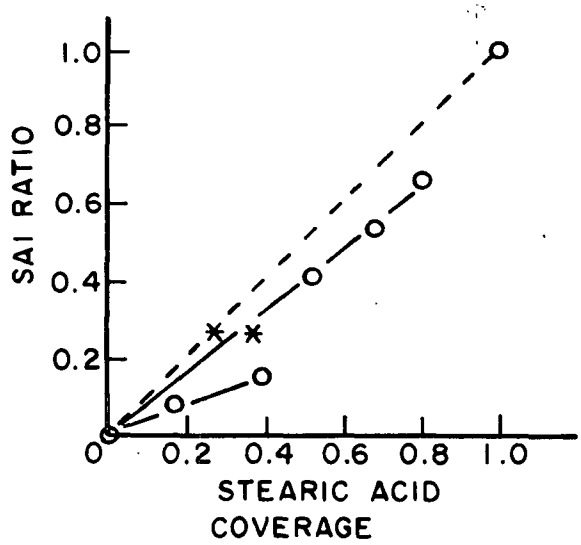

Figure 13. SAI Ratio for Hexanol on Stearic Acid Modified Fibers at 45°C

ISOTHERM ANALYSIS

Adsorption Isotherms

Adsorption isotherms were measured for hexanol on all seven surfaces in the physisorbed modified series. Figure 14 shows hexanol isotherms at 45°C on these surfaces. Hexanol is preferentially adsorbed on any portions of the fiber surfaces not covered with stearic acid. The isotherms in Fig. 14 group into low coverage and high coverage sets as do SAI values.

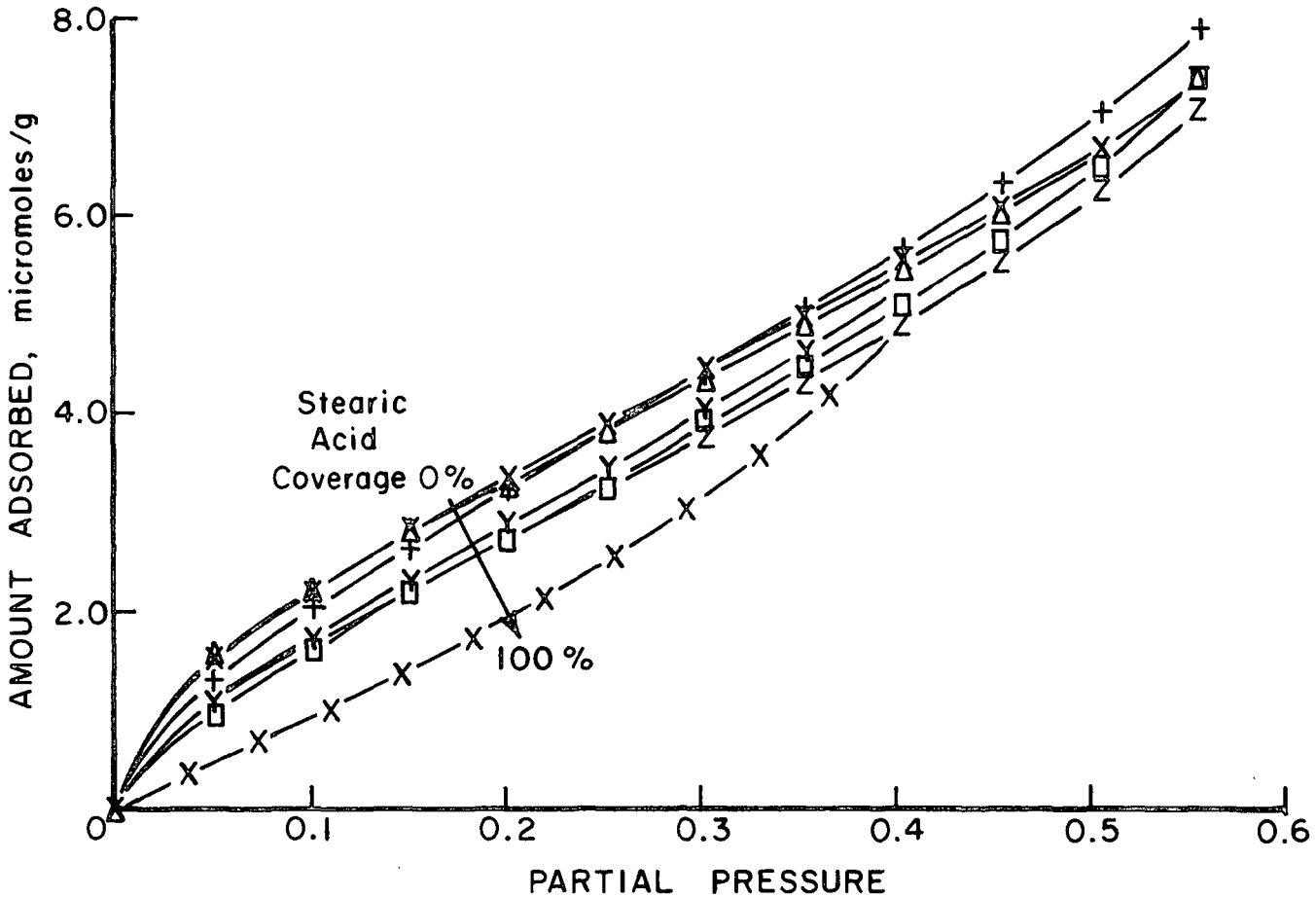

Figure 14. Hexanol Isotherms at 45°C on Stearic Acid Modified Surfaces

SAI characterization showed a small, regular change in decane behavior on the family of modified surfaces. Therefore, decane adsorption isotherm data were gathered on only three surfaces. Figure 15 presents decane isotherms at 45°C on these three surfaces. Decane is also preferentially adsorbed by portions of the fiber surfaces not covered with stearic acid. Lack of strong, specific interaction between cellulose and decane results in nearly linear decane adsorption isotherms.

Figure 16 shows the changes which occurred in the behavior of decane and hexanol isotherms when fiber surfaces were covered with stearic acid. Hexanol behavior changes to a greater degree than that of decane.

Analysis of these isotherms by the BET approach would not provide any information about distribution of stearic acid on fiber surfaces. BET surface areas would show the same trends as sorptometer surface areas, indicating a decrease in surface area as fiber roughness and porosity become filled with stearic acid. Decane isotherms are nearly linear. BET "c" values would be low and nearly equal. For hexanol, "c" values would change markedly from unmodified to fully covered surfaces. However, Fig. 14 indicates that "c" values would not change in a regular manner for the series of surfaces. Columns 4 and 14 display nearly identical isotherms, as do Columns 13 and 15. This would result in identical BET parameters for these two pairs of surfaces.

Thermodynamic Adsorption Parameters

Chromatographic adsorption data for hexanol on all seven surfaces and decane on three surfaces were measured at 5°C intervals from 35 to 55°C. The Clausius-Clapeyron equation was used to calculate isosteric heats and entropies of adsorption from the five isotherms for each adsorbate-surface pair investigated. A representative set of isotherms for hexanol is given by Fig. 17. Figure 18 shows a set of isotherms for decane.

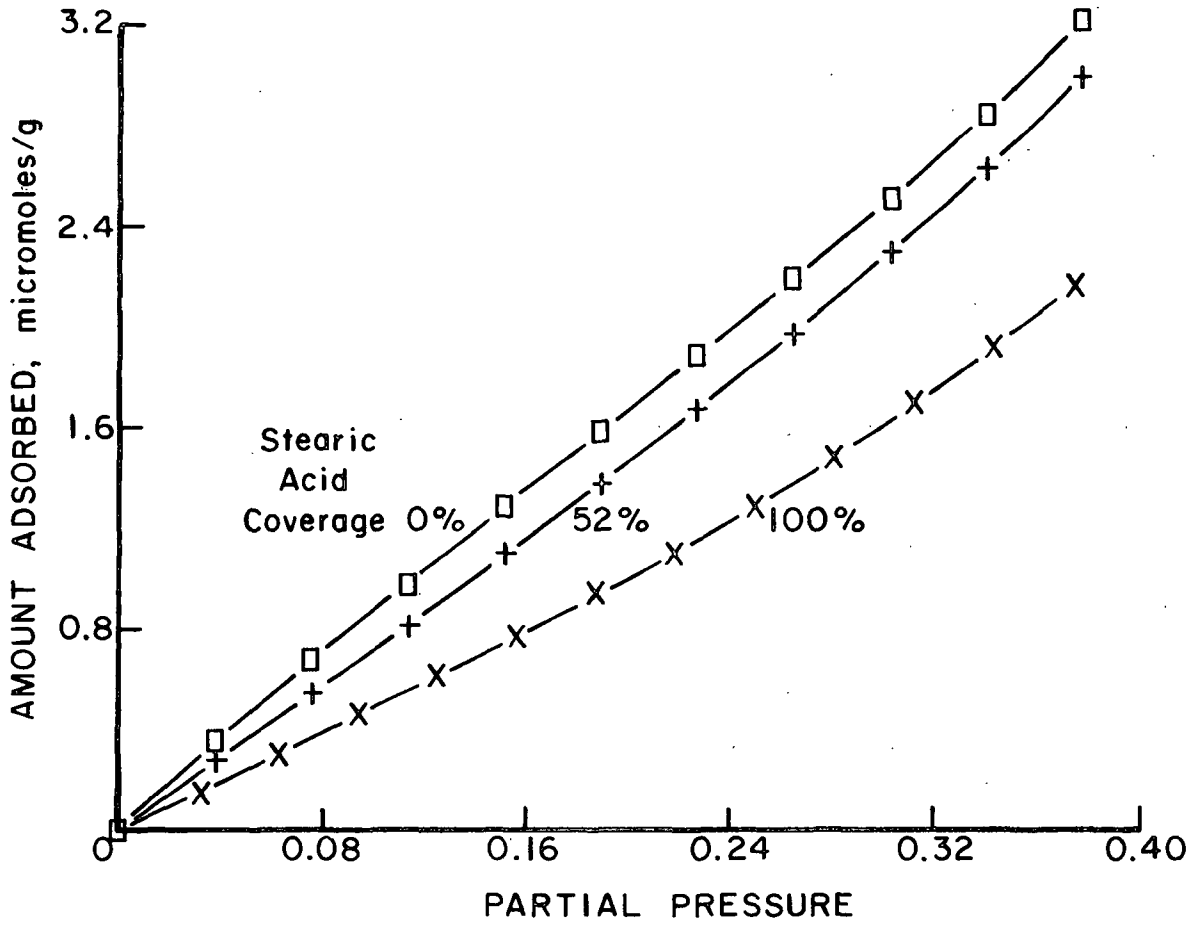

Figure 15. Decane Isotherms at 45°C on Stearic Acid Modified Surfaces

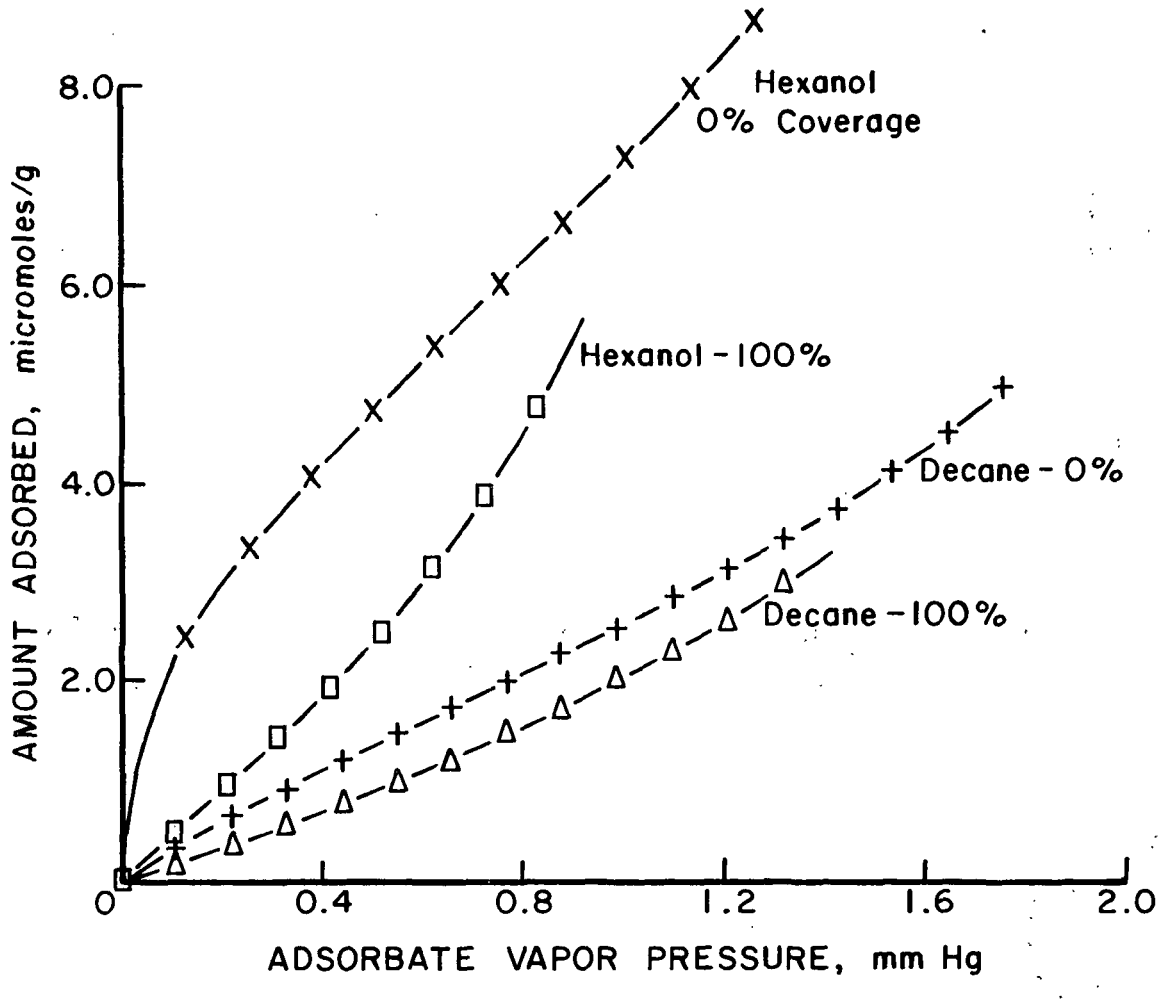

Figure 16. Decane and Hexanol Isotherms Measured at 45°C on Untreated Cotton Fibers (0% Coverage) and Fibers Completely Covered with Stearic Acid (100% Coverage)

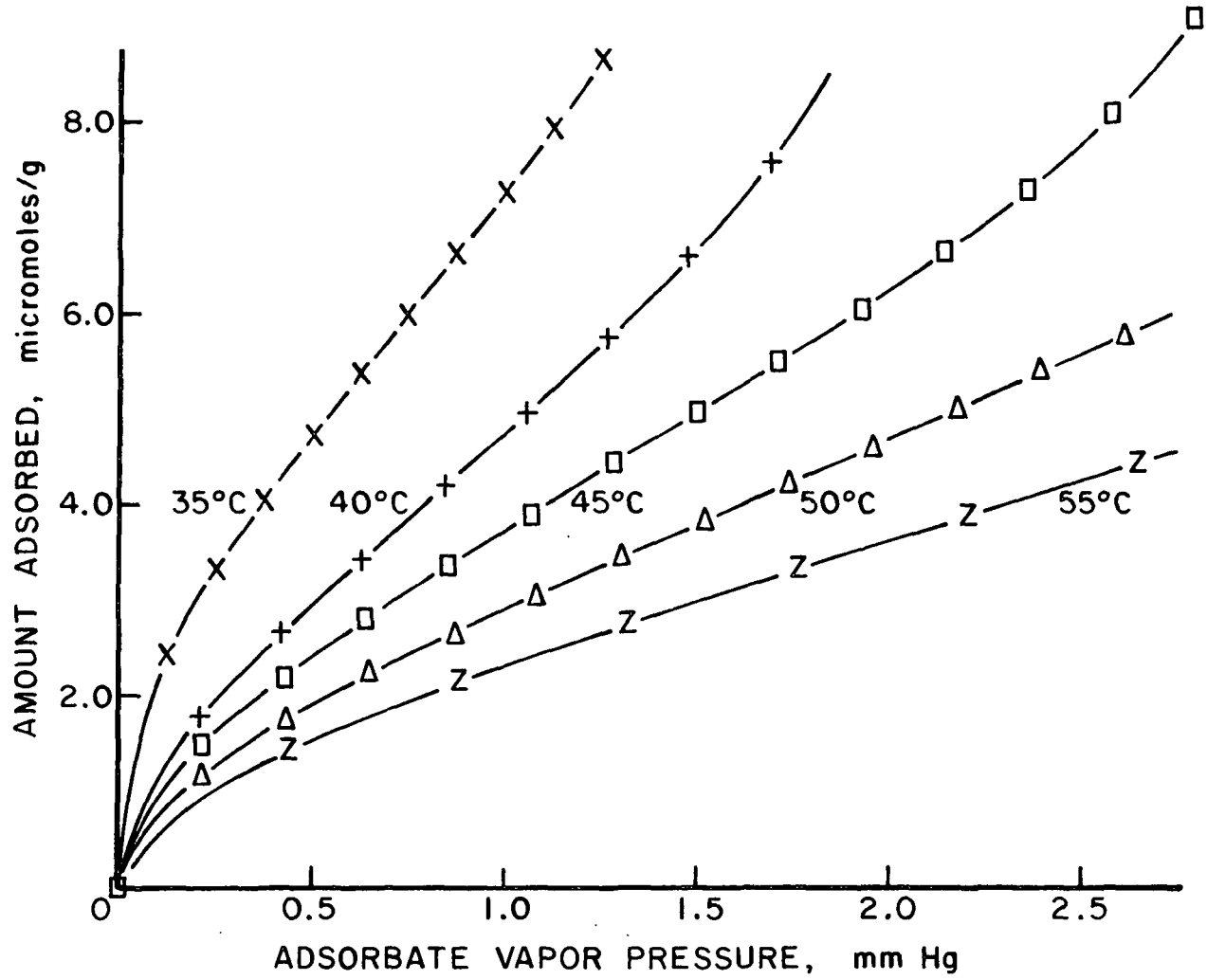

Figure 17. Hexanol Adsorption Isotherms on Untreated Cellulose Fibers

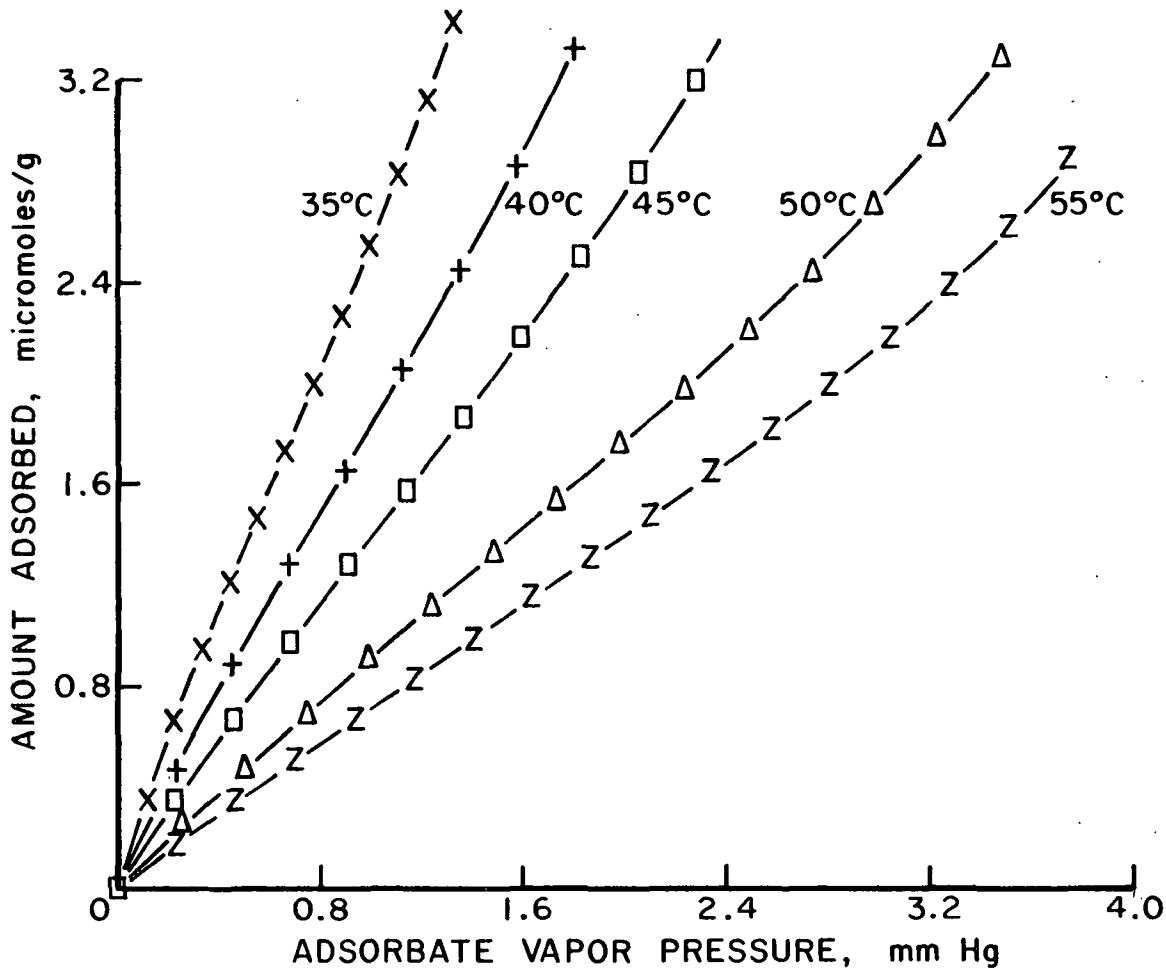

Figure 18. Decane Adsorption Isotherms on Untreated Cellulose Fibers

To apply the Clausius-Clapeyron equation for calculation of isosteric thermodynamic adsorption parameters, adsorption data must first be tabulated as vapor pressures required for a given amount of adsorption at each temperature. This was accomplished for each isotherm set by a nonlinear interpolation program based on polynomial extraction from a table of divided difference. Results of this interpolation on the data of Fig. 17 are shown in Table X. Each row of this table is, in fact, an adsorption isostere.

Each row of this interpolation was then fitted to the Clausius-Clapeyron equation in the form:

$$\Delta\bar{H} = - R \, \partial \ln p / \partial(1/T) \qquad (4)$$

A least squares fitting program was used to obtain $\partial \ln p / \partial(1/T)$. Free energy of adsorption was calculated at 45°C as:

$$\Delta\bar{G} = - RT \ln p \qquad (5)$$

The entropy of adsorption at 45°C was calculated as:

$$\Delta\bar{S} = (\Delta\bar{H} - \Delta\bar{G})/T \qquad (6)$$

These quantities are tabulated for the data of Table X in Table XI.

The correlation coefficient indicates how well each set of five data points fit the calculated straight line. Table XI presents data with the lowest correlation coefficients. For 90% of the isotherm data the correlation coefficients were 0.99 or higher. This indicates the experimental data fit the Clausius equation quite well. However, these indicated good fits are somewhat misleading. Slopes of ln p vs. reciprocal absolute temperature determined by this analysis are very large negative numbers, in the region of ~ -6000. Very small differences in slopes are producing all of the difference

TABLE X

ADSORPTION ISOTHERMS FOR HEXANOL
ON UNTREATED CELLULOSE FIBERS INTERPOLATED
FOR FITTING TO THE CLAUSIUS-CLAPEYRON EQUATION

Amount Adsorbed, moles/g	Adsorbate Vapor Pressure at Designated Temperature - MM. Hg.				
	308°K	313°K	318°K	323°K	328°K
0.160	0.003	0.010	0.012	0.017	0.026
0.320	0.007	0.021	0.025	0.035	0.054
0.480	0.011	0.033	0.040	0.057	0.087
0.640	0.015	0.046	0.058	0.083	0.127
0.800	0.020	0.062	0.080	0.115	0.175
0.960	0.025	0.080	0.104	0.153	0.227
1.120	0.031	0.100	0.132	0.198	0.288
1.280	0.037	0.123	0.164	0.249	0.361
1.440	0.046	0.149	0.201	0.305	0.444
1.600	0.055	0.176	0.243	0.366	0.533
1.760	0.066	0.206	0.288	0.432	0.629
1.920	0.078	0.240	0.336	0.502	0.730
2.080	0.091	0.277	0.387	0.575	0.835
2.240	0.105	0.315	0.439	0.652	0.945
2.400	0.121	0.355	0.494	0.731	1.058
2.560	0.138	0.396	0.550	0.813	1.174
2.720	0.159	0.438	0.608	0.897	1.292
2.880	0.181	0.481	0.668	0.983	1.413
3.040	0.204	0.525	0.729	1.072	1.535
3.200	0.228	0.569	0.791	1.161	1.659
3.360	0.254	0.613	0.853	1.251	1.784
3.520	0.280	0.658	0.917	1.341	1.911
3.680	0.308	0.703	0.980	1.431	2.037
3.840	0.336	0.747	1.044	1.521	2.165
4.000	0.365	0.792	1.108	1.611	2.292
4.160	0.394	0.836	1.172	1.700	2.420
4.320	0.424	0.881	1.237	1.789	2.548
4.480	0.454	0.925	1.302	1.877	2.676
4.640	0.484	0.969	1.366	1.966	2.804
4.800	0.514	1.013	1.430	2.055	2.932
4.960	0.545	1.057	1.494	2.144	3.059
5.120	0.576	1.101	1.558	2.232	3.185
5.280	0.607	1.144	1.621	2.321	3.309
5.440	0.639	1.187	1.684	2.409	3.432
5.600	0.670	1.230	1.747	2.497	3.554
5.760	0.702	1.272	1.809	2.585	3.674
5.920	0.734	1.313	1.871	2.673	3.792
6.080	0.766	1.354	1.932	2.760	3.908
6.240	0.797	1.395	1.992	2.847	4.022
6.400	0.829	1.434	2.051	2.932	4.133
6.560	0.861	1.471	2.108	3.017	4.241
6.720	0.893	1.508	2.164	3.100	4.345
6.880	0.924	1.543	2.218	3.181	4.445
7.040	0.955	1.578	2.270	3.259	4.540
7.200	0.986	1.611	2.320	3.334	4.630
7.360	1.017	1.642	2.368	3.406	4.715
7.520	1.047	1.673	2.415	3.474	4.796
7.680	1.077	1.702	2.460	3.539	4.872
7.840	1.107	1.730	2.503	3.601	4.943
8.000	1.136	1.757	2.544	3.667	5.010

TABLE XI

THERMODYNAMIC ADSORPTION PARAMETERS FOR HEXANOL ADSORPTION ON UNTREATED CELLULOSE FIBERS AT 45°C

Amount Adsorbed, Micmole/gM	-Heat of Adsorption, Kcal/mole	Free Energy of Adsorption, Kcal/mole	Entropy of Adsorption, Cal/M-deg	Correlation Coefficient
0.160	19.0347	6.9563	-37.9825	-0.9498
0.320	18.8514	6.5009	-38.8380	-0.9549
0.480	19.0553	6.2034	-40.4149	-0.9579
0.640	19.4899	5.9679	-42.5222	-0.9592
0.800	20.0370	5.7703	-44.8639	-0.9600
0.960	20.4325	5.6005	-46.6415	-0.9593
1.120	20.7780	5.4500	-48.2014	-0.9591
1.280	21.0731	5.3138	-49.5577	-0.9602
1.440	21.1851	5.1856	-50.3131	-0.9620
1.600	21.1726	5.0672	-50.6458	-0.9641
1.760	21.0906	4.9600	-50.7253	-0.9657
1.920	20.9594	4.8625	-50.6193	-0.9661
2.080	20.7909	4.7749	-50.3649	-0.9664
2.240	20.6013	4.6948	-50.0204	-0.9670
2.400	20.3679	4.6212	-49.5178	-0.9680
2.560	20.0833	4.5530	-48.8373	-0.9695
2.720	19.7487	4.4895	-47.9848	-0.9715
2.880	19.4023	4.4306	-47.0811	-0.9736
3.040	19.0857	4.3756	-46.2582	-0.9755
3.200	18.7985	4.3244	-45.5161	-0.9774
3.360	18.5270	4.2765	-44.8130	-0.9793
3.520	18.2725	4.2315	-44.1541	-0.9810
3.680	18.0321	4.1891	-43.5315	-0.9826
3.840	17.8099	4.1493	-42.9578	-0.9841
4.000	17.6042	4.1119	-42.4288	-0.9855
4.160	17.4171	4.0764	-41.9518	-0.9868
4.320	17.2465	4.0427	-41.5214	-0.9879
4.480	17.0886	4.0107	-41.1255	-0.9889
4.640	16.9438	3.9802	-40.7658	-0.9899
4.800	16.8082	3.9514	-40.4304	-0.9907
4.960	16.6803	3.9238	-40.1146	-0.9916
5.120	16.5594	3.8975	-39.8171	-0.9923
5.280	16.4436	3.8724	-39.5320	-0.9930
5.440	16.3307	3.8484	-39.2524	-0.9936
5.600	16.2226	3.8254	-38.9850	-0.9941
5.760	16.1200	3.8033	-38.7318	-0.9947
5.920	16.0221	3.7821	-38.4905	-0.9952
6.080	15.9282	3.7619	-38.2589	-0.9956
6.240	15.8374	3.7426	-38.0339	-0.9961
6.400	15.7492	3.7244	-37.8140	-0.9965
6.560	15.6642	3.7070	-37.6012	-0.9969
6.720	15.5800	3.6906	-37.3879	-0.9973
6.880	15.4942	3.6752	-37.1667	-0.9976

in calculated values. Thus, small differences in experimental data make very large differences in the calculated parameters. This factor influences the choice of temperature range to be considered.

Application of the Clausius-Clapeyron equation to analysis of adsorption isotherms assumes that heat of adsorption is constant over the temperature range selected. Of course, heat of adsorption would not be expected to be constant over too wide a temperature range. The adsorption data were analyzed over the 20° range from 35 to 55°C. Analysis was also done over three 10° ranges: 35 to 45°C, 40 to 50°C, and 45 to 55°C. No systematic pattern could be found in parameter variations. However, variations for a given surface were often quite large. Correlation coefficients were always quite high, that is, different groupings of the same data fit the Clausius equation equally well. Parameter differences were due to small variations in calculated slopes. The 35 to 55°C range was selected since it made best use of the experimental data.

Figure 19 summarizes the results for isosteric heats and entropies of adsorption for hexanol and decane over a range of $\theta = 0 \rightarrow 2$ on the family of stearic acid modified surfaces. Heats of adsorption are usually higher at low coverages, decreasing as higher energy adsorption sites are covered. At several layers coverage, heat of adsorption approaches heat of vaporization for the liquid adsorbate. Entropies of adsorption also show this decrease toward liquid properties. Decane behavior on the three surfaces analyzed shows this type behavior. For decane at 45°C, liquid properties are $\Delta h_{vap} = -11.4$ Kcal/mole and $\Delta s_{vap} = -28$ cal/mole °K. Column 8 seems to show the effect of decane absorption into the stearic acid surface phase.

For surfaces with up to 40% stearic acid coverage, initial hexanol adsorption up to $\theta \sim 0.5$ causes increasing heats of adsorption with corre-

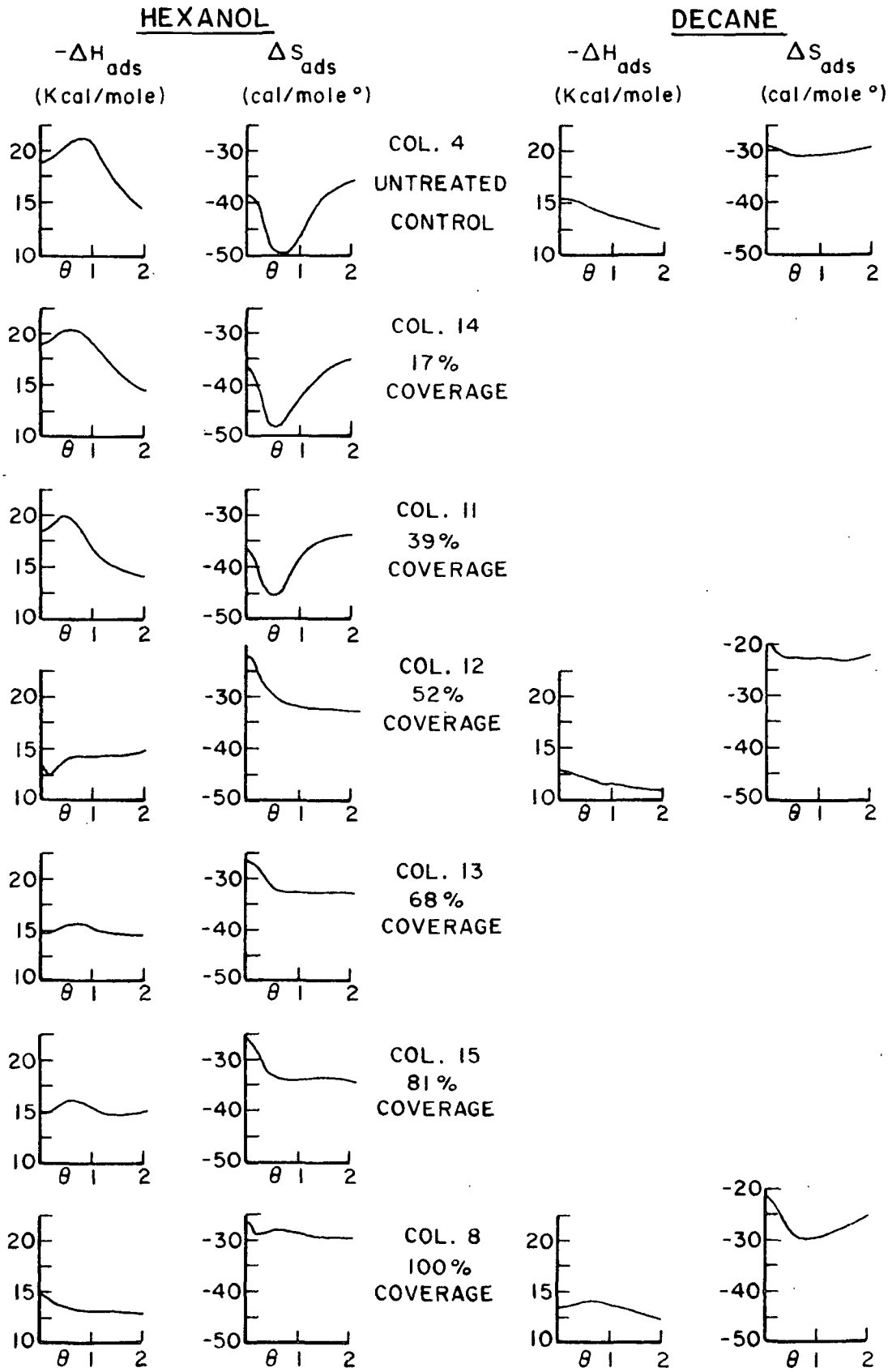

Figure 19. Hexanol and Decane Adsorption Parameters Calculated at 45°C on Stearic Acid Modified Cotton Fiber Surfaces

sponding entropy minimums. This behavior was also noted by Tremain and Gray (42) and is best explained by clustering of adsorbed hexanol molecules forming higher energy sites on the surface. Due to strong adsorbate/adsorbent interactions, initially adsorbed molecules are relatively immobile on the surface. An adsorbed hexanol molecule provides additional interaction with gaseous hexanol molecules by sorbate-sorbate hydrogen bonding. These lateral interactions make the surface immediately surrounding adsorbed hexanol more attractive than bare cellulose. Two adsorbed hexanol molecules are still more favorable, and so on. These small clusters of adsorbed hexanol build up until overlap between clusters occurs and adsorbed hexanol is no longer immobile. At this point heat of adsorption begins to decrease in a normal manner. For hexanol at 45°C, liquid properties are:

$$\Delta h_{vap} = -13.4 \text{ Kcal/mole}; \qquad \Delta s_{vap} = -32 \text{ cal/mole } °K$$

After the fiber surfaces are about half covered with stearic acid, this clustering is almost eliminated, as is shown for Columns 12, 13 and 15. Figure 19 helps to explain hexanol SAI behavior. Below 40% stearic acid coverage clustering of hexanol on cellulose causes increased interaction. This "specific interaction" is eliminated when fiber surfaces become more than 50% covered with stearic acid. SAI values depend on a difference between maximum retention volume, probably affected by clustering, and minimum retention volume, probably not affected by clustering. Thus, hexanol SAI values decrease as the cellulose surface is covered by more and more stearic acid. However, rate of decrease changes due to loss of the clustering mechanism.

Results of this isotherm analysis were relatively independent of experimental variables. Carrier gas flow rates and detector sensitivities were randomly varied ±10% for computing hexanol adsorption on Columns 11, 12 and 13. Resulting plots were relatively unchanged in shape although shifted somewhat

in absolute value. Therefore, the results shown in Fig. 19 should be fairly independent of experimental variables such as detector sensitivity changes.

Treatment by Analysis of Spreading Behavior

Thermodynamic analysis indicates a clustering of hexanol molecules on cellulosic surfaces less than half covered with stearic acid. For this clustering to create higher energy adsorption sites, adsorbed hexanol molecules must be localized on the surface. Absence of clustering could indicate that adsorbed hexanol molecules are more mobile on cellulose surfaces which are more than 50% covered with stearic acid. One way of estimating mobility of adsorbed molecules is by calculating changes in two dimensional spreading pressure as adsorbate molecules cover the surface to an increasing extent. Nonmobile molecules will exhibit no spreading pressure.

Except for special systems (55), spreading pressure cannot be measured directly for a gas-solid system but must be estimated from the adsorption isotherm by the generalized Gibbs adsorption equation:

$$-d\gamma' = \sum_i \Gamma_d^i \mu^i \qquad (7)$$

For a single gas-solid system this may be written as:

$$-d\,\gamma' = RT\,\Gamma^s\,d\ln p \qquad (8)$$

Where Γ^s is the surface concentration and p the vapor pressure of the adsorbate. Integration of Equation (8) yields:

$$\gamma_o' - \gamma' = \pi = RT \int^p \Gamma^s\, d\ln p \qquad (9)$$

If N micromoles are adsorbed on 1 gram of solid with surface area of S m^2/g, then:

$$\pi = \frac{RT}{S} \int_{p=o}^{p} N\, d\ln p \qquad (10)$$

The spreading pressure, π, corresponding to any equilibrium gas pressure between 0 and p may be obtained by graphical integration of a plot of N vs. ln p. The area, a, occupied by one adsorbate molecule on the surface is:

$$a = 166 \frac{S}{N} \text{ square angstroms} \qquad (11)$$

This treatment assumes the adsorbed state is that of a two dimensional ideal gas. Obviously this is not accurate since adsorbate molecules have both size and lateral interactions. However, Equation (10) is easily applied to gas chromatographic data. Even if a more realistic adsorbed state were assumed, any calculation of spreading pressure from adsorption isotherms assumes monolayer adsorption up to $\theta = 1$. This is a far more serious limitation than assumption of two-dimensional ideal gas behavior. Nevertheless π vs. a diagrams calculated with Equation (10) should be interpreted only in the most general terms.

Adsorption isotherms for decane and hexanol at 35°C on Columns 4, 12, and 8 were analyzed by a computer program which calculated spreading pressure as a function of surface area available per adsorbate molecule on the surface. Refer to Appendix VI – C for this program. Figure 20 shows the results of this analysis. On untreated control fibers no spreading pressure develops until hexanol surface concentration reaches one molecule for every 150 A^2 of surface. On surfaces half covered with stearic acid, spreading pressure begins at one hexanol molecule for every 400 A^2. Decane exhibits spreading pressure at very low surface concentrations. As fiber surfaces become increasingly covered by stearic acid, hexanol spreading behavior approaches that of decane.

Calculation of Adsorptive Site Energy Distributions

The Rudzinski approach was utilized to calculate a rough, first-order approximation of adsorptive site energy distributions for decane and hexanol

at 45°C on the surfaces under investigation. A computer program (see Appendix VI – B) was developed to analyze microcomparator data by differentiating a calculated table of retention volume as a function of adsorbate vapor pressure. The Rudzinski method utilizes the condensation approximation of Hobson and assumes no lateral interactions between adsorbate molecules. This last assumption is quite inappropriate considering the discussion of initial clustering of hexanol molecules. This clustering is due to lateral interactions, but will be interpreted by the Rudzinski approach as interactions between cellulose and hexanol.

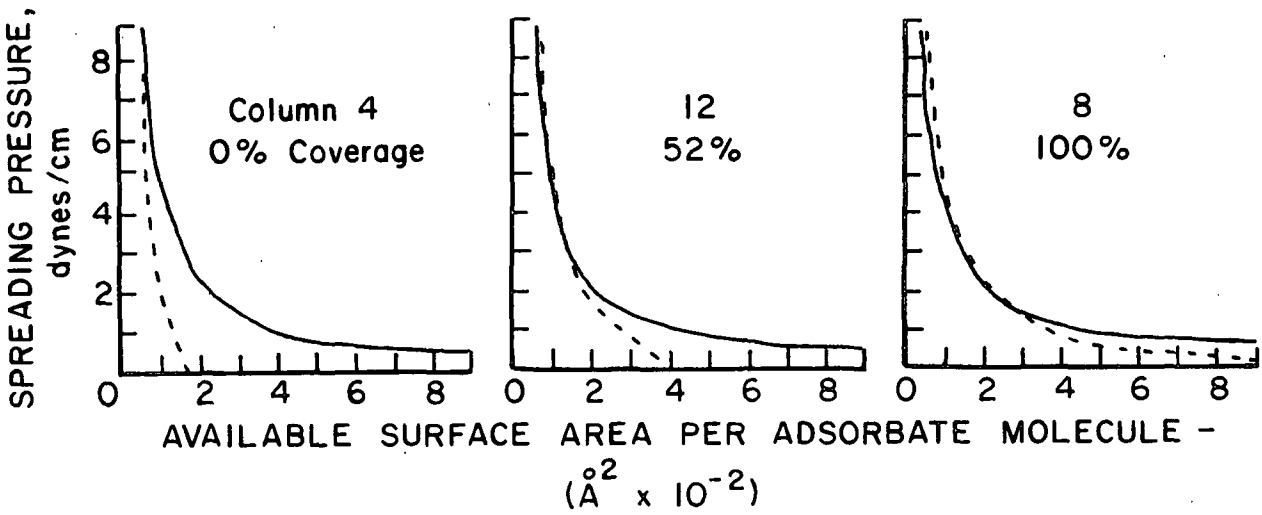

Figure 20. Spreading Pressure Diagrams for Decane and Hexanol on Stearic Acid Modified Cellulose Fiber Surfaces

Results of this analysis are shown for decane in Fig. 21. Rudzinski type site energy distributions are primarily functions of isotherm curvature. Based on Fig. 21, decane adsorption on fully covered fibers would be expected to be slight compared to adsorption on unmodified fibers. Reference to Fig. 15 will show that decane adsorption at 100% coverage is about half that at 0% coverage at any given vapor pressure. The site energy distributions should reflect this relative amount of adsorption. However, total adsorption area for fibers 100% covered with stearic acid is only 1/25 that of untreated fibers in Fig. 21. Therefore, chart area at 100% coverage should be 12 times larger than shown in Fig. 21. Likewise, chart area at 52% coverage should be five times larger than is shown in Fig. 21. Area adjustments were carried out by estimation without any detailed calculations. Figure 22 shows the results of this normalization procedure. These distributions show a decrease in available decane adsorption sites as cellulose becomes covered with stearic acid.

A similar normalization procedure using appropriate (different) factors was done for hexanol. Results of this analysis are shown in Fig. 23. Hexanol distributions are broader and higher than decane distributions. Above 2.5 Kcal/mole a high energy tail asymptotically approaches the energy axis. Distributions for 0 and 17% coverage (not shown) have two distinct peaks. One of these could be attributed to clustering of hexanol molecules. However, clustering also occurs on 39% stearic acid covered fibers where only one peak is present.

These site energy distributions are not too useful for characterizing fiber surfaces as to stearic acid coverage. However, changes in the distributions are quite evident as the surfaces are modified. The Rudzinski approach appears to be quite useful for determining adsorbent site energy distributions using complex adsorbates. Hexanol and decane would be nearly impossible to treat

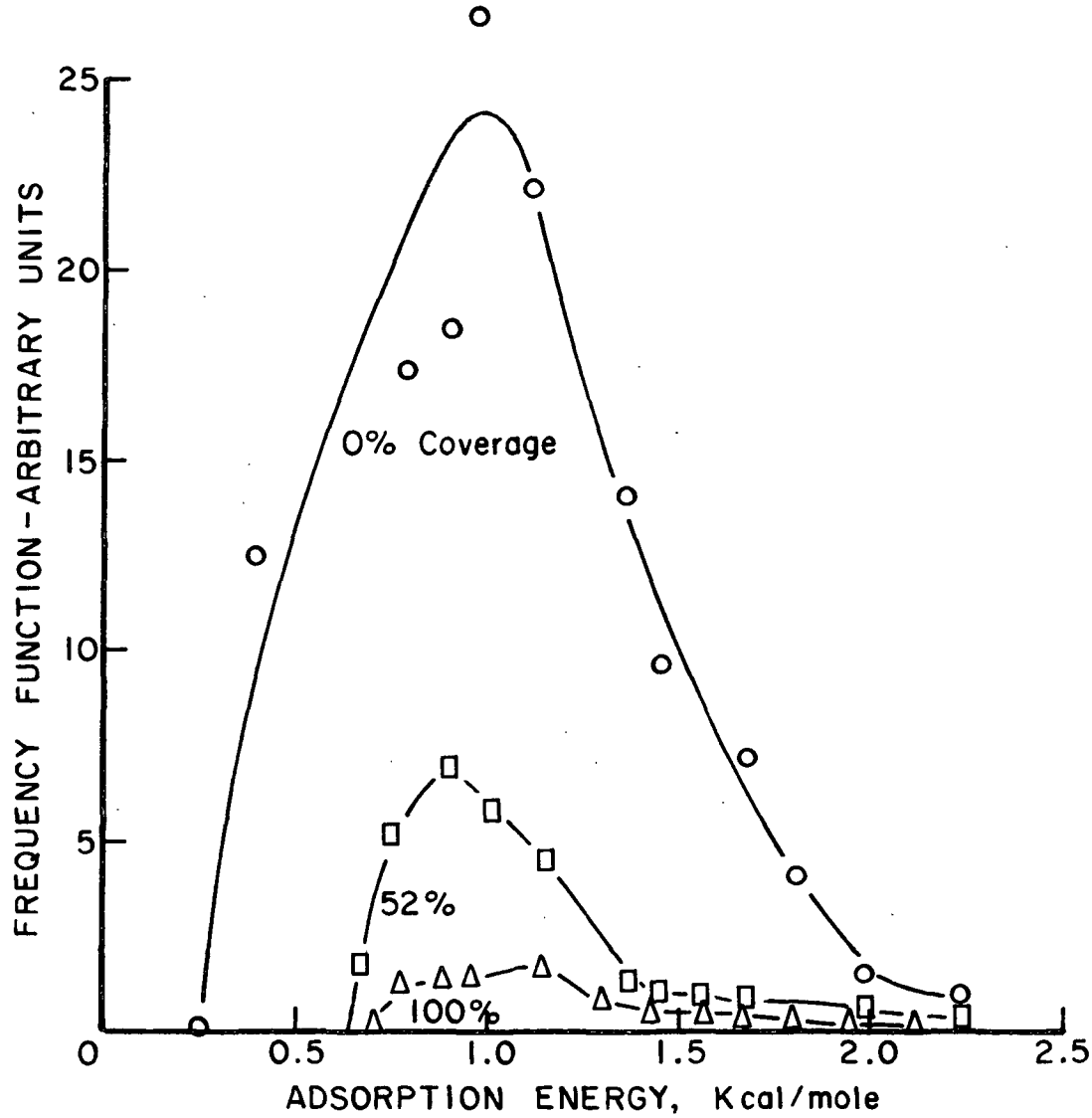

Figure 21. Rudzinski Type Adsorptive Site Energy Distributions for n-Decane on Stearic Acid Modified Cotton Surfaces at 45°C.

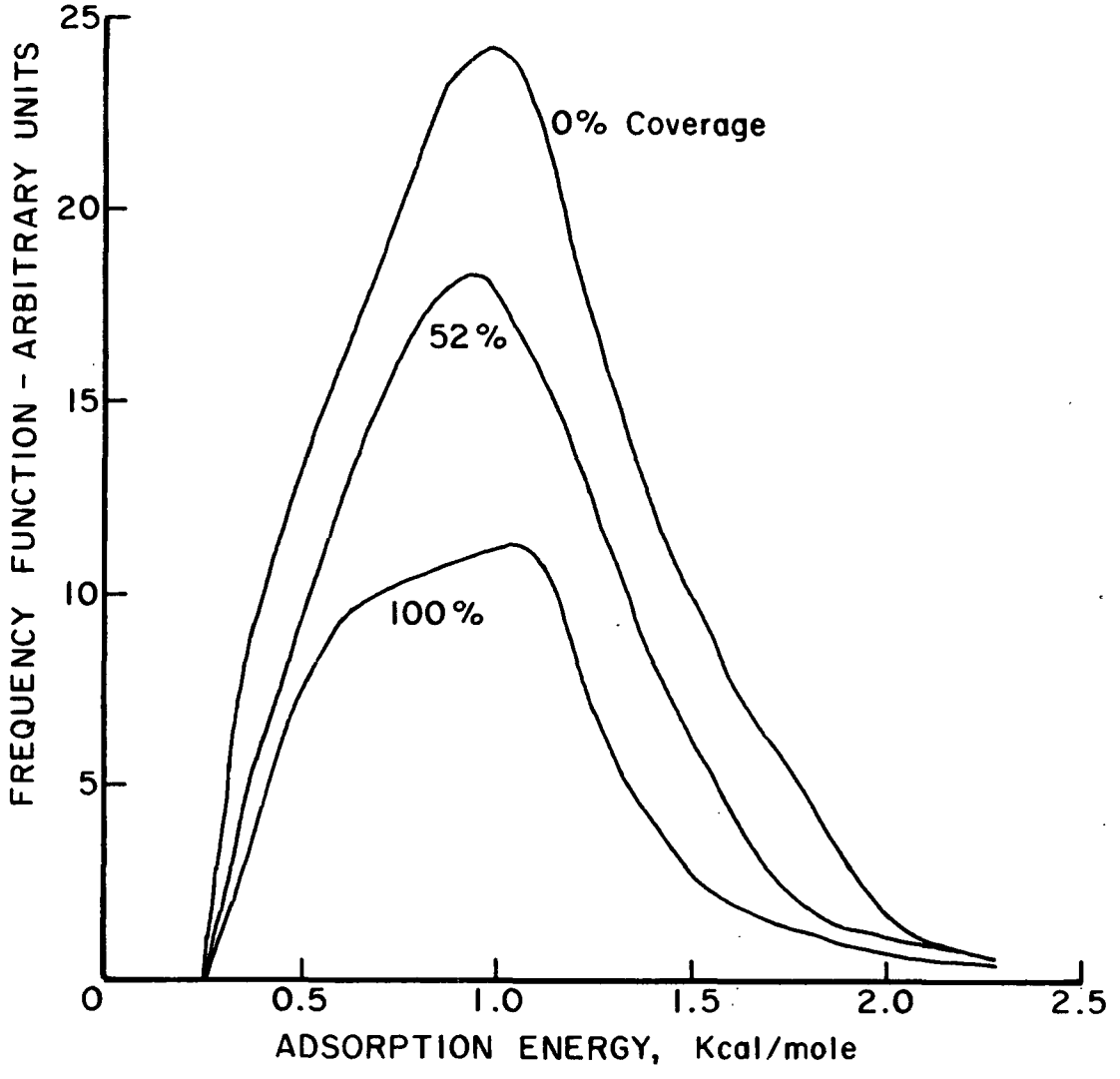

Figure 22. Normalized Rudzinski Type Site Energy Distributions for n-Decane on Stearic Acid Modified Cotton Surfaces at 45°C

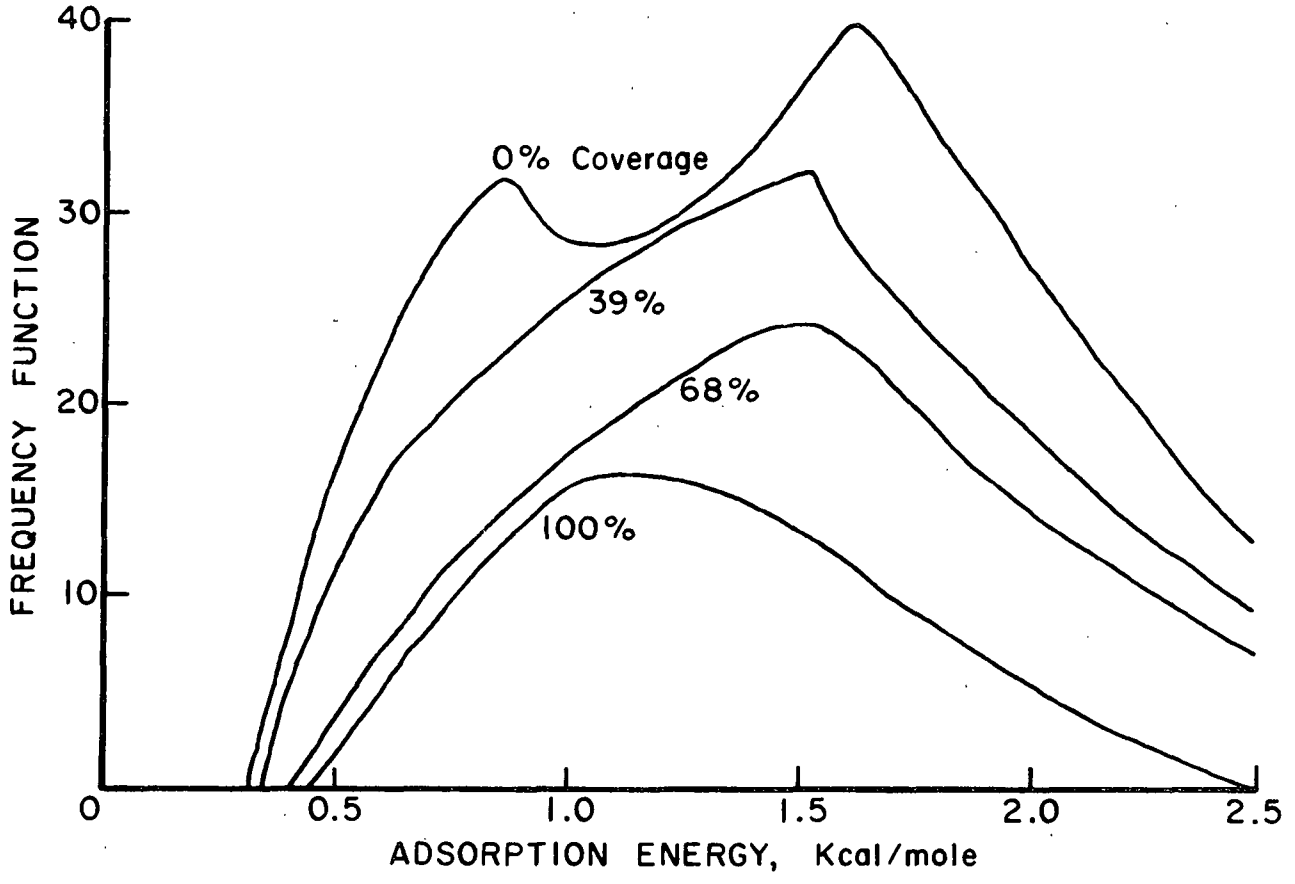

Figure 23. Normalized Rudzinski Type Energy Distributions for n-Hexanol on Stearic Acid Modified Cotton Surfaces at 45°C

in an exact mathematical model since changes in configurations on adsorption would be complex. Calculation of both site energy distributions and spreading pressure behavior would probably yield more useful information if a more realistic state for adsorbed gas molecules was used. However, the resulting equations for more realistic adsorbed states would be quite complex and not easily applied to chromatographic data.

Isotherm Analysis for Water Repellent Fibers

SAI characterization indicated that water repellent fibers with 0.28 POML chemisorbed stearic acid share the hexanol adsorption mechanism common to surfaces more than half covered by physisorbed stearic acid. Based on this interpretation of SAI data, clustering of hexanol moleclues would not be expected on fibers modified with 0.28 POML chemisorbed stearic acid, although it does occur on fibers modified with 0.29 POML physisorbed stearic acid. Chromatographic isotherm data were gathered for hexanol on Column 6 at 5°C intervals from 35 to 55°C. These data were analyzed by the computer based application of the Clausius-Clapeyron equation which has been previously outlined. Figure 24 clearly demonstrates absence of initial clustering of adsorbed hexanol. These results are similar to those for Columns 12, 13, 15 and 8 shown in Fig. 19. These surfaces all have high coverages of physisorbed stearic acid.

Swanson (74) and Ferris (73) hypothesized that development of water repellency results from cones of surface coverage swept out by firmly anchored, chemisorbed stearic acid tails. SAI results indicate that gaseous adsorbate molecules can elude these tails to interact with the surface. However, chemisorbed stearic acid does have a greater effect on hexanol adsorption than does physisorbed stearic acid. The initial clustering of hexanol molecules is

eliminated at lower coverages of chemisorbed stearic acid. In this way, chemisorbed stearic acid is more efficient at protecting the cellulose surface from hexanol vapor than an equal coverage of physisorbed stearic acid.

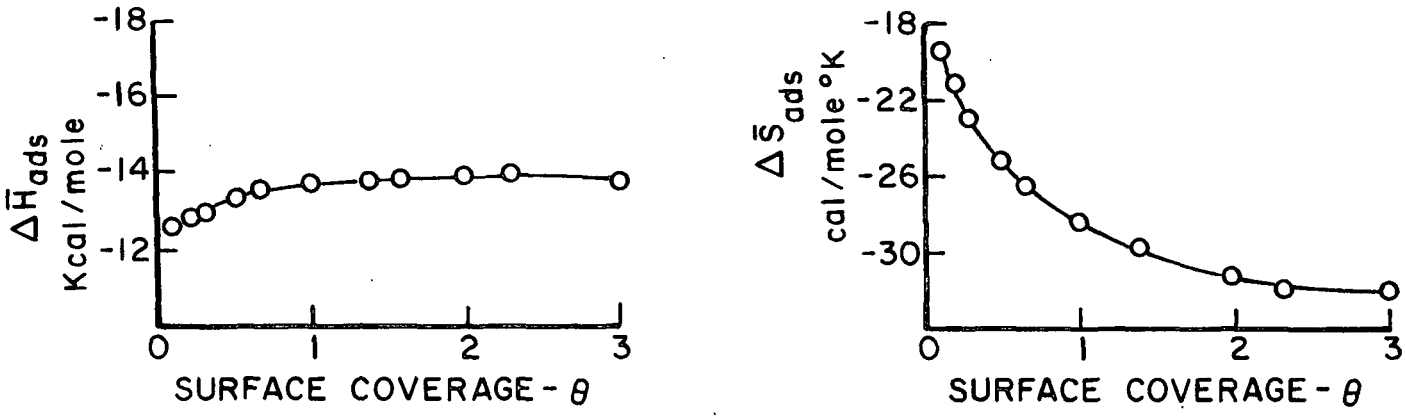

Figure 24. Heats and Entropies of Adsorption for Hexanol at 45°C on Water Repellent Cotton Fibers Modified by 0.28 POML Chemisorbed Stearic Acid

GAS ADSORPTION SURFACE CHARACTERIZATION UTILIZING SURFACE ADSORPTION INDICES

Inverse gas adsorption chromatography eliminates tedious, time consuming techniques associated with vacuum adsorption studies. Organic vapors may be routinely used as adsorbates. A wide range of temperatures is readily available. Easily measured surface adsorption indices have been shown to be as useful for characterizing adsorbent surfaces as more time consuming isotherm analysis approaches. Chromatographic surface characterizations are best carried out using adsorbates with low, nearly equal, saturation vapor pressures. Inverse gas chromatography is an order of magnitude more rapid and simple than vacuum adsorption techniques. The SAI analysis is an order of magnitude more rapid and straightforward than techniques of isotherm analysis.

Calculation of adsorption isotherms from gas chromatographic retention data is relatively straightforward. However, the resulting isotherms must be analyzed with care. It is quite easy to treat these isotherms as if they were determined by equilibrium, vacuum measurements. In most cases this presents few problems if experimental conditions have been correctly chosen. However, the nature of the chromatographic experiments must always be kept in mind. For instance, it is impossible for a chromatographically measured isotherm to show a hysteresis loop since chromatograms are a result of a great many adsorption-desorption steps. Therefore, inverse gas adsorption chromatography would not be suitable for studying adsorbent porous structure.

It is much easier to remember the chromatographic nature of these experiments when using surface adsorption indices to characterize adsorbent surfaces. Surface adsorption indices are calculated as the difference between maximum and minimum retention volumes. The maximum retention volume reflects adsorbate-adsorbent interactions, adsorbate properties, and chromatographic conditions. The minimum, constant retention volume depends on adsorbate properties and chromatographic conditions. Surface adsorption indices, therefore, strongly reflect interactions between adsorbate molecules and adsorbent surfaces. When characterizing surfaces by the SAI approach, care must be taken to assure that maximum retention volumes are measured at equal adsorbate vapor pressures. This is much easier to achieve for systems which exhibit nearly linear isotherms such as decane on cellulose. The best way to insure measurement of $V_{R_{max}}$ at equal adsorbate vapor pressures is to determine detector sensitivity for each adsorbate. Then Equation (1) [p. 14] can be used to calculate peak height corresponding to the desired vapor pressure.

Surface adsorption indices are sensitive to specific surface areas of adsorbent materials. SAI values are relatively independent of column packing

variables as long as the column diameter is constant. SAI values are independent of carrier gas flow rates. However, the flow rate must be measured to allow index calculation. Different carrier gas flow rates can be used to check for penetration of adsorbate into the adsorbent surface. Conditions of instantaneous equilibrium between adsorbate molecules and adsorbent surfaces can also be confirmed by working at different carrier gas flow rates.

Gas adsorption proved very useful for characterizing a group of cotton cellulose fiber surfaces modified by exposure to stearic acid vapors. Sorptometer surface area measurements showed that adsorbed stearic acid filled in surface features opened up by the extraction of natural waxes and pectins. Decane SAI ratio values were directly proportional to fractional coverage of the surface by stearic acid. Although not capable of specific interactions with cellulose, decane is nevertheless preferentially adsorbed on unmodified portions of the cellulose fiber surfaces. No parameter resulting from any type of isotherm analysis was proportional to stearic acid surface coverage. Thus, decane SAI characterization would be a good approach for evaluating stearic acid coverage of cellulose surfaces.

SAI values were not dependent on stearic acid surface coverage alone. The mechanism of adsorption also affected these values. Hexanol interacted with the cellulosic surface by strong, specific hydrogen bonding forces. Hexanol SAI values decreased as stearic acid coverage of fiber surfaces increased. This decrease was quite large compared to changes in decane SAI values. On unmodified fibers, the hexanol SAI value was ten times that for decane. On fibers completely covered with stearic acid, hexanol and decane SAI values were nearly equal. Thus, specific interactions between hexanol and cellulose, probably of a hydrogen bonding nature, were eliminated by covering cellulose

fiber surfaces with stearic acid. SAI behavior suggested that a change in the mechanism of hexanol adsorption on cellulose occurred in a region between 40 and 50% coverage of cellulose surfaces with stearic acid. SAI behavior indicated this by a change in slope of the SAI vs. stearic acid coverage plot. SAI values, however, did not indicate anything about the nature of this change in mechanism.

Heats and entropies of adsorption calculated by application of the Clausius-Clapeyron equation to chromatographically determined adsorption isotherms gave details of the adsorption mechanism. Below 40% stearic acid surface coverage, initially adsorbed hexanol molecules apparently clustered together forming more favorable adsorption sites. This caused increasing heats of adsorption and a corresponding entropy "well" in the $\theta \sim 0.5$ region. At and above 50% stearic acid coverage this clustering was eliminated. Cellulose surfaces remaining unmodified were less attractive to hexanol than at lower stearic acid coverages. Hexanol SAI values decreased at a higher rate above 50% coverage than below 40% coverage.

Neither spreading pressure behavior nor adsorptive site energy distributions were much help in either characterizing or clarifying this change in adsorption mechanism. Spreading pressure plots indicated that hexanol mobility increased on cellulose surfaces more than half covered with stearic acid. Rudzinski site energy distributions showed a loss in adsorption sites as the surfaces became covered with stearic acid.

Thus, SAI values appear to be quite useful for routine, straightforward characterization of surfaces. However, if detailed information about adsorption mechanisms is required, adsorption isotherms must be analyzed. The SAI approach is entirely relative. Standard surfaces must be available. These

standard surfaces must be identical to the unknown surfaces in all respects save the property being evaluated. The good results found with stearic acid modified surfaces were due in great part to availability of good standard surfaces.

Gas adsorption characterization of surfaces modified with stearic acid vapors tend to confirm many ideas proposed by earlier workers (72-74). Water repellent, chemisorbed modified surfaces affect SAI values only to degree of POML coverage. The water repellency, therefore, is probably due to hydrocarbon tails of the anchored molecules sweeping out hemispheres and cones of coverage, effectively shielding the surface from liquid water. Gaseous adsorbate molecules can elude these tails and reach the surface. Physisorbed acid dimers must also be oriented in a "standing up" configuration. Dimerized carboxyl groups provide points of interaction with the surface. If the physisorbed molecules were "lying down" on the surface, effective coverage should have been higher than the observed 40% increase above POML coverage.

Permanent anchoring of the stearic acid molecule is necessary for water repellency. None of the physisorbed modified fibers were water repellent, even when fully covered with stearic acid. Chemical bonds are necessary to prevent the molecular overturning first proposed by Yiannos (75). Gaseous adsorbate molecules, however, are incapable of overturning physisorbed molecules or otherwise displacing them from the surface. That is, overturning is not possible when there is no bulk liquid phase into which amphipathic molecules can overturn.

Chemisorbed stearic acid molecules, however, do affect hexanol adsorption to a greater extent than physisorbed stearic acid dimers. Chemisorbed acid molecules eliminate the initial clustering of adsorbed hexanol molecules at

lower stearic acid coverage than do physisorbed dimers. The most likely explanation for this is probably that hexanol molecules are able to slightly displace (push aside) physisorbed dimers and form clusters. Chemisorbed acid molecules do not move aside so hexanol clusters are not able to form. Eventually, physisorbed coverage becomes high enough that dimers are not easily displaced. At this point the adsorbed stearic acid phase is probably continuous. Adsorbed dimers can no longer be pushed aside by hexanol molecules and clustering is prevented. Of course, elimination of clustering may be due to the presence of chemisorbed species at higher physisorbed coverage. At and above 50% stearic acid coverage about 0.02 POML chemisorbed molecules are present.

Physisorbed stearic acid displacement at low acid coverage may also occur by a solution-evaporation effect caused by adsorbate. The injected adsorbate plug might act as a solvent, dissolving adsorbed stearic acid. As the adsorbate vaporized, stearic acid would remain in solution and be concentrated at the point of final evaporation. This process would result in an increase of uncovered cellulose. At high enough stearic acid coverage, the injection would not be as effective in this mechanism. An injection could only dissolve a given amount of acid. At higher coverages redistribution of acid would produce little change in effective surface coverage. Chemisorbed molecules, of course, could not enter solution.

This solvation-evaporation mechanism would result in a redistribution of physisorbed stearic acid on fiber surfaces. If this occurred to any great extent, adsorbate behavior would change with each injection. Since no such changes were noted, this mechanism cannot be too important. Stearic acid redistribution would be most likely on the first inch or so of the column

packing material where adsorbate injections would initially condense as a plug. Solvation effects would become important if a great many very large injections (>100 μL) were made for some reason on a surface covered with physisorbed stearic acid.

EXTENSION TO LIQUID SYSTEMS

The chromatographic approach to surface characterization presented in this work could be extended directly to liquid systems. Either regular column chromatography or high pressure liquid chromatography (HPLC) could be utilized. Chromatograms would probably be quite similar to gas chromatograms. However, diffusion of adsorbate molecules in the liquid phase would be much slower than in gaseous systems. In gas chromatography, diffusion was considered to be much more rapid than the adsorption-desorption process and did not have to be considered. In liquid systems diffusion times would have to be measured or estimated. Diffusion broadening of chromatographic peaks would have to be accounted for if adsorption isotherms were to be calculated.

The relative SAI approach for surface characterization would not require such an exact treatment. For example, adsorbates such as polyethylene oxide or other polymeric molecules could be characterized as to relative degree of interaction with various cellulosic fiber surfaces by the SAI approach.

SUMMARY OF CONCLUSIONS

Surface adsorption index (SAI) values calculated directly from gas chromatographic retention volumes gave a useful characterization of cellulose fiber surfaces.

SAI values are sensitive to adsorbate-adsorbent interactions. They reflect adsorbent surface areas and both general and specific adsorbate-surface interactions.

The SAI approach is a relative method. Standard surfaces must be available for comparison with unknown surfaces. Usefulness of an SAI characterization will depend upon proper choice of both standard surfaces and adsorbates. The SAI approach characterizes an adsorbent surface as to degree of interaction with an adsorbate relative to a standard surface of known properties.

For cotton fibers partially covered with stearic acid SAI characterization was more useful for following changes in coverage of fiber surfaces with stearic acid than parameters calculated by traditional isotherm analysis techniques.

Decane SAI values were directly proportional to coverage of cellulose fiber surfaces with physisorbed stearic acid. Traditional isotherm analysis of these surfaces by calculation of isosteric heats and entropies of adsorption, investigation of adsorbate spreading pressure behavior, or calculation of adsorptive site energy distributions produced no parameter which was proportional to stearic acid surface coverage.

SAI values, however, gave no details about the exact nature of adsorption processes. Hexanol SAI values on the series of stearic acid modified cellulose fiber surfaces indicated a change in adsorption mechanism for surfaces more than half covered with physisorbed stearic acid. It was necessary to calculate

isosteric heats and entropies of adsorption from adsorption isotherms to elucidate this change in mechanism.

For cellulose surfaces less than half covered with physisorbed stearic acid, hexanol molecules initially clustered together during adsorption of 0.1 to 0.5 monolayer. This initial clustering was eliminated on surfaces more than half covered with physisorbed stearic acid.

Chemisorbed stearic acid was necessary for water repellency to develop in cellulose fibers. Coverage of 28% of the fiber surface with chemisorbed acid produced complete water repellency. However, gaseous adsorbate molecules could still reach the surface, eluding the chemisorbed acid tails which protect the surface from liquid water.

Chemisorbed stearic acid was more effective at eliminating initial clustering of adsorbed hexanol molecules than physisorbed stearic acid of an equal percent coverage.

POSSIBLE APPLICATIONS AND SUGGESTIONS FOR FURTHER WORK

Self-sizing of absorbent materials is often a problem. This phenomenon is usually attributed to fatty and resin acids diffusing from ray cells and resin canal fragments present with the pulp fibers. Self-sizing often takes some time to develop. Absorbent materials leaving a mill are sometimes water repellent when received by a customer. This time dependency is undoubtedly due to a combination of diffusion processes and slow chemical esterification reactions. SAI studies of stearic acid modified fibers are, in fact, evaluating the self-sizing potential of these fibers. None of the physisorbed modified fibers is water repellent, but all of the fibers would develop water repellency with time.

Gas chromatographic SAI characterization might therefore be useful for evaluating self-sizing potentials of pulp fibers. Standard surfaces would have to be fibers or paper "confetti" which had been extracted to remove all fatty and resin acids. Comparison with this standard would indicate the presence of physisorbed fatty acids on the surfaces of unsized fibers. Diffusion of fatty acids onto fiber surfaces from ray cells could also be monitored. Perhaps fatty and resin acids are physisorbed on fiber surfaces in the dryer section. The time dependency of self-sizing may be primarily due to the slow esterification reaction.

Selection of proper adsorbate for a self-sizing study would be important. Decane SAI differences would be small, requiring careful measurement. Hexanol SAI changes would be much larger. However, hexanol SAI values are not directly proportional to coverage of fiber surfaces by fatty acids due to clustering of hexanol molecules. Hexanol is both a hydrogen bond doner and acceptor which facilitates clustering behavior. A compound like 2-octanone can function only as a hydrogen bond acceptor. This compound might well be a better adsorbate

for characterizing surfaces as to fatty acid coverage. SAI changes would be expected to be large but clustering may be eliminated. Octanone behavior on stearic acid modified surfaces would have to be checked to determine the suitability of this adsorbate.

Future work with the adsorption chromatograph would be much easier if a strip chart recorder fitted with a Disc integrator were used. This would eliminate the need for separate peak area measurements. Detector sensitivity could be easily measured and monitored on a continuous basis. Since there is no bleed-off of liquid phase, chromatograph base line is quite stable. A Disc integrator would be ideal for application to such a system.

The configuration of precipitated rosin size on fiber surfaces may possibly lend itself to characterization by SAI values. Sometimes rosin sizing results in poor water repellency. This may be due to failure of the precipitated aluminum-rosin size particles to adhere properly to fiber surfaces. Or the rosin-aluminum hydroxide material may "ball up" due to improper sizing conditions. Evenly distributed sizing materials which are easily displaced by water may well shield the fiber surfaces from gaseous adsorbate molecules, just like physically adsorbed stearic acid. SAI characterization may be able to distinguish between these two extremes in precipitated rosin size configuration.

Evaluation of pitch in pulps may also be possible by a slight modification of the SAI procedure. An adsorbate like benzene would be capable of penetrating and absorbing into pitch particles. Benzene SAI values would be measured at two different flow rates on pulp fibers or confetti containing pitch particles. SAI values could be much higher at the slower flow rate due to penetration into pitch particles. Fibers which had been extracted with alcohol-benzene to remove all pitchy materials would serve as the standard surface. A series of pulps

with known concentrations of pitch particles could be evaluated. A correlation between pitch content and SAI increase would probably be possible.

Evaluation of fiber surfaces for lignin and hemicellulose content should also be possible. A system of model compounds and standard surfaces would have to be developed. Adsorbates which preferentially interact with lignin and/or hemicellulosic compounds would be desirable. These adsorbates could preferentially adsorb, penetrate, or chemically react with lignin or hemicellulose areas on fiber surfaces. Haselton (7), for instance, found that carbon dioxide was absorbed by lignin. This suggests that carbon dioxide might be a good adsorbate for evaluation of lignin areas on fiber surfaces by the approach previously outlined for pitch evaluation. Chlorine would be an adsorbate capable of chemical reactions with lignin.

All future work with the SAI approach will have to make use of carefully selected and evaluated standard surfaces. Although SAI values are quickly measured, interpretation of these indices is possible only relative to standard surfaces of known composition. Proper selection of adsorbates with low saturation vapor pressures and other properties leading to maximized interaction with certain specific areas of cellulose fiber surfaces is also important.

Kinetics of stearic acid vapor-phase sizing could possibly be studied by gas chromatography. Although the SAI approach could probably not be used directly, a brief presentation of some possible approaches will be made. Fibers fully covered with physisorbed, tagged stearic acid would exchange tagged material with an injection of untagged acid. As chemisorption proceeded on the fiber surfaces, less of the tagged material would be available for exchange. The ratio of tagged to untagged material in the eluted injection would be determined by first passing the carrier gas flow through a proportional Geiger

tube followed by a flame ionization detector. The rate of chemisorption should be proportional to the rate of change of tagged to untagged stearic acid in an injection of initially untagged stearic acid. The monomer-dimer equilibrium constant could be determined by similar experiments with injections of tagged acid into fibers covered with untagged stearic acid. Activity would disappear due to incorporation of tagged monomers into physisorbed dimers. Amount of tagged acid incorporated would depend on injections size. Thus different sized injections of tagged acid could be used to determine the monomer-dimer equilibrium.

The Rudzinski approach to evaluation of adsorptive site energy distributions does not produce a particularly useful characterization of fiber surfaces as to stearic acid coverage. However, this type approach is conveniently applied to chromatographic data and is the only practical approach for complex organic adsorbates. Perhaps a very general mathematical model of a chromatographic column from the standpoint of adsorption could be developed. No attempt would be made to model a chromatography column in detail. The column can be assumed to be a system which causes a great many adsorption-desorption cycles to occur on an average injected adsorbate molecule. The elution chromatogram is the distribution of retention times of injected molecules. As such it is definitely log-normal in shape for small injections of strongly adsorbed material. It may be possible to combine DeBoer's equation for surface residence time of adsorbed molecules (11), a general parameter for adsorbate lateral interactions, and adsorbent surface area to produce an equation for the elution chromatogram. Fitting experimental data to this equation would give parameters characterizing the surface.

NOMENCLATURE

A^2 = square Angstrom unit

D = gas chromatograph detector sensitivity

N = adsorbate molecules injected/adsorbed

N_{ads} = adsorbate molecules in adsorbed phase

N_{gas} = adsorbate molecules in gas phase

OD = outside diameter

P_o = adsorbate saturation vapor pressure

P/P_o = adsorbate partial pressure

POML = planar oriented monolayer

R = ideal gas constant

RH = relative humidity

S = specific surface area

S_a = gas chromatogram chart area corresponding to amount adsorbed

SAI = surface adsorption index

T = absolute temperature

U' = Ross-Olivier mean adsorptive potential energy

V_m = volume of adsorbed gas at monolayer coverage

V_β = Ross-Olivier monolayer coverage

V_R = gas chromatogram retention volume

$V_{R_{min}}$ = minimum retention volume

$V_{R_{max}}$ = maximum retention volume

WAN = water-alcohol-nonpolar solvent

c = BET adsorption constant

g = gas chromatograph recorder chart speed

h = gas chromatograph recorder pen height

h_s = maximum pen height occurring at saturation of carrier gas with adsorbate

$\underline{k}$ = Langmuir adsorption constant

$\underline{m}$ = grams adsorbent in gas chromatography column

m^2/g = square meters per gram surface area

nm^2 = square nanometer

$\underline{p}$ = adsorbate vapor pressure

$\underline{r}$ = radius of gas chromatography column

$\underline{w}$ = carrier gas flow rate

$\Delta\overline{H}$ = heat of adsorption

$\Delta\overline{G}$ = Gibbs free energy of adsorption

$\Delta\overline{S}$ = entropy of adsorption

Δh_{vap} = heat of vaporization

Δs_{vap} = entropy of vaporization

Γ^s = surface concentration

$\theta(\underline{P},\underline{T})$ = experimentally observed adsorption isotherm

γ = Ross Olivier heterogeneity parameter

γ' = surface tension

μi = chemical potential

$\mu Ci/mg$ = microcuries per milligram

μL = microliter

θ = surface coverage

$\theta(\varepsilon,\underline{p},\underline{T})$ = localized isotherm function on a subpatch of the surface

σ = standard deviation of the mean

π = spreading pressure

ε = adsorption energy

$\mathcal{f}(\varepsilon)$ = adsorptive site energy distribution function

ACKNOWLEDGMENTS

The successful completion of a Ph.D. thesis is far from an easy task. The author is indebted to a great many people for their time and efforts which aided this project. Above all, thanks to the Chairman of the Advisory Committee, John W. Swanson, who provided the initial direction, continued guidance and enthusiastic encouragement throughout the course of this work. Special thanks are also due Lynden Stryker and Rajai Atalla, the other members of the Thesis Advisory Committee. Thanks also to Donald Johnson who initially served on the Advisory Committee.

In no small way, every member of the Institute faculty and staff, past and present, contributed to this work. I would like to thank faculty members for the excellent course work presented to me during my stay at the Institute. Special thanks are due to members of A-200 preparation for research problem committees. This phase of my education was unique, challenging, and will be long remembered. While it is impossible to acknowledge every member of the staff who aided me individually, special recognition is given to John Bachhuber for computer assistance; Fred Sweeney and Don Beyer for photography work; Keith Hardacker for electronic assistance; John Carlson for help with the microcomparator; and Marvin Filz and Paul Van Rossum for assistance with shop work.

The financial support of the Institute and its member companies is deeply appreciated.

LITERATURE CITED

1. Brunauer, S. The adsorption of gases and vapors. Vol. I, Chap. 3. Physical adsorption. Princeton, N.J., Princeton University Press, 1945. 505 p.

2. Papanu, S. Surface structure of kaolinite from the detailed analysis of gas/solid adsorption isotherms. Doctor's Dissertation. Troy, N.Y., Rensselaer Polytechnic Institute, 1976. 87 p.

3. Grace, N. H. and Maass, O., J. Phys. Chem. 36:3046(1932).

4. Salley, D. J., Textile Res. 5:493(1935).

5. Emmett, P. H. and DeWitt, T., Ind. Eng. Chem., Anal. Ed., 13:28(1941).

6. Hunt, C. M., Blaine, R. L., and Rowen, J. W., J. Res. Natl. Bur. Std. 43:547(1949).

7. Haywood, G., Tappi 33:370(1950).

8. Haselton, W. R. An investigation of the adsorption of gases by wood and its components and of gas adsorption techniques as a means of studying the area and structure of pulp and paper. Doctor's Dissertation. Appleton, Wis., The Institute of Paper Chemistry, 1953. 172 p.

9. Merchant, M. V. A study of certain phenomena of liquid exchange of water-swollen cellulose fibers and their subsequent drying from hydrocarbons. Doctor's Dissertation. Appleton, Wis., The Institute of Paper Chemistry, 1957. 124 p.

10. Sommers, R. A. A surface-area study of cotton dried from liquid carbon dioxide at zero surface tension. Doctor's Dissertation. Appleton, Wis., The Institute of Paper Chemistry, 1963. 157 p.

11. DeBoer, J. H. The dynamical character of adsorption. Oxford, England, Calendon Press, 1953. 239 p.

12. Claesson, S., Arkiv. Kemi. 23A:1(1946). Work cited In Littlewood's Gas chromatography.

13. James, A. T. and Martin, A. J. P., Biochem. J. 50:679(1952). Work cited In Littlewood's Gas chromatography.

14. Littlewood, A. B. Gas chromatography. 2nd ed., Chap. 3. New York, N.Y., Academic Press, 1970. 546 p.

15. Braun, J. M. and Guillet, J. E., Adv. Polymer Sci. 21:107(1976).

16. Gray, D. G., Prog. Polymer Sci. 5:1-60(1977).

17. Littlewood, A. B., op. cit., Chap. 4.

18. Kiselev, A. V. and Yashin, Y. I. Gas adsorption chromatography. New York, N.Y., Plenum Press, 1969. 254 p.

19. Brunauer, S., Deming, L. S., Deming, W. E., and Teller, E. J., J. Am. Chem. Soc. 62:1723(1940).

20. Gregg, S. J. and Sing, S. W. Adsorption, surface area, and porosity. New York, N.Y., Academic Press, 1967. 371 p.

21. Glueckauf, E., J. Chem. Soc. 187:1302(1947).

22. Kiselev, A. V. and Yashin, Y. I., op. cit., Chap. 4.

23. Gregg, S. J. The surface chemistry of solids. Chap. 8. New York, N.Y., Reinhold, 1961.

24. Huber, J. F. K. and Gerritse, R. G., J. Chromat. 58:137(1971).

25. Sevcik, J., J. Chromat. 135:183(1977).

26. Vink, H., J. Chromat. 135:1(1977).

27. Dollimore, D., Heal, G. R., and Martin, D. R., J. Chromat. 50:209(1970).

28. Gray, D. G. and Guillet, J. E., Macromols. 5:316(1972).

29. Courval, G. J. and Gray, D. G., Macromols. 8:916(1975).

30. Brunauer, S., op. cit., p. 120-39, Chap. 11.

31. Brunauer, S., op. cit., Chap. 5.

32. Langmuir, I., J. Am. Chem. Soc. 38:2221(1916).

33. Brunauer, S., Emmett, P. H., and Teller, E. J., J. Am. Chem. Soc. 66:309 (1938).

34. Ross, S. and Olivier, J. P. On physical adsorption. New York, N.Y., Interscience, 1964. 401 p.

35. Barber, H. A. The determination of the site energy distribution of the surface of cellulose fibers by gas adsorption methods. Doctor's Dissertation. Appleton, Wis., The Institute of Paper Chemistry, 1968. 107 p.

36. Brown, G. W. Adsorptive potential distributions for water dried cellulose. Doctor's Dissertation. Appleton, Wis., The Institute of Paper Chemistry, 1972. 304 p.

37. Hoory, S. E. Adsorption of gases on homogeneous and heterogeneous surfaces. Doctor's Dissertation. Berkeley, Calif., The University of California, 1966. 165 p.

38. Ross, S. and Morrison, I. D., Surface Sci. 52:103(1975).

39. House, W. A. and Jaycock, M. J., J. Colloid Interface Sci. 59:252(1977).

40. Adamson, A. W. and Ling, I., Adv. Chem. Ser. 33:51(1961).

41. Mohlin, U. B. and Gray, D. G., J. Colloid Interface Sci. 47:747(1974).

42. Tremain, P. R. and Gray, D. G., J. Chem. Soc., Faraday Trans. I 71:2170 (1975).

43. Tremain, P. R., Mohlin, U. B., and Gray, D. G., J. Colloid Interface Sci. 60:548(1977).

44. Gray, D. G., Trans. 6th Symp. Fiber-Water Interactions (Oxford), 1977.

45. Rudzinski, W., Suprynowicz, Z., Waksmundzki, A., and Rayss, J., J. Chromat. 91:67(1974).

46. Suprynowicz, Z., Waksmundzki, A., Rudzinski, W., and Leboda, R., J. Chromat. 92:9(1974).

47. Rudzinski, W., Waksmundzki, A., Leboda, R., and Suprynowicz, Z., J. Chromat. 92:25(1974).

48. Hobson, J. P. and Armstrong, R. A., J. Phys. Chem. 67:2000(1963).

49. Hobson, J. P., Can. J. Phys. 43:1934(1965).

50. Hobson, J. P., Can. J. Phys. 43:1941(1965).

51. Harris, L. B., Surface Sci. 10:129(1968).

52. Harris, L. B., Surface Sci. 13:377(1969).

53. Van Dongen, R. H., Surface Sci. 39:341(1973).

54. Van Dongen, R. H. and Broekhoff, C. P., Surface Sci. 18:462(1969).

55. Dash, J. G. Films on solid surfaces. New York, N.Y., Academic Press, 1975.

56. Davis, B. W. and Pierce, C., J. Phys. Chem. 70:1051(1966).

57. Nonaka, A. and Ishizaki, E., J. Colloid Interface Sci. 62:381(1977).

58. Adamson, A. W., Ling, I., Dormant, L. M., and Orem, M., J. Colloid Interface Sci. 21:445(1966).

59. Adamson, A. W. Physical chemistry of surfaces. 2nd ed. New York, N.Y., Interscience, 1967. 747 p.

60. Morrison, J. W. and Ross, S., Surface Sci. 62:331(1977).

61. Waksmundzki, A., Jaroniec, M., and Suprynowicz, Z., J. Chromat. 110:381 (1975).

62. Sokalowski, J. and Jaroniec, M., Surface Sci. 47:492(1975).

63. Rudzinski, W., Jaroniec, M., and Sokalowski, J., Surface Sci. 54:189(1976).

64. Waksmundzki, A. and Rayss, J., J. Chromat. 119:557(1976).

65. Deitrich, W. H. A comparison of adsorptive potential energies for argon and nitrogen adsorption on the surface of cellulose fibers. Doctor's Dissertation. Appleton, Wis., The Institute of Paper Chemistry, 1970. 181 p.

66. Thode, E. F. and Guide, R. C., Tappi 42:35(1959).

67. Robertson, A. A., Pulp Paper Mag. Can. 65:T171(1964).

68. Robertson, A. A., Tappi 53:1332(1970).

69. Craver, J. K., J. Appl. Polymer Sci. 14:1755(1970).

70. Nelson, F. M. and Eggertsen, F. T., Analytical Chem. 30:1387(1958).

71. Stone, J. E. and Nickerson, L. F., Pulp Paper Mag. Can. 64:T155(1963).

72. Tremain, P. R. and Gray, D. G., Analytical Chem. 48:380(1976).

73. Ferris, J. L. The wettability of cellulose film as affected by vapor-phase adsorption of amphipathic molecules. Doctor's Dissertation. Appleton, Wis., The Institute of Paper Chemistry, 1974. 154 p.

74. Swanson, R. E. The influence of molecular structure of vapor phase chemisorbed fatty acids present in fractional monolayer concentrations on the wettability of cellulose film. Doctor's Dissertation. Appleton, Wis., The Institute of Paper Chemistry, 1976. 153 p.

75. Yiannos, P. N. Molecular reorientation of some fatty acids when in contact with water. Doctor's Dissertation. Appleton, Wis., The Institute of Paper Chemistry, 1960. 115 p.

APPENDIX I

CALCULATION OF ADSORPTION ISOTHERMS FROM GAS CHROMATOGRAMS

Glueckauf (20), Gregg (22), Huber and Gerritse (23), and Kiselev and Yashin (21) have all developed mathematical relations between diffuse boundaries of elution chromatograms and the corresponding adsorption (or solution) isotherm. The following derivation is primarily the approach of Kiselev and Yashin.

Although gas chromatography is a kinetic process, it must be assumed that instantaneous (relatively) equilibrium is established between the adsorbed and gaseous phases. Calculation of adsorption isotherms from gas chromatographic data also assumes that broadening of chromatographic peaks is due entirely to deviation from a linear Henry isotherm. Diffusion and kinetic peak broadening are assumed to be negligible. The adsorption isotherm relates $\underline{a}$, the quantity adsorbed, and $\underline{c}$, the adsorbate concentration. That is, $\underline{a} = \Phi(\underline{c})$. Since $\underline{p} = n\underline{RT}/\underline{v}$, and $\underline{c} = n/\underline{v}$, $\underline{p} = \underline{cRT}$ where $\underline{p}$ is the partial pressure of the adsorbate, the adsorption isotherm is most generally expressed as $\underline{a} = f(\underline{p})$.

To derive an expression for $\underline{a} = \Phi(\underline{c})$, consider the material balance for an elementary layer of adsorbate in carrier gas moving over the adsorbent surface (Fig. 25).

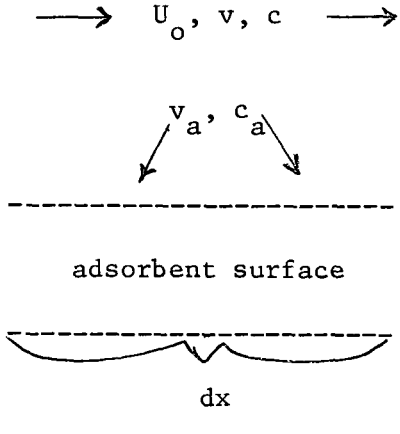

Figure 25. Elementary Layer in Gas Adsorption Chromatography

A material balance (21) gives:

$$U_o v\left(\frac{\partial c}{\partial x}\right) = v\left(\frac{\partial c}{\partial t}\right)x + v_a\left(\frac{\partial c_a}{\partial t}\right)_x \qquad (12)$$

This material balance represents the change in adsorbate concentration in the carrier gas across a length of the column at any given time as equal to the sum of adsorbate concentration changes in the gas and adsorbed phases with time at any fixed point along the column. Dividing both sides of the material balance by $(\partial c/\partial t)_x$ yields:

$$\frac{U_o v\left(\frac{\partial c}{\partial x}\right)t}{\left(\frac{\partial c}{\partial t}\right)_x} = \frac{v\left(\frac{\partial c}{\partial t}\right)_x}{\left(\frac{\partial c}{\partial t}\right)_x} + \frac{v_a\left(\frac{\partial c}{\partial t}\ a\right)_x}{\left(\frac{\partial c}{\partial t}\right)_x}$$

Since at any fixed location along the column, $x = x_i$, partial derivatives may be treated as exact functions:

$$\left(\frac{\partial c}{\partial t}\right)_x = \left(\frac{\partial c}{\partial x}\right)_t \left(\frac{\partial x}{\partial t}\right)_c ,$$

and

$$\left(\frac{\partial c_a}{\partial t}\right) \Big/ \left(\frac{\partial c}{\partial t}\right)_x = \left(\frac{\partial c_a}{\partial c}\right)_x$$

Then:

$$\frac{U_o v\left(\frac{\partial c}{\partial x}\right)_t}{\left(\frac{\partial c}{\partial x}\right)_t \left(\frac{\partial x}{\partial t}\right)_c} = v + v_a\left(\frac{\partial c_a}{\partial c}\right)_x$$

$$\frac{U_o v}{\left(\frac{\partial x}{\partial t}\right)_c} = v + v_a\left(\frac{\partial c_a}{\partial t}\right)_x$$

Let: $(\partial x/\partial t)_c = U_c$ - the linear velocity of a point of constant c:

$$\frac{U_o v}{U_c} = v + v_a\left(\frac{\partial c_a}{\partial c}\right)_x \qquad (13)$$

The term $\left(\frac{\partial c_a}{\partial c}\right)_x$ represents the slope of the adsorption isotherm at concentration c (read: "the change in concentration of the adsorbed phase with change in adsorbate concentration in the gas phase"). In terms of a, the amount

adsorbed, c, the adsorbate concentration, and x, the mass of adsorbent, $v_a(\frac{\partial c_a}{\partial c})_x$ may be replaced by $m\, da/dc$ (21) yielding:

$$\frac{U_o v}{U_c} = v + m\frac{da}{dc}$$

$$\frac{da}{dc} = \frac{vU_o - vU_c}{mU_c} = \frac{v}{m}\left(\frac{U_o}{U_c} - 1\right) \tag{14}$$

The term U_o/U_c is the ratio of carrier gas velocity to the velocity of a point of given concentration of adsorbate. The velocities are inversely proportional to retention time, i.e.: the faster moving component (carrier gas) has a shorter retention time than the slower moving adsorbate. Thus:

$$\frac{da}{dc} = \frac{v}{m}\left(\frac{t_c}{t_o} - 1\right) = \frac{v}{mt_o}(t_c - t_o) = \frac{w}{m}(t_c - t_o),$$

where t_c = retention time of adsorbate at concentration c

t_o = retention time of nonadsorbed gas moving at carrier gas velocity i.e., the "retention time" of a differential volume of carrier gas

$w = v/t_o$ = the flow rate of carrier gas

Let $V_c = w(t_c - t_o)$ be the retained volume of adsorbate at concentration c. Now:

$$\frac{da}{dc} = \frac{V_c}{m}$$

and

$$a = \frac{1}{m}\int_o^c V_c\, dc \tag{15}$$

Equation (15) gives "a" as a function of c, i.e., the adsorption isotherm. In order to calculate an isotherm form quantities recorded on the gas chromatograph chart, it is necessary to derive the integral of Eq. (15) in terms of detector reading and chart speed. The recorder response, h, is usually proportional to c:

$$c = kh, \tag{16}$$

in which k is a constant for a given compound and a given sensitivity range of the detector. By injecting an accurately measured amount of adsorbate, m_a, a corresponding peak is produced on the recorder chart:

$$m_a = \int_0^\infty c\,dV,$$

where V is the volume of gas flowing through the column while the limits of integration correspond to injection and complete elution. Application of Equation (16) gives:

$$m_a = k \int_0^\infty h\,dV \tag{17}$$

The recorder chart is calibrated in units of length, z. The chart speed, q, is:

$$q = \frac{dz}{dt} \tag{18}$$

The flow rate of the carrier gas, w, is:

$$w = \frac{dV}{dt} \tag{19}$$

Combining Equations (18) and (19) gives:

$$w = \frac{dV}{dt} \qquad q = \frac{dz}{dt}$$

$$dV = w\,dt \qquad dt = dz/q$$

$$dV = \frac{w}{q}\,dz \tag{20}$$

Substitution of Equation (20) into Equation (17) gives:

$$m_a = k \int_0^\infty h \frac{w}{q}\,dz = \frac{kw}{q} \int_0^\infty h\,dz = \frac{kw}{q} S, \tag{21}$$

where $S = \int_0^\infty h\,dz$ = the area of the peak.

The calibration constant may now be expressed as:

$$k = \frac{m_a q}{Sw} \tag{22}$$

Looking now at Equation (15) for the adsorption isotherm:

$$a = \frac{1}{m} \int_o^c V_c \, dc \tag{15}$$

Let $dc = k\,dh$ — from differentiation of Equation (16) and

$$V_c = w\,(t_c - t_o) = \frac{w}{q}\,(z_h - z_o),$$

Where $(z_h - z_o)$ is the distance on the chart from the point of emergence of an unadsorbed component to the point on the chart where adsorbate of concentration c (deflection h) elutes, then:

$$a = \frac{1}{m} \int_o^h \frac{w}{q}\,(z_h - z_o)\,k\,dh = \frac{kw}{mq} \int_o^h (z_h - z_o)\,dh \quad a = \frac{kw}{mq}\,S_a, \tag{23}$$

in which m = mass of adsorbent

$S_a = \int_o^h (z_h - z_o)\,dh$ — the area on the chart between the axis of h at $z = z_o$ and the edge of the peak (see Fig. 3)(p. 15)

Substitution of Equation (22) into Equation (23) for the value of k yields:

$$a = \frac{kw}{mq}\,S_a \quad (23) \qquad k = \frac{m_a q}{Sw} \quad (22)$$

$$a = \frac{m_a S_a}{m\,S} \tag{24}$$

The term m_a/S is simply the detector "sensitivity," i.e., the chart area traced out by a given amount, m_a (or 1 μmole) of injected adsorbate. If $D = m_a/S$, then Equation (24) becomes:

$$a = \frac{DS_a}{m} \tag{25}$$

The corresponding c follows directly:

$$c = k\,h \tag{16}$$

$$k = \frac{m_a\,q}{S\,w} \tag{22}$$

$$c = \frac{m_a\,q\,h}{S\,w} = \frac{D\,q\,h}{w} \tag{26}$$

If vapor pressure is desired:

$$p = c\,R\,T$$

$$p = \frac{D\,q\,h\,R\,T}{w} \tag{27}$$

Detector sensitivity is usually expressed as chart area per micromole, $D' = S/m_a$. With this definition of D' Equations (25) and (27) become:

$$a = \frac{S_a}{mD'} \tag{28}$$

$$p = \frac{q\,h\,R\,T}{w\,D'} \tag{29}$$

To calculate an isotherm in terms of a vs. p, Equations (28) and (29) are applied to gas chromatographic data. The resulting units of vapor pressure are millimeters mercury. The relative partial pressure may be calculated from the ratio of h/h_s, where h_s is the recorder pen response to a very large sample injection which saturates the carrier gas with a concentration of adsorbate corresponding to the vapor pressure of the adsorbate at column temperature.

NOMENCLATURE FOR APPENDIX I

D, D' = detector sensitivity

R = ideal gas constant

S = total peak area of known amount of injected adsorbate

S_a = chart area corresponding to amount adsorbed

T = absolute temperature

U_o = linear velocity of carrier gas

U_c = linear velocity of a point of constant adsorbate concentration

V = total volume of gas flowing through column

V_c = retained volume of adsorbate at concentration c

a = amount of adsorbed adsorbate

c = concentration of adsorbate in gas phase

c_a = concentration of adsorbate in adsorbed layer

$f(p)$ = the adsorption isotherm as a function of adsorbate pressure

h = recorder pen height

k = sensitivity constant for adsorbate

m = adsorbent mass in column

m_a = amount of adsorbate injected

p = adsorbate vapor pressure

q = recorder chart speed

t = time elapsed from injection of sample

t_o = retention time of nonadsorbed gas

t_c = adsorbate retention time at concentration c

v = volume of gas phase in column

v_a = volume of adsorbed layer

w = carrier gas flow rate

$\underline{x}$ = distance along column

$\underline{z}$ = length units of recorder chart

$\Phi(\underline{c})$ = adsorption isotherm as a function of adsorbate concentration

APPENDIX II

CALCULATION OF ADSORPTIVE SITE ENERGY DISTRIBUTIONS FROM GAS CHROMATOGRAMS BY THE RUDZINSKI APPROACH

The adsorbent surface is assumed to be of a patchwork nature. Each subpatch is considered to be heterogeneous and unique from all other subpatches. Henry's Law is obeyed in the limiting case of extremely low adsorbate pressure. Hobson's application of the condensation approximation (48) is used for the special case of no adsorbate lateral interactions. In this application the Langmuir isotherm is approximated by a linear function. Although not stated as such, Rudzinski's approach assumes ideal gas behavior of the adsorbate, both in the gas phase and the adsorbed state.

The local isotherm function, $\theta(\varepsilon, p, T)$, on each small patch of surface with energy ε_i follows the relation:

$$\theta_i(\varepsilon,p,T) = \frac{p}{K} \exp\left(\frac{\varepsilon_i}{RT}\right) \quad \text{for } p<p'_i, \tag{30}$$

$$\theta_i(\varepsilon,p,T) = 1 \quad \text{for } p>p'_i, \tag{31}$$

$$p'_i = K\exp(-\varepsilon_i/RT), \tag{31a}$$

where $K = 1.76 \times 10^4 (MT)^{1/2}$

M = adsorbate molecular weight

The term p'_i is the adsorbate pressure above which the extremely small localized patch is completely covered. This treatment, therefore, approximates the Langmuir isotherm at pressures below p'_i and should be employed only at very low surface coverages. Multilayer coverage is accounted for indirectly, by assuming that a covered patch of surface in effect simply becomes a new patch for adsorption.

In the case of no adsorbate lateral interactions, Hobson's approach yields:

$$\chi(\varepsilon) = -\left(\frac{\partial \theta_t}{\partial \varepsilon}\right)_T - RT \left(\frac{\partial^2 \theta_t}{\partial \varepsilon^2}\right)_T \tag{32}$$

In order to be able to determine $\chi(\varepsilon)$ (the frequency of a particular site energy) from pressure data, Equation (31) is applied. This relates adsorbate vapor pressure and adsorptive site energy through the condensation approximation.

$$p'_i = K \exp\left(-\varepsilon_i/RT\right) \tag{31a}$$

Solving for ε_i in terms of p'_i gives:

$$\varepsilon_i = -RT \ln\left(p'_i/K\right) \tag{33}$$

Now, consider the interval $i \rightarrow i + \Delta i$ to become so small that a continuous distribution of energies and pressures results. This case will apply for a highly heterogeneous surface such as cellulose.

$$\varepsilon = -RT \ln\left(p/K\right) \tag{34}$$

$$\left(\frac{\partial \varepsilon}{\partial p}\right)_T = -\left(RT/p\right) \tag{35}$$

Using Equation (35) to calculate $\chi(\varepsilon)$ from pressure data via Equation (32) yields:

$$\chi(\varepsilon) = -\left(\frac{\partial \theta_t}{\partial \varepsilon}\right)_T - RT \left(\frac{\partial^2 \theta_t}{\partial \varepsilon^2}\right)_T \tag{36}$$

Applying the chain rule:

$$\chi(\varepsilon) = -\left(\frac{\partial \theta_t}{\partial p}\right)_T \left(\frac{\partial p}{\partial \varepsilon}\right)_T - RT \left\{\frac{\partial}{\partial p}\left[\left(\frac{\partial \theta_t}{\partial p}\right)_T \left(\frac{\partial p}{\partial \varepsilon}\right)\right]\right\} \left(\frac{\partial p}{\partial \varepsilon}\right)_T \tag{37}$$

Now:

$$\left(\frac{\partial p}{\partial \varepsilon}\right)_T = \frac{1}{\left(\partial \varepsilon/\partial p\right)_T} = -\,p/RT \tag{38}$$

Therefore:

$$\chi(\varepsilon) = -\left(\frac{\partial\theta_t}{\partial p}\right)(-p/RT) - RT\left\{\frac{\partial}{\partial p}\left[\left(\frac{\partial\theta_t}{\partial p}\right)_T(-p/RT)\right]\right\}(-p/RT)$$

$$\chi(\varepsilon) = -\left(\frac{\partial\theta_t}{\partial p}\right)(-p/RT) - (-p)\left\{\left[\left(\frac{\partial\theta_t}{\partial p}\right)_T\left(-\frac{1}{RT}\right) = \left(\frac{\partial^2\theta_t}{\partial p^2}\right)(-p/RT)\right]\right\}$$

$$\chi(\varepsilon) = \left(\frac{\partial\theta_t}{\partial p}\right)(p/RT) - \left(\frac{\partial\theta_t}{\partial p}\right)(p/RT) - (p^2/RT)\left(\frac{\partial^2\theta_t}{\partial p^2}\right)$$

$$\chi(\varepsilon) = -p^2/RT\left(\frac{\partial^2\theta_t}{\partial p^2}\right) \tag{39}$$

Equation (39) relates $\chi(\varepsilon)$ to the second derivative of the dependence of total adsorbent surface coverage on adsorbate pressure. As has already been shown in Appendix I, both surface coverage and adsorbate pressure can be calculated from chromatographic data. Following Rudzinski's approach (45-47), retention volume is expressed as the variation in amount adsorbed with pressure:

$$V_R = FRT\,(\partial N_t/\partial p)_T \tag{40}$$

If N_t is the number of molecules adsorbed and θ_t is the fractional coverage, then

$$N_t = \theta_t\, N_\infty\,, \tag{41}$$

where N_∞ = monolayer capacity, a constant. Therefore:

$$\partial N_t = N_\infty\, \partial\theta_t \tag{42}$$

and Equation (40) becomes:

$$V_R = N_\infty\, FRT\left(\frac{\partial\theta_t}{\partial p}\right)_T \tag{43}$$

Differentiating Equation (43) with respect to pressure gives:

$$\left(\frac{\partial V_R}{\partial p}\right)_T = N_\infty\, FRT\left(\frac{\partial^2\theta_t}{\partial p^2}\right) \tag{44}$$

Solving Equation (44) for $(\partial^2\theta_t/\partial p^2)_T$ and substituting into Equation (39) gives:

$$\left(\frac{\partial^2\theta_t}{\partial p^2}\right)_T = \frac{1}{N_\infty FRT}\left(\frac{\partial V_R}{\partial p}\right)_T \tag{45}$$

Now:

$$\chi(\varepsilon) = -\, p^2/RT \left(\frac{\partial^2\theta_t}{\partial p^2}\right)_T \tag{39}$$

$$\chi(\varepsilon) = -\frac{1}{N_\infty F}\,(p/RT)^2 \left(\frac{\partial V_R}{\partial p}\right)_T \tag{46}$$

Let:

$$\chi'(\varepsilon) = N_\infty F\, \chi(\varepsilon),$$

then:

$$\chi'(\varepsilon) = -\,(p/RT)^2 \left(\frac{\partial V_R}{\partial p}\right)_T \tag{47}$$

Equation (47) can be used to calculate the adsorptive site energy distribution from a plot of retention volume vs. adsorbate pressure. The Rudzinski analysis of gas chromatographic retention data to give adsorptive site energy distribution involves many important assumptions. The method would be most applicable to a highly heterogeneous adsorbent at low surface coverages. Rudzinski makes no claims as to the exactness of his approach. Rather, he stresses the speed and accuracy of chromatographic measurements. He suggests the approach could be useful in industrial process control applications involving adsorbent and/or catalytic surfaces which require monitoring.

NOMENCLATURE FOR APPENDIX II

$\underline{F}$ = James-Martin compressibility factor

$\underline{K}$ = adsorbate pressure-energy constant

$\underline{N_t}$ = number of molecules adsorbed

$\underline{N_\infty}$ = number of molecules adsorbed at monolayer coverage

$\underline{R}$ = ideal gas constant

$\underline{T}$ = absolute temperature

$\underline{V_R}$ = gas chromatographic retention volume

$\underline{i}$ = identifier for small localized patch on the adsorbent surface

$\underline{p}$ = adsorbate vapor pressure

$\underline{p'_i}$ = pressure necessary for adsorbate condensation on patch

ε = adsorption energy

$\varepsilon_{\underline{i}}$ = adsorption energy on patch $\underline{i}$

$\theta_{\underline{i}}(\varepsilon,\underline{p},\underline{T})$ = local isotherm function on patch $\underline{i}$

$\theta_{\underline{t}}$ = total, overall observed experimental isotherm

$\chi(\varepsilon)$ = site energy frequency function

$\chi'(\varepsilon)$ = modified site energy frequency function

APPENDIX III

C-14 STEARIC ACID DILUTION

Labeled stearic acid activity	0.24 μ Ci/mg @ 6.3
Cross-sectional area/POML molecule	20 A^2
Surface area of 1 g fibers	0.7 m^2
1 POML on 1 g fibers	3.5×10^{18} molecules stearic acid
Weight fibers analyzed	0.1 g
Minimum detectable POML coverage	0.01 POML
Number stearic acid molecules at 0.01 POML on 0.1 g fibers	3.5×10^{15} molecules stearic acid
1 μCi	2.22×10^{6} cpm @ 6.3
Desire 100 cpm @ 0.01 POML on 0.1 g	4.5×10^{-5} μCi activity
0.01 POML stearic acid on 0.1 g	5.8×10^{-3} μmole stearic acid
Desired stearic acid activity	0.0078 μCi/μmole
	0.0275 μCi/mg
Weight labeled stearic acid	0.37 g
Microcuries labeled stearic acid	89 μCi
Enough for 89/0.0275 =	3236 mg stearic acid
Add 3.0 g unlabeled stearic acid	
Count 1 mg samples prepared by dissolving 10 mg acid in 5 mL benzene. Count 0.5 mL sample	69,029 67,829 ± 0.5% @ 6.3 ± 0.2 quenching constant 72,557
Average	69,805 ± 4%

$$\frac{6.98 \times 10^{4}}{2.22 \times 10^{6}} = 3.14 \times 10^{-2} = 0.031 \text{ μCi/mg activity}$$

Counting rate for 0.01 POML on 0.1 g fiber = 111 cpm @ 6.3

Note — a microcurie is defined as 2.2×10^{6} <u>disintegrations</u> per minute. In this work the term microcurie has been defined as 2.2×10^{6} <u>counts</u> per minute as measured on a Beckman DPM-100 liquid scintillation counter at a quenching

constant of 6.3. As long as all counting is done with this instrument, identical vials, and a quenching constant close to 6.3, this redefinition of the microcurie is inconsequential to the results of the work.

APPENDIX IV

STEARIC ACID SURFACE ANALYSIS

Approximately 0.1 g samples of fibers were analyzed. Fibers were extracted 15 min in boiling benzene or toluene kept at 80°C. Extraction was accomplished by submerging the fibers in solvent contained in a 250 mL beaker on a hot plate. About 200 mL of solvent were used. After extraction, fibers were removed with tweezers, held over the solvent, and rinsed with about 50 mL of solvent. The rinsings fell into the beaker. The fibers were placed in a clean glass evaporating dish to dry. The extraction solvent was concentrated to about 5 mL by boiling on the hot plate. This 5 mL concentrate was carefully poured into a 20 mL counting vial. The beaker was rinsed with about 12 mL of solvent from a plastic squeeze bottle, allowing the rinsings to fill the vial. The contents of the vial were concentrated to about 0.5 mL by boiling on the hot plate.

The dried, solvent extracted fibers were placed in about 200 mL room temperature water for 10-15 min, removed with tweezers, rinsed with water and set aside. The extraction water and rinsings were concentrated to 5 mL in a vacuum flash cyclone evaporator. After transfer to a counting vial, the evaporator was filled with 150 mL water which was then concentrated to 5 mL and added to the vial. The contents of the vial were concentrated to 0.5 mL on a hot plate. Concentration was done below the boiling point to prevent bumping of the vial contents.

The wet, solvent and water extracted fibers were placed in a 150 mL beaker. About 25 mL of 0.1M KOH in methanol were added. The contents of the beaker were boiled 5 min. Fibers were removed with tweezers and rinsed with about 50 mL of methanol, the rinsings falling into the beaker. The contents of the beaker were reduced to about 5 mL by evaporation on a hot plate and

carefully poured into a counting vial. The beaker was rinsed with methanol, the rinsings added to the vial. Total volume in the vial was 12-15 mL. The methanol extract was reduced to about 0.5 mL by evaporation on a small rotary evaporator at 35°C under 20-30 inches mercury vacuum. Initially vacuum was kept low to prevent explosive foaming. After the volume was reduced to about 5 mL, maximum vacuum was applied.

Temperatures of evaporation were minimized as much as possible to prevent loss of volatile stearic acid. Loss was judged to be unimportant unless a vial or beaker was allowed to evaporate to dryness on the hot plate. When this occurred the procedure was repeated. Large volumes of solvent and water were used to insure complete extraction of each type of adsorbed stearic acid. Volumes less than 50 mL were not able to insure removal of all of each phase. Duplicate extractions on one sample with the procedure outlined above gave no activity above background for the second extraction with each solvent. Duplicate samples for Column 7 gave agreement of ±5% for benzene and water extractions and ±8% for basic methanol extraction.

Immediately after concentration each vial was counted. About 20 mL of counting cocktail (composition: 100 g napthalene, 5 g diphenyloxazole, Baker's analyzed dioxane to make 1000 mL) were added to each vial. Activity was counted to a confidence limit of ±2% with a Beckman DPM-100 liquid scintillation counter. Liquid scintillation counting functions by counting flashes of light given off by an organic molecule when hit by a beta particle from decay of a carbon-14 atom. This method is extremely sensitive to species in solution which absorb light or beta particles. A quenching constant was measured for each vial counted. This constant is determined automatically by the counter which positions a cesium-137 source outside the vial. The measured activity is

compared to the known activity. A vial of pure counting cocktail gives a quenching constant of about 6.6.

All samples were counted with a quenching constant of 6.3 ± 0.2. If volume was not evaporated to less than 0.5 mL, quenching constants were lower, indicating interference with scintillation. If more than about 30 min were allowed to pass between addition of cocktail and counting, quenching constants would be around 6.0. The basic methanol extract was most troublesome in this regard. If more than 10-15 min elapsed between concentration to 0.5 mL and counting, quenching constants would be 6.0 or less. A definite yellow color developed in basic extracts 12-15 hr after concentration or addition of cocktail. Quenching constants in these cases were below 3.0. By counting as soon as possible and immediately after addition of cocktail, quenching constants could be kept in the 6.3 region.

Table XII shows results of surface analysis for stearic acid modified adsorbents used in this study.

TABLE XII

RESULTS OF STEARIC ACID ANALYSIS

Column No.	Hours Stearic Acid Treatment	Weight Sample, g	Counts per Minute: Benzene Extract	Water Extract	Base Extract	POML Stearic Acid: On Surface	In Surface	Chemisorbed
14	2.5	0.0663	489	.416	40			
		0.10	738	627	60	0.07	0.06	0.00
11	5	0.0775	1566	916	66			
		0.10	2020	1182	85	0.18	0.11	0.005
12	13	0.0691	1725	1163	132			
		0.10	2496	1683	191	0.22	0.15	0.02
13	15	0.0685	2029	1682	207			
		0.10	2962	2456	302	0.27	0.22	0.02
15	19	0.0530	2041	1366	157			
		0.10	3851	2577	296	0.35	0.23	0.03
8	24	0.0801	4403	2035	187			
		0.10	5497	2541	233	0.50	0.23	0.02
7	144	0.0823	4850	2610	1900			
		0.10	5893	3171	2309	0.53	0.29	0.21
6	130	0.0743	--	--	2099			
benzene,		0.10	--	--	2825	--	--	0.254
water		0.0738	--	--	2428			
extraction		0.10	--	--	3290	--	--	0.296
		Average	--	--		--	--	0.275

APPENDIX V

MEASUREMENT OF SURFACE AREAS WITH INSTITUTE SORPTOMETER

The Institute sorptometer is an equilibrium, flow-through chromatographic device. The approach used for measurement of adsorbent surface areas is the single point comparison with a standard as described by Stone and Nickerson (71). About 0.6 g of adsorbent fibers are packed into a sample tube. Flow gas is 15% nitrogen and 85% helium. The gas flows through the reference arm of a standard gas chromatographic thermal conductivity detector before flowing through the sample tube. After passing through the sample tube the gas flows through the other side of the detector. Any change in composition of the flow gas as a result of adsorption/desorption in the sample tube is detected as an unbalance in the Wheatstone bridge circuit of the detector and recorded on a standard chart recorder.

After packing, the sample tube is connected to the gas flow and allowed to equilibrate at least 15 min in a room temperature water bath. The tube is then slowly immersed in liquid nitrogen. Nitrogen adsorbs, depleting N_2 content of the flow gas until adsorption is complete. Adsorption is recorded as a peak on the chart. After adsorption is complete, as judged by return of the recorder pen to zero, the tube is removed from the liquid nitrogen and replaced in the water bath. Desorption of N_2 occurs, enriching the nitrogen content of the gas flowing from the sample tube. Recorder polarity is reversed and the desorbed gas peak is recorded. Peak areas are measured with a Technicon pen tracing integrator. A standard tube containing 0.7697 g Whatman No. 1 filter paper is run at the beginning and end of each batch of sample tubes. Based on equilibrium, vacuum measurements, this standard is assigned a surface area of 1 m^2/g.

Adsorbed and desorbed chart areas are averaged and proportioned directly to the areas for the standard tube. From adsorbent weight in each sample tube surface areas are calculated as square meter per gram. In the following data some surfaces were run in triplicate determinations of separate tubes. Some were run in triplicate measurements of the same tube. Most stearic acid modified surfaces were run one time on one sample. This was to save time since experience had been gained with the equipment and technique, Tables XIII-XIX.

TABLE XIII

SORPTOMETER SURFACE AREAS FOR ADSORBENT III
WAN DRIED - BEFORE PACKING INTO COLUMNS
JUNE 7, 1977

Tube No.	Weight Adsorbent, g	Adsorbed Chart Area	Desorbed Chart Area	Average	Surface Area, m^2/g	
Reference	0.7697	3664	3888	--	1.00	
III	0.5951	7109	9953	8531	2.92	
I	0.5828	7413	9423	8418	2.94	2.98±0.09
7	0.6695	8462	11,782	10,122	3.08	
Reference	0.7697	3698	3887	3784	1.00	

TABLE XIV

SORPTOMETER SURFACE AREAS FOR ADSORBENT II
WAN DRIED — RESIDUE AFTER PACKING INTO COLUMNS
JUNE 7, 1977

Tube No.	Weight Adsorbent, g	Adsorbed Chart Area	Desorbed Chart Area	Average	Surface Area, m^2/g	
Reference	0.7697	7409	7800	--	1.00	
16	0.5637	6567	8935	7751	1.37	1.33±0.04
17	0.5425	6049	8128	7088	1.30	
Reference	0.7697	7742	8055	7751	1.00	

TABLE XV

SORPTOMETER SURFACE AREAS FOR RAW COTTON
OCTOBER 3, 1977

Tube No.	Weight Adsorbent, g	Adsorbed Chart Area	Desorbed Chart Area	Average	Surface Area, m^2/g	
Reference	0.7697	915	966	940	1.00	
1	0.7302	388	504	446	0.51	
2	0.7440	402	516	409	0.46	0.52±0.06
3	0.6537	380	527	453	0.58	
Reference	0.7697	911	932	922	1.00	

TABLE XVI

SORPTOMETER SURFACE AREAS FOR ADSORBENT IV
WATER DRIED JANUARY 4, 1978

Tube No.	Weight Adsorbent, g	Adsorbed Chart Area	Desorbed Chart Area	Average	Surface Area, m^2/g	
Reference	0.7697	368	365	366	1.00	
I	0.4715	142	141	142	0.63	
III	0.5947	195	241	218	0.76	0.73±0.09
16	0.5587	201	236	218	0.81	
Reference	0.7697	359	389	374	1.00	

TABLE XVII

SORPTOMETER SURFACE AREAS FOR BENZENE EXTRACTED, WATER EXTRACTED SURFACES — FEBRUARY 22, 1978

Tube No. and Description	Weight Adsorbent, g	Adsorbed Chart Area	Desorbed Chart Area	Average	Surface Area, m^2/g
Reference	0.7697	5768	6086	--	1.00
VI-Control fibers - untreated Column 5	0.8878 0.8878 0.8878	4466 4485 4572	6603 7284 7172	5534 5884 5872	0.83±0.02
IV-0.28 POML chemisorbed stearic acid Column 6	0.6392 0.6392 0.6392	2582 2697 2668	3334 3419 3422	2958 3058 3045	0.60±0.02
Reference	0.7697	6124	6186	6041	1.00

TABLE XVIII

SORPTOMETER SURFACE AREAS FOR FIBERS FULLY COVERED WITH STEARIC ACID — MARCH 9, 1978

Tube No. and Description	Weight Adsorbent, g	Adsorbed Chart Area	Desorbed Chart Area	Average	Surface Area, m^2/g
Reference	0.7697	1813	1832	1822	1.00
II-1.03 POML Col. 7-water repellent	0.677	762	980	871	0.54
28-0.75 POML Col. 8-not water repellent	0.5791	690	781	735	0.54

TABLE XIX

SORPTOMETER SURFACE AREAS FOR FIBERS MODIFIED WITH PHYSISORBED STEARIC ACID APRIL 17, 1978

Tube No. and Description	Weight Adsorbent, g	Adsorbed Chart Area	Desorbed Chart Area	Average	Surface Area, m^2/g
Reference	0.7697	504	539	522	1.00
9-Col. 4(0%)	0.6171	246	343	294	0.70
7-Col. 14(17%)	0.6116	206	285	246	0.59
V-Col. 11(39%)	0.6804	230	298	264	0.57
4-Col. 12(52%)	0.6765	245	272	258	0.56
2 Col. 13(68%)	0.6219	198	242	220	0.52
I-Col. 15(81%)	0.6172	206	293	244	0.53
Reference	0.7697	513	543	528	1.00

In all the above sorptometer work it will be noted that desorbed peak area of various cotton fiber surfaces is always greater than adsorbed peak area for the same sample. This is also true for the reference filter paper sample but to a lesser degree. This probably has something to do with the kinetics of adsorption on filter paper strips and packed masses of cotton fibers. For reference tubes the desorbed peaks are slightly higher and more narrow than the adsorbed peaks. This indicates that desorption is quicker than adsorption. On the various cotton surfaces desorption peaks are always lower and broader than the adsorption peaks. This indicates that desorption out of these samples is a slower process than adsorption.

The discrepancies are impossible to avoid by any variations in experimental techniques. The average of adsorbed and desorbed peak area is used in each case to calculate adsorbent surface area. Because of this discrepancy and based on triplicate samples, the precision of the sorptometer for these surfaces is estimated at ± 0.09 m^2/g regardless of sorbent surface area.

APPENDIX VI

COMPUTER PROGRAMS

These programs, along with experimental data, have been stored on magnetic tape in the Computing Center of The Institute of Paper Chemistry. Program VI-A is stored with data representing 55 adsorption isotherms at various temperatures for decane and hexanol on the series of stearic acid modified surfaces. Program VI-B is stored with data representing hexanol and decane adsorption at 45°C on this series of surfaces. Program VI-C is stored with data representing adsorption of decane and hexanol at 35°C on these surfaces.

In each set of data the first cards after / DATA are the labels of graph axes. Program VI-A has five labels, the other programs have only two labels. Each subset of experimental data has two identifier cards, a card with experimental chromatographic conditions, a card with specialized program information, and a card with the microcomparator reference point before the data points. The fourth card in a subset deck contains specialized information required by the program. This card is different for each data deck appearing in more than one program. Except for this card, data decks may be used in all programs.

Sufficient comments have been included to allow understanding of the basic operating principles of each program. Photographically reduced, superimposed chromatogram common boundaries were digitized with a Hewlett-Packard K02 5211 B microcomparator. A Dymec 2526A coupler connected the digitization unit to an IBM card punch. Four data points were punched on each card. The chromatogram common boundaries were reduced to 1/5 actual size. Digitization resulted in a five digit representation of each data point. In each program, these data points were converted to 1/10-inch chart squares by dividing differences

APPENDIX VI

COMPUTER PROGRAMS

VI-A — ISOTHERM ANALYSIS

```
C                                                                      C
C  THIS PROGRAM WILL COMPUTE,PLOT,AND ANALYZE ADSORPTION ISOTHERMS FROM
C  SUPERIMPOSED GAS CHROMATOGRAMS OF A SERIES OF SAMPLE  INJECTIONS OF
C  INCREASING SIZE. EXPERIMENTAL DATA IS ENTERED  AS  MICROCOMPARATOR DA
C  OBTAINED FROM THE EXPERIMENTAL PLOTS.ISOTHERMS ARE CALCULATED AND
C  PLOTTED.ISOTHERMS AT 5 TEMPS. ARE ANALYZED BY APPLICATION OF THE
C  CLAUSIUS-CLAPEYRON EQUATION.HEATS,ENTROPIES,AND FREE ENERGIES OF
C  ADSORPTION ARE CALCULATED AND PLOTTED AS FUNCTIONS OF AMT.ADS.
      DOUBLE PRECISION SX,SY,SSX,SSY,SXY,YLNVP(5),S,EE,DR,CEPT
      DIMENSION A (200,6),X(200),HEAD(20),B(200,6),AMAD(200),F(200,5),
     2 XRT(5),C(100,7),LAB1X(6),LAB1Y(6),LAB2Y(6),LAB3Y(6),LAB4Y(6)
      COMMON LX(7),LY(7),ID(13),SVAL(4)
      REAL M
      ID(13) = 0
      R=0.0624
      IO=5
      READ(IO,9020) LAB1X,LAB1Y,LAB2Y,LAB3Y,LAB4Y
C  THESE ARE THE FIRST 5 CARDS AFTER /DATA AND BEFORE ISOTHERM DATA
C  THESE CARDS ARE THE AXIS LABELS FOR THE PLOTS OF ISOTHERMS AND
C  THERMODYNAMIC ADSORPTION PARAMETERS FROM ISOTHERM ANALYSIS.
 9020 FORMAT (6A4)
      LX(7)=24
      LY(7)=24
COMMENT OUT NEXT STMT.IF DESIRE TO ONLY CALCULATE AND PLOT ISOTHERMS
      DO 800 ITIME=1,5
 1000 CONTINUE
      H=-0.5
      DH = 0.5
C  EACH ISOTHERM DATA SET MUST START WITH THE FOLLOWING 4 CARDS
C  ENTER TABLE AND GRAPH HEADINGS
      CALL GET (HEAD,80,IO)
     IF(IVER(HEAD,1,80))  1001,1002,1001
 1001 CALL GET (ID,48,IO)
C  ENTER EXPERIMENTAL CONDITIONS
      READ (IO,9001) N,T,Q,W,M,D
C  N=DATA PTS T=ABS.TEMP Q=CHT.SPD IN 0.1 SQUARES/MIN W=GAS FLOW,ML/MIN
C  M=GRAMS ADSORBENT IN COLUMN D=DETECTOR SENS.,CHT.SQ./MICROMOLE
9001  FORMAT (1I4,1F4.0,3F6.3,1F8.3)
C  ENTER PROGRAM OPTION CONTROL INTERGERS
      READ (IO,9002) KZ,L,NX,NY,IEQ,LJ
C  KZ=0,MAX V.P.IS CALCULATED,KZ=1,MAX V.P.MUST BE ENTERED.
C  L=-1 FOR GRAPH ONLY,L=0 FOR GRAPH AND TABLE,L=1 FOR TABLE ONLY
C  NX AND NY ARE +1 FOR NEW SET OF GRAPH AXIS,-1 TO PLOT ON SAME AXIS
C  NOTE, THE FIRST DATA DECK MUST HAVE NX AND NY +1
C  IEQ DEFINES SYMBOL FOR PLOT USUALLY DIFFERENT FOR EACH DECK
C  LJ LABELS EACH DATA DECK AS TO TEMPERATURE
9002  FORMAT (6I3)
C  ENTER THE EXPERIMENTAL CURVE AS MICROCOMPARATOR DATA
      READ (IO,9003) XREF
9003  FORMAT (1F5.0)
      VMAX = -9999.
      READ (IO,9004)(X(I),I=1,N)
9004  FORMAT (4(F5.0,5X))
```

```
      DO 10 I=1,N
      H = H+0.5
      A(I,1) = H
      A(I,2) = (XREF-X(I))/240
      A(I,3) =   Q*A(I,1)*R*T/(W*D)
      VMAX = AMAX1 (A(I,3),VMAX)
 10   CONTINUE
      IF (KZ) 6,6,5
C FOR KZ=1, SATN.VAP.PRES.OF ADSORBATE MUST BE LAST CARD IN EACH
C ISOTHERM DATA DECK AS MM.HG.
  5   READ (IO,9005) VMAX
9005  FORMAT (1F5.2)
  6   DO 11 I=1,N
      A(I,4) = A(I,3)/VMAX
      IF (I-1) 11,11,12
 12   A(I,5) = (A(I,2) + A(I-1,2))/2*DH+ A(I-1,5)
      A(I,6) =   A(I,5)/(M*D)
 11   CONTINUE
C THE 'A' MATRIX IS THE EXPERIMENTAL DATA AND THE CALCULATED ISOTHERM
      IF (L) 13,13,14
 13   DO 8 I=1,6
      LX(I)=LAB1X(I)
  8   LY(I)=LAB1Y(I)
      CALL GRAPH (A(1,3),A(1,6),NX,NY,N,10,IEQ)
      IF (L) 16,14,14
 14   WRITE (6,9006) HEAD
9006  FORMAT (' ',20A4)
      WRITE (6,9007)
9007  FORMAT ('      H       X      VAP.PRES.    PART.PRES.       AREA
     2 AMT.ADS.  ')
      WRITE (6,9008)
9008  FORMAT ('   CHARTSQUARES     MM.HG.      (RELATIVE)      SQUARES
     2 MICROMOLES/GM. ')
      IJK=N-10
C ADJUST IJK VALUE TO PRINT OUT MORE OF THE ISOTHERM TABLE IF DESIRED
C NOW ONLY LAST 10 ENTRIES ARE PRINTED
      DO 15 I=IJK,N
 15   WRITE (6,9009) (A(I,J),J=1,6)
9009  FORMAT (1H ,2F7.2,2F12.4,1F12.2,1F12.4)
 16   CONTINUE
COMMENT OUT NEXT STMT.IF DESIRE TO ANALYZE ISOTHERMS
C     GO TO 1000
C ISOTHERM CALCULATION NOW COMPLETE. BEFORE CALCULATION OF
C THERMODYNAMIC QUANTITIES CALCULATE ADSORBATE VAPOR PRESSURES
C FOR A REGULARLY SPACED SERIES OF SURFACE COVERAGES.
C DONE BY INTERPOLATION WITH TABLE OF DIVIDED DIFFERENCES
C  FIRST ENTER DATA FROM 'A' MATRIX FOR ANALYSIS. SURFACE
COVERAGE, THETA, IS LEFT IN MICROMOLES ADSORBED/GRAM ADSORBENT
      THETA = 0.0
      DO 18 I = 1,50
C ADJUST COVERAGE LIMIT BY CHANGING VALUE ADDED TO THETA IN NEXT STMT.
      THETA = THETA + 0.1900
      B(I,1) = THETA
 18   CONTINUE
      DO 19 I=1,N
      AMAD(I)=A(I,6)
      F(I,1)=A(I,3)
 19   CONTINUE
C CONSTRUCT DIVIDED DIFFERENCE TABLES
 20   DO 101 I=2,N
      DO 101 J=2,5
      IF (I-J) 101,105,105
105   K=(I-J+1)
      F(I,J)=(F(I,J-1)-F(I-1,J-1))/(AMAD(I)-AMAD(K))
```

```
  101 CONTINUE
C NOW DO INTERPOLATION
      DO 800 IPT=1,50
      XA=B(IPT,1)
      DO 705 II=1,N
      I=II
      IF(XA-AMAD(I)) 735,770,705
  705 CONTINUE
      GO TO 740
  735 I=I-3
      IF (I-1) 736,750,737
  737 IF (I-N+4) 750,750,740
  736 I=1
      GO TO 750
  740 I=N-4
      GO TO 750
  770 FA=F(I,1)
      GO TO 753
  750 FA=F(I+4,5)
      DO 707 J=1,4
      K=I+4-J
      LN=5-J
  707 FA=FA*(XA-AMAD(K))+F(K,LN)
  753 B(IPT,LJ)=FA
  800 CONTINUE
C THE 'B' MATRIX IS 5 ISOTHERMS TABULIZED AT REGULAR INTERVALS OF AMT.ADS
      WRITE (6,9006) HEAD
   22 WRITE (6,9010)
 9010 FORMAT (' AMOUNT                ADSORBATE VAPOR PRESSURE-MM.HG')
      WRITE (6,9011)
 9011 FORMAT (' ADSORBED      308K      313K      318K      323K      328K'
      DO 23 I=1,50
   23 WRITE (6,9012) (B(I,J),J=1,6)
 9012 FORMAT (1H ,1F5.3,5X,5F9.3)
C NOW PLOT NATURAL LOG OF VAPOR PRESSURE VS.RECIPROCAL OF ABSOLUTE
C TEMPERATURE IN A CLAUSIUS-CLAPEYRON PLOT. DO THIS FOR EACH VALUE
C OF AMOUNT ADSORBED. FIT DATA FROM JUST GENERATED 'B' MATRIX TO
C STRAIGHT LINE BY LEAST SQUARES. GET THERMODYNAMIC ADSORPTION
C FUNCTIONS FROM SLOPE GENERATED AT EACH FIXED LEVEL OF AMOUNT
C ADSORBED.
      XRT(1)=0.0032452
      XRT(2)=0.0031934
      XRT(3)=0.0031432
      XRT(4)=0.0030945
      XRT(5)=0.0030474
C THESE XRT VALUES ARE RECIPROCALS OF THE ABSOLUTE TEMPERATURES OF
C THE FIVE EXPERIMENTAL ISOTHERMS.CHANGE AS NECESSARY
      DO 40 I=1,50
      SX=0.0
      SY=0.0
      SSX=0.0
      SSY=0.0
      SXY=0.0
      C(I,1)=B(I,1)
```

```
      DO 30 LJ=2,6
C LJ RANGE,J VALUE,AND NC RANGE MUST BE ADJUSTED FOR <5 ISOTHERMS
   30 YLNVP(LJ-1)=ALOG(B(I,LJ))
      J=5
      DO 31 NC=1,5
      SX=SX+XRT(NC)
      SY=SY+YLNVP(NC)
      SSX=SSX+XRT(NC)**2
      SSY=SSY+YLNVP(NC)**2
   31 SXY=SXY+XRT(NC)*YLNVP(NC)
      AVGX=SX/J
      AVGY=SY/J
      DR=((SSX-(SX**2)/J)*(SSY-(SY**2)/J))
      IF (DR) 32,32,33
   32 CR=90.9090
      GO TO 34
   33 CR=(SXY-J*AVGX*AVGY)/(SQRT(DR))
   34 CEPT=(SSX*SY-SX*SXY)/(J*SSX-SX**2)
      S=(J*SXY-SX*SY)/(J*SSX-SX**2)
      EE=(SSY-((CEPT*SY)+(S*SXY)))/J
      IF (EE) 36,36,37
   36 EF=EE
      GO TO 38
   37 EF=SQRT(EE)
   38 C(I,5)=EF
      C(I,2)=S*(-0.00198)
      C(I,3)=0.00198*318*(-ALOG(B(I,4)/760))
      C(I,4)=(C(I,2)-C(I,3))/(-0.318)
      C(I,6)=AVGY
      C(I,7)=CR
   40 CONTINUE
C THE 'C' MATRIX IS ISOSTEARIC,THERMODYNAMIC,ADSORPTION PARAMETERS.
      IF (L) 41,41,45
   41 DO 42 I=1,6
      LX(I)=LAB1Y(I)
   42 LY(I)=LAB2Y(I)
      CALL GRAPH (C(1,1),C(1,2),1,1,50,3,1)
      DO 43 I=1,6
   43 LY(I)=LAB3Y(I)
      CALL GRAPH (C(1,1),C(1,3),1,1,50,3,1)
      DO 44 I=1,6
   44 LY(I)=LAB4Y(I)
      CALL GRAPH (C(1,1),C(1,4),1,1,50,3,1)
      IF (L) 1002,45,45
   45 WRITE (6,9006) HEAD
      WRITE (6,9013)
 9013 FORMAT (' AMOUNT     -HEAT OF     -FREE ENERGY  ENTROPY OF    ERRO
     2       AVGERAGE     CORR.')
      WRITE (6,9014)
 9014 FORMAT(' ADSORBED    ADSORPT.      OF ADSORPT.  ADSORPT.     IN A
     2      Y VALUE      COEFF.')
      WRITE (6,9015)
 9015 FORMAT(' MICMOLE/GM  KCAL/MOLE     KCAL/MOLE    CAL/M-DEG     Y')
      DO 46 I=1,50
   46 WRITE (6,9016) (C(I,J),J=1,7)
 9016 FORMAT (1H ,1F6.3,6X,6(F8.4,4X))
 1002 CALL FINAL
      CALL EXIT
      END
```

VI-B — CALCULATION OF ADSORPTIVE SITE ENERGY DISTRIBUTION

```
C THIS PROGRAM CALCULATES AND PLOTS A ROUGH FIRST APPROXIMATION TO
C THE DISTRIBUTION OF ADSORPTIVE SITE ENERGIES ON A SURFACE. AN
C EXPERIMENTAL PLOT OF RETENTION VOLUME VS.PEAK HEIGHT IS ENTERED
C AS A MICROCOMPARATOR PRODUCED SERIES OF DATA POINTS.THE CONDENSATION
C APPROXIMATION AND ABSENSE OF LATERAL INTERACTIONS OF ADSORBED
C MOLECULES IS ASSUMED. THE APPROACH OF RUDZINSKI AND CO-WORKERS
C AS PRESENTED IN J.CHROMATOG.,VOL.92,PGS.25-32,(1974), IS UTILIZED
C FOR THIS CALCULATION.
      DIMENSION A(100,9),Y(200),HEAD(20),LAB1X(6),LAB1Y(6)
      COMMON LX(7),LY(7),ID(13),SVAL(4)
      REAL M
      ID(13)=0
      R=0.00198
      IO=5
C ENTER THE GRAPH AXES LABELS AS FIRST TWO CARDS AFTER /DATA
      READ(IO,9001)LAB1X,LAB1Y
 9001 FORMAT(6A4)
      LX(7)=24
      LY(7)=24
 1000 CONTINUE
      H=-0.5
      DH=0.5
C ENTER TABLE AND GRAPH HEADINGS
      CALL GET (HEAD,80,IO)
      IF(IVER(HEAD,1,80)) 1001,1002,1001
 1001 CALL GET (ID,48,IO)
C ENTER EXPERIMENTAL CONDITIONS AND PROGRAM CONTROL INTEGERS
      READ(IO,9002) N,T,Q,W,M,D
 9002 FORMAT(1I4,1F4.0,3F6.3,1F8.3)
C N=DATA PTS,T=ABSOLUTE TEMP,Q=CHT.SPD.INSQUARES/MIN,W=GAS FLOW,ML/MIN,
C M=GRAMS ADSORBENT IN COL.,D=DETECTOR SENS.IN CHT.SQ./MICROMOLE
      READ(IO,9003) NX,NY,IEQ,Z,ENGO
 9003 FORMAT(3I3,2F6.3)
C NX AND NY ARE +1 FOR NEW AXIS SET, AND -1 FOR REPLOT ON SAME SET.
C FIRST DATA DECK IN STACK MUST HAVE NX AND NY=+1.
C IEQ=GRAPH PLOTTING SYMBOL,Z=ADSORBATE MOL.WT.IN GRAMS.,
C ENGO=ESTIMATED ADSORBATE LATERAL INTERACTION ENERGY.
C NOW ENTER EXPERIMENTAL DATA.
      READ(IO,9004)YREF
 9004 FORMAT (1F5.0)
      READ(IO,9005)(Y(I),I=1,N)
 9005 FORMAT(4(F5.0,5X))
      J=N/2
      B=17600*(SQRT(Z*T))
      DP=Q*DH*(0.0624)*T/(W*D)
      DO 10 I=1,J
      H=H+0.5
      A(I,1)=H
CALCULATION OF VAPOR PRESSURE AT EACH RECORDER PEN HEIGHT
      A(I,2)=Q*A(I,1)*(0.0624)*T/(W*D)
CALCULATION OF CORRESPONDING ADSORPTION ENERGY FROM CONDENS.APPROX.
      IF (I-1) 2,2,3
    2 A(I,3)=0
      GO TO 4
    3 A(I,3)=(-R*T*(ALOG(A(I,2)/B)))-ENGO
    4 CONTINUE
CALCULATION OF Y VALUE IN 0.1 INCH CHART SQUARES
      A(I,4)=(YREF-Y(I))/240
CALCULATION OF SPECIFIC RETENTION VOLUME
      A(I,5)=((A(I,4)/Q)*W)/M
CALCULATION OF DERIVATIVE MULTIPLIER TERM
      A(I,6)=(A(I,2)/(R*T))**2
CALCULATION OF D(R.V.)/DP TERM.NOTE,SIMPLE SLOPE ESTIMATE IS USED.
      IF (I-1) 5,5,6
    5 A(I,7)=0
      GO TO 7
    6 A(I,7)=-(A(I-1,5)-A(I,5))/DP
    7 CONTINUE
```

```
CALCULATION OF SITE ENERGY DISTRIBUTION FREQUENCY TERM
      A(I,8)=-A(I,6)*A(I,7)
   10 CONTINUE
      DO 12 I=1,6
      LX(I)=LAB1X(I)
   12 LY(I)=LAB1Y(I)
      CALL GRAPH (A(1,3),A(1,8),NX,NY,J,-1,IEQ)
      WRITE (6,9006) HEAD
 9006 FORMAT (' ',20A4)
      WRITE (6,9007)
 9007 FORMAT('  VAPOR     ADSORPTION    SPECIFIC    FREQUENCY  ')
      WRITE (6,9008)
 9008 FORMAT(' PRESSURE    ENERGY      RETENT.VOL.   FUNCTION  ')
      WRITE (6,9009)
 9009 FORMAT('   MM.HG.    KCAL/MOLE      ML/GRAM  ')
      DO 15 I=1,J
   15 WRITE (6,9010) A(I,2),A(I,3),A(I,5),A(I,8)
 9010 FORMAT (1H ,1F6.4,4X,3(F8.4,4X))
      GO TO 1000
 1002 CALL FINAL
      CALL EXIT
      END
```

VI-C — CALCULATION OF SPREADING PRESSURE BEHAVIOR

```
C THIS PROGRAM CALCULATES AND PLOTS SPREADING PRESSURE AS A FUNCTION OF
C ADSORBENT SURFACE AREA AVAILABLE PER ADSORBATE MOLECULE.TRAPEZOIDAL
C INTEGRATION IS USED TWICE TO CONVERT MICROCOMPARATOR DIGITALIZED
C ADSORPTION DATA. THIS PROGRAM FIRST CALCULATES THE ADSORPTION
C ISOTHERM BEFORE PROCEEDING FURTHER WITH THE CALCULATION OF SPREADING
C PRESSURE. THE GIBBS ADSORPTION EQUATION FOR A SINGLE GAS-SOLID
C SYSTEM IS UTILIZED. SPREADING PRESSURE IS CALCULATED INDIRECTLY FROM
C THE ADSORPTION ISOTHERM. SINCE ALL ADSORPTION IS ASSUMED TO OCCUR AS A
C MONOLAYER,THE INTERPRETATION OF THIS CALCULATION SHOULD BE APPROACHED
C WITH EXTREME CAUTION.
      DIMENSION A(200,9),X(200),HEAD(20),LAB1X(6),LAB1Y(6)
      COMMON LX(7),LY(7),ID(13),SVAL(4)
      REAL M
      ID(13)=0
      R=0.0624
      IO=5
C ENTER THE GRAPH AXES LABELS AS THE FIRST TWO CARDS AFTER /DATA
      READ(IO,9001)LAB1X,LAB1Y
 9001 FORMAT(6A4)
      LX(7)=24
      LY(7)=24
 1000 CONTINUE
      H=-0.5
      DH=0.5
C ENTER TABLE AND GRAPH HEADINGS
      CALL GET (HEAD,80,IO)
      IF(IVER(HEAD,1,80)) 1001,1002,1001
 1001 CALL GET (ID,48,IO)
C ENTER EXPERIMENTAL CONDITIONS AND PROGRAM CONTROL INTEGERS
      READ (IO,9002) N,T,Q,W,M,D
 9002 FORMAT(1I4,1F4.0,3F6.3,1F8.3)
C N=NUMBER DATA PTS,T=ABSOLUTE TEMP,Q=CHT SPD(SQ/MIN),W=GAS FLOW(ML/MIN)
C M=GM.ADSORBENT IN COL.,D=DETECTOR SENSITIVITY(CHT.SQ./MICROMOLE)
      READ(IO,9003)NX,NY,IEQ,SURFA
 9003 FORMAT(3I3,1F6.3)
C NX AND NY ARE +1 FOR NEW AXIS SET AND -1 FOR REPLOT ON SAME SET
C FIRST DATA DECK IN STACK MUST HAVE NX AND NY=+1
C IEQ=GRAPH PLOTTING SYMBOL
C SURFA=MEASURED(NITROGEN AT 76DEG K) ADSORBENT SURFACE AREA IN SQ.M/GM
C NOW ENTER EXPERIMENTAL DATA FROM MICROCOMPARATOR
      READ(IO,9004)XREF
 9004 FORMAT(1F5.0)
      READ(IO,9005)(X(I),I=1,N)
```

```
 9005 FORMAT(4(F5.0,5X))
      J=N/2
      DO 10 I=1,J
      H=H+0.5
      A(I,1)=H
CALCULATION OF ADSORBATE VAPOR PRESSURE AT EACH RECORDER PEN HEIGHT
      A(I,2)=Q*A(I,1)*R*T/(W*D)
      IF(I-1) 2,2,3
    2 A(I,3)=0
      GO TO 4
    3 A(I,3)=ALOG(A(I,2))
    4 CONTINUE
CALCULATION OF X IN 0.1 INCH CHART SQUARES
      A(I,4)=(XREF-X(I))/240
CALCULATION OF AMOUNT ADSORBED AT EACH PRESSURE IN MICROMOLES ADSORBED
C PER GRAM ADSORBENT. THIS IS THE ADSORPTION ISOTHERM,(WITH A(I,2)).
      A(I,5)=(A(I,4)+A(I-1,4))/2*DH+A(I-1,5)
      A(I,6)=A(I,5)/(M*D)
CALCULATION OF INTEGRAL OF AMT.ADS.VS.LNP AT EACH PRESSURE
      IF(I-2) 5,5,6
    5 A(I,7)=0
      GO TO 7
    6 A(I,7)=(A(I,6)+A(I-1,6))/2*(A(I,3)-A(I-1,3))+A(I-1,7)
    7 CONTINUE
CALCULATION OF SPREADING PRESSURE IN MN/M(DYNES/CM)OR MJ/SQ.M(ERG/SQ.CM)
      A(I,8)=((0.1333*R*T)/SURFA)*A(I,7)
CALCULATION OF AREA PER MOLECULE ON THE SURFACE IN SQ.NANOM/MOLECULE
      A(I,9)=(1.66*SURFA)/A(I,6)
   10 CONTINUE
      DO 12 I=1,6
      LX(I)=LABIX(I)
   12 LY(I)=LABIY(I)
      CALL GRAPH(A(3,9),A(3,8),NX,NY,J,-1,IEQ)
      WRITE(6,9006) HEAD
 9006 FORMAT (' ',20A4)
      WRITE(6,9007)
 9007 FORMAT('  VAPOR    AMT.ADS.-    SPREADING     SURF.AREA  ')
      WRITE(6,9008)
 9008 FORMAT('PRESSURE  MICROMOLES   PRESSURE     PER SORBATE ')
      WRITE(6,9009)
 9009 FORMAT(' MM.HG.     PER GRAM     MILI.N/M     MOLECULE- ')
      WRITE(6,9010)
 9010 FORMAT('             ADSORBENT   (DYNES/CM)   SQ.NM./MOLECULE ')
      DO 15 I=1,J
   15 WRITE(6,9011) A(I,2),A(I,6),A(I,8),A(I,9)
 9011 FORMAT(1H ,1F6.4,4X,3(F8.4,4X))
      GO TO 1000
 1002 CALL FINAL
      CALL EXIT
      END
```

between the microcomparator reference point and individual data points by a scale factor of 240. Different data formats would require modification of this portion of each program.

APPENDIX VII

GAS CHROMATOGRAPH FLAME IONIZATION DETECTOR SENSITIVITY CALCULATIONS

Detector sensitivities were measured for each adsorption isotherm. Chromatogram areas of the 0.1, 0.2, and 0.3 μL injections for each isotherm were measured on the Technicon integrator. The integrator was calibrated before each measurement to read directly in 0.1 inch x 0.1 inch chart squares. Table XX shows the chart areas for these chromatograms. On Column 6 peak areas of 0.2, 0.3, and 0.4 μL injections were measured.

Except for Column 6, all data for each adsorbate were averaged together. This was done by taking into account injection size, chart speed, and detector sensitivity setting. Data of Table XX were averaged in terms of chart area for a 0.1 μL injection of hexanol at 1 inch/min chart speed and sensitivity of range 10^{-9}, attenuation x 32. For example, a 0.3 μL injection at 2 inches/min and 10^{-9} x 128 gave a peak area of 401 chart squares. At 1 inch/min chart speed the area would be 200 chart squares. At attenuation x 32, chart area would be 128/32 = 4 times larger or 800 chart squares. For a 0.1 μL injection at 1 inch/min and 10^{-9} x 32, the chart area would be 800/3 = 267 chart squares. This would be the number going into the average. All entries for hexanol (except Column 6) were thus treated and averaged. Standard deviation was calculated. Entries outside the limit of one standard deviation of the mean ($\pm\sigma$) were discarded. The average was recalculated as 246 ± 11 chart squares for a 0.1 μL injection of hexanol at 1 inch/min and 10^{-9} x 32. Injections that were discarded for exceeding $\pm\sigma$ were examined. If only one injection out of 3 for a given column at a certain temperature was outside limits, the average sensitivity was used. If 2 or 3 of the injections were outside of limits, the average sensitivity of the 3 injections was used.

TABLE XX

CHART AREAS FOR DETECTOR SENSITIVITY CALCULATIONS

Isotherm Col. No.	Isotherm Temp., °C	Chart Speed Inches Per Min	Attenuation 10^{-9} x	Adsorbate	Peak Areas 0.1 µL	0.2 µL	0.3 µL	(Sensitivity)
8	35	1	32	Hexanol	232	508	808	
8	40	1	32	Hexanol	208	522	--	
8[a]	45	2	10^{-10} x 256	Hexanol	317	724	--	(425)[a]
8	50	2	64	Hexanol	237	513	844	
8[a]	55	2	64	Hexanol	273	528	900	(351)[a]
8	35	2	64	Decane	287	575	1037	
8[a]	40	2	128	Decane	116	160	274	(292)[a]
8[a]	45	4	10^{-10} x 512	Decane	372	--	1057	(706)[a]
8	50	4	128	Decane	287	720	1084	
8	55	4	128	Decane	290	698	1014	
11	35	1	32	Hexanol	185	466	857	
11	40	1	32	Hexanol	183	545	900	
11	45	1	64	Hexanol	91	252	468	
11	50	2	64	Hexanol	260	529	831	
11	55	2	128	Hexanol	122	205	398	
15[a]	35	1	32	Hexanol	175	441	--	(248)[a]
15	40	1	32	Hexanol	199	518	779	
15	45	1	64	Hexanol	118	236	401	
15	50	2	64	Hexanol	241	501	807	
15	55	2	128	Hexanol	107	249	406	
12	35	1	32	Hexanol	239	493	699	
12	40	1	32	Hexanol	243	540	--	
12	45	1	64	Hexanol	129	257	406	
12	50	2	64	Hexanol	246	517	797	
12	55	2	128	Hexanol	127	265	--	
12	35	2	64	Decane	252	641	1058	
12	40	2	128	Decane	126	308	509	
12[a]	45	2	128	Decane	155	331	527	(323)[a]
12	50	4	128	Decane	265	610	--	
12	55	4	128	Decane	296	600	957	
14[a]	35	1	32	Hexanol	129	387	608	(220)[a]
14	40	1	32	Hexanol	246	414	758	
14	45	1	64	Hexanol	117	213	385	
14	50	2	64	Hexanol	243	423	757	
14	55	2	128	Hexanol	131	221	382	
13[a]	35	1	32	Hexanol	210	431	719	(279)[a]
13	40	1	32	Hexanol	251	518	774	
13	45	1	64	Hexanol	243	541	762	
13	50	2	128	Hexanol	165	243	396	
13	55	2	128	Hexanol	140	244	399	
4[a]	35	1/2	32	Hexanol	94	191	345	(128)[a]
4	40	1	64	Hexanol	69	202	382	
4	45	1	64	Hexanol	93	236	427	
4	50	1	64	Hexanol	109	245	395	
4	55	2	128	Hexanol	104	228	401	
4	35	2	64	Decane	306	578	951	
4	40	2	128	Decane	137	277	441	
4	45	2	128	Decane	146	291	412	
4	50	4	128	Decane	274	593	871	
4	55	4	128	Decane	331	616	862	
					0.2 µL	0.3 µL	0.4 µL	
6[a]	35	1	32	Hexanol	368	668	756	(254)[a]
6[a]	40	1	32	Hexanol	359	376	752	(254)[a]
6[a]	45	1	64	Hexanol	193	301	451	(127)[a]
6[a]	50	2	64	Hexanol	392	611	856	(254)[a]
6[a]	55	2	128	Hexanol	234	303	550	(127)[a]

[a]Average sensitivities not used for calculation. Those used are given in parentheses.

For decane, calculations were made for 0.1 μL injection at 2 inches/min and 10^{-9} x 64. Eighty-one peaks were analyzed for hexanol and 33 peaks for decane. For hexanol, detector sensitivity is calculated as:

D = 246 squares/0.1 μL = 246 squares/0.796 μmole = 309 squares/μmole

Therefore at:

1/2 inch/min and 10^{-9} x 32 - D = 154.5

1 inch/min and 10^{-9} x 32 = D = 309

1 inch/min and 10^{-9} x 64 - D = 154.5

2 inches/min and 10^{-9} x 64 - D = 309

2 inches/min and 10^{-9} x 128 - D = 154.5

For decane the average peak area was 300 ± 12 for 0.1 μL at 2 inches/min and 10^{-9} x 64.

D = 300 squares/0.1 μL = 300 squares/0.513 μmole = 585 squares/μmole

Therefore at:

2 inches/min and 10^{-9} x 64 - D = 585

2 inches/min and 10^{-9} x 128 - D = 292

4 inches/min and 10^{-9} x 128 - D = 585

In Table XX isotherms that were not calculated with these average sensitivities are marked with an asterisk. The sensitivity used is given in parentheses. Except for Column 6, all isotherms were measured in a four-week period from April 23 to May 19, 1978. The chromatograph was run almost continuously for this time. At night the flame was extinguished but detector temperature was maintained. Air flow was maintained at 400 mL/min with the air pump. Work on Column 6 was done after a 3-month shutdown of the chromatograph. Detector sensitivity was

calculated as 254 squares/μmole at 1 inch/min and 10^{-9} x 32 for hexanol. This is a 17% decrease in detector sensitivity, and is not easily explained. Therefore it is strongly suggested that detector sensitivity always be determined for a given set of experimental conditions.

Detector sensitivities also are important for SAI measurements. In this work SAI values were measured at 45°C. At this constant temperature adsorbate vapor pressure should be constant. Relative detector sensitivities were evaluated from the maximum plateau peak heights of 2 μL injections. These relative sensitivities were used to calculate the corresponding peak heights for $\underline{V}_{R_{max}}$ measurements at equal adsorbate vapor pressures.

APPENDIX VIII

SAI ADSORPTION DATA

Experimental retention data used to calculate surface adsorption indices for stearic acid modified surfaces are contained in Table XXI. Temperature was 45°C and 30 mL helium/min carrier gas flow rate was used in all cases. Maximum peak height refers to the plateau height of a 2 liter injection measured in centimeters at 10^{-10} x 128. Maximum retention time peak height was chosen as 1.00 inch for hexanol and 1.66 inches for decane on Column 4 at 10^{-10} x 16. For maximum retention time peak heights on other columns the ratio of maximum peak height to maximum peak height on Column 4 was multiplied by 1.00 and 1.66. Injection temperature was 145°C, detector temperature was 160°C.

The large changes in detector sensitivity as indicated by variations in maximum peak heights shown in Table XXI were due to insufficient air flow to the detector. With insufficient air flow, detector sensitivity is highly dependent on hydrogen flow, as well as air flow. These flows are extremely difficult to monitor and set exactly. At air flows above 400 mL/min detector sensitivity is independent of hydrogen flow variations of ±1-2 mL/min. A better but more time consuming way to insure measurement of $\underline{R}_{V_{max}}$ at equal vapor pressures would be to measure detector sensitivity before determining $\underline{R}_{V_{max}}$. Then the proper peak height corresponding to the selected, constant adsorbate vapor pressure could be calculated.

TABLE XXI

SAI ADSORPTION DATA

Col. No.	Adsorbent, g	Adsorbate	Peak Height cm. at 10^{-10} x 128	$\frac{R_V}{R_V \text{ min}}$ Peak Height inch at 10^{-10} x 16	Retention Time, cm	Chart Speed, inch/min	Retention Volume, mL	SAI, mL	SAI, mL/g
44	1.23	Hexanol	16.2	1.00	Max. 28.3 Min. 7.3	1	334 86	248	202
		Decane	8.7	1.66	Max. 12.7 Min. 9.1	2	75 54	21	17
14	1.16	Hexanol	7.3	0.45	Max. 25.1 Min. 6.8	1	296 80	216	185
		Decane	10.8	2.06	Max. 23.4 Min. 17.1	4	69 52	17	15
11	1.15	Hexanol	5.4	0.33	Max. 24.1 Min. 7.3	1	285 86	199	173
		Decane	7.4	1.41	Max. 22.7 Min. 17.7	4	66 51	15	13
12	1.19	Hexanol	4.7	0.29	Max. 19.3 Min. 7.0	1	228 83	145	123
		Decane	7.6	1.45	Max. 21.2 Min. 16.3	4	62 49	13	11
13	1.36	Hexanol	8.6	0.53	Max. 37.6 Min. 14.9	2	222 88	134	98
		Decane	11.6	2.21	Max. 22.0 Min. 18.0	4	65 53	12	9
15	1.36	Hexanol	7.7	0.48	Max. 34.0 Min. 16.6	2	200 98	102	75
		Decane	10.0	1.91	Max. 23.2 Min. 19.9	4	68 59	9	7
5	1.22	Hexanol	5.5	0.34	Max. 39.1 Min. 8.3	1	462 98	364	298
		Decane	8.2	1.56	Max. 15.5 Min. 10.5	2	92 62	30	24
6	1.50	Hexanol	8.1	0.50	Max. 37.6 Min. 8.8	1	444 104	340	227
		Decane	11.3	2.16	Max. 15.8 Min. 10.9	2	93 64	29	19
7	1.72	Hexanol	8.1	0.50	Max. 11.8 Min. 8.3	1	139 98	41	24
		Decane	5.0	0.95	Max. 23.1 Min. 20.1	4	68 59	9	6
8	1.46	Hexanol	4.1	0.25	Max. 8.5 Min. 7.5	1	101 89	12	7
		Decane	4.2	0.60	Max. 9.8 Min. 8.6	2	58 51	7	5